



Assessing the Life Cycle Environmental Impacts and Benefits of PV-Microgrid Systems in Off-Grid Communities

Authors: Andy Bilich; Love Goyal;

James Hansen; Anjana Krishnan; Kevin Langham

Faculty Advisor: Roland Geyer, Bren School

External Advisor: Joe Bergesen, Bren School

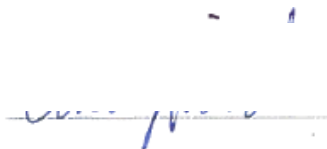
Client Advisor: Parikhit Sinha, First Solar

March 2016




Signature Page


As authors of this Group Project report, we are proud to archive this report on the Bren School's website such that the results of our research are available for all to read. Our signatures on the document signify our joint responsibility to fulfill the archiving standards set by the Bren School of Environmental Science & Management:




Andy Bilich



Anjana Krishnan



Love Goyal



Kevin Langham



James Hansen

The mission of the Bren School of Environmental Science & Management is to produce professionals with unrivaled training in environmental science and management who will devote their unique skills to diagnosis, assessment, mitigation, prevention, and remedy of the environmental problems of today and the future. A guiding principle of the School is that the analysis of environmental problems requires quantitative training in more than one discipline and an awareness of the physical, biological, social, political, and economic consequences that arise from scientific or technological decisions.

The Group Project is required of all students in the Masters of Environmental Science & Management (MESM) Program. It is a yearlong activity in which small groups of students conduct focused, interdisciplinary research on the scientific, management, and policy dimensions of a specific environmental issue. This Final Group Project Report is authored by the MESM students and has been reviewed and approved by:



Dr. Roland Geyer

Acknowledgements

The authors would like to thank the Bren School of Environmental Science & Management at the University of California, Santa Barbara, and First Solar for providing the opportunity to pursue this project.

The authors would also like to thank the following people and organizations for their support and guidance throughout the development of this project:

Faculty Advisor: Roland Geyer, Bren School of Environmental Science and Management

External Advisor: Joe Bergesen, Bren School of Environmental Science and Management

Other Bren Advisors:

- Kyle Meng, Bren School of Environmental Science and Management
- Sangwon Suh, Bren School of Environmental Science and Management
- Allison Horst, Bren School of Environmental Science and Management

Client Advisors:

- Parikhith Sinha, First Solar
- Lee Kraemer, First Solar
- Mitchell Lee, First Solar

Other External Advisors:

- João Arsénio, PROSOLIA Solar Energy
- Daniel Soto, Sonoma State University

External Funding: Yardi Corporation

Table of Contents

SIGNATURE PAGE	2
LIST OF FIGURES	7
LIST OF TABLES	8
ABSTRACT	9
EXECUTIVE SUMMARY	10
BACKGROUND	14
PROJECT OBJECTIVES	19
PROJECT SIGNIFICANCE	20
METHODOLOGY	22
GENERAL METHODOLOGY	22
<i>Baseline Parameters and Scenario Analysis</i>	24
<i>Life Cycle Modeling</i>	24
<i>PV-Battery system</i>	25
<i>PV-Diesel system</i>	25
<i>PV-Hybrid system</i>	25
<i>GaBi modeling</i>	26
<i>Impact Assessment</i>	27
PV MODULE METHODOLOGY	28
<i>PV Panels</i>	28
<i>Cadmium Telluride (CdTe)</i>	28
<i>Mono Crystalline Silicon</i>	29
<i>Module AC/DC Cabling</i>	30
<i>Retaining Clips</i>	30
BALANCE OF SYSTEMS INVENTORY MODELING	31
<i>Baseline CdTe Balance of Systems</i>	31
<i>Mounting</i>	31
<i>Inverter</i>	31
<i>Transformer</i>	31
<i>Construction, Operation, and Maintenance</i>	32
<i>Transport</i>	32
<i>Other Support Structures</i>	32
<i>Mono-Si Balance of Systems</i>	32
LITHIUM-ION BATTERY METHODOLOGY	32
<i>Battery Model</i>	34
<i>Battery Manufacturing</i>	34
<i>Battery Cell</i>	35
<i>Packaging</i>	36
<i>Battery Management System</i>	36

<i>Battery Sizing</i>	36
CHARGE CONTROLLER METHODOLOGY	37
<i>Modeling</i>	38
<i>Sizing</i>	38
DIESEL GENERATOR METHODOLOGY	39
<i>Generator Production</i>	40
<i>Generator Use Phase</i>	41
<i>PV-Diesel Generator System</i>	41
<i>PV- Hybrid Generator System</i>	43
DISTRIBUTION SYSTEM METHODOLOGY	44
<i>Residential Electricity Meters</i>	44
<i>Residential Electricity Wiring</i>	44
SECURITY FENCING METHODOLOGY	44
END OF LIFE METHODOLOGY	44
<i>Baseline Landfilling of Microgrid Systems</i>	44
<i>Recycling of CdTe Modules</i>	45
<i>Recycling of BOS</i>	45
<i>Recycling of Charge Controllers</i>	45
<i>Battery End of Life</i>	46
<i>Generator Recycling</i>	47
TRADITIONAL ELECTRIFICATION SOLUTION.....	47
<i>Average Kenya Electricity Grid Mix</i>	47
<i>Marginal Kenya Electricity Grid Mix</i>	47
SMALL-SCALE DIESEL COMPARISON	48
<i>Home Diesel Genset</i>	48
MANUFACTURING ELECTRICITY GRID MIXES	48
<i>Malaysia</i>	48
<i>South Korea</i>	48
DATA QUALITY AND UNCERTAINTIES	49
<i>Input Uncertainties</i>	49
<i>Processing uncertainties</i>	49
<i>Output Uncertainties</i>	49
RESULTS	50
OVERALL MICROGRID IMPACTS	50
ELEMENTARY FLOW ANALYSIS	52
MICROGRID COMPARISONS.....	54
<i>Microgrids versus Small-scale Diesel Gensets</i>	54
<i>Microgrids versus Traditional Electrification</i>	56
PV-BATTERY CONTRIBUTION ANALYSIS	58
SCENARIO 1: ELECTRICITY GRID MIX FOR BATTERY MANUFACTURING	61
SCENARIO 2: MICROGRID END OF LIFE RECYCLING.....	62
<i>Recycling: PV-Microgrid Impacts</i>	62
<i>Recycling: System Comparisons and Tradeoffs</i>	64

SCENARIO 3: CHOICE OF PV TECHNOLOGY- CdTe vs. MONO-Si	67
SCENARIO 4: APPLICATION TO LARGER SCALES - POWERHIVE’S PLANNED EXPANSION.....	71
DISCUSSION	74
OVERALL COMPARISON OF MICROGRID SYSTEM DESIGNS	74
MICROGRIDS VERSUS SMALL-SCALE DIESEL GENERATORS	76
MICROGRIDS VERSUS TRADITIONAL ELECTRIFICATION SOLUTION.....	77
PV-BATTERY CONTRIBUTION ANALYSIS	78
IMPACT HOTSPOTS	80
<i>Scenario 1: Electricity Grid Mix for Battery Manufacturing.....</i>	<i>80</i>
<i>Scenario 2: Microgrid End of Life Recycling</i>	<i>81</i>
SCENARIO 3: CHOICE OF PV TECHNOLOGY- CdTe vs. MONO-Si	83
SCENARIO 4: APPLICATION TO LARGER SCALES - POWERHIVE’S PLANNED EXPANSION.....	84
LIMITATIONS	84
SUGGESTIONS FOR FUTURE RESEARCH.....	85
IMPACTS TO STAKEHOLDERS	86
<i>Solar Developers</i>	<i>86</i>
<i>Off-grid communities</i>	<i>87</i>
CONCLUSION.....	89
APPENDIX.....	91
APPENDIX 1: COMPONENT BENCHMARKING.....	91
APPENDIX 2: LIFE CYCLE INVENTORIES.....	93
<i>Section A: PV Modules</i>	<i>93</i>
<i>Section B: Module Balance of Systems (BOS)</i>	<i>104</i>
<i>Section C: Life Cycle Inventory of Li-ion Battery pack and Charge Controller.....</i>	<i>110</i>
<i>Section D: Life Cycle Inventory of Diesel Generator</i>	<i>132</i>
<i>Section E: Life Cycle Inventory of Microgrid Distribution and Security Systems</i>	<i>134</i>
<i>Section F: Life Cycle Inventory of Microgrid End of Life</i>	<i>137</i>
<i>Section G: Life Cycle Inventory of Electricity Grid Mixes</i>	<i>145</i>
APPENDIX 3: BREAKDOWN OF UNCERTAINTIES	148
APPENDIX 4: PV-HYBRID AND PV-DIESEL CONTRIBUTION ANALYSIS	149
WORKS CITED.....	152

List of Figures

Figure 1: Global Map of Rural Electrification Rates by Country (2013).	14
Figure 2: General Setup of a PV Microgrid.	22
Figure 3: General Manufacturing Process for Thin Film CdTe Laminate	28
Figure 4: General Manufacturing Process for Mono-Si PV Panels	29
Figure 5: Manufacturing of a Lithium-ion Battery Pack.....	35
Figure 6: Hourly Electricity Load and Supply Profile for village.	42
Figure 7: Variation of PV Installed Capacity and PV Electricity Use with PV Demand Contribution Threshold.....	43
Figure 7: Comparison of PV Microgrid Life Cycle Impacts.	52
Figure 8: Category Impacts per kWh of PV Microgrids and Home Diesel Gensets.....	55
Figure 9: Category Impacts per kWh of PV Microgrids and Traditional Electrification.	57
Figure 10: Contribution Analysis of PV-Battery Components.	58
Figure 11: Contribution Analysis of Lithium-ion Battery Components.....	59
Figure 12: Contribution Analysis of Battery Cell Components.	60
Figure 13: Battery Electricity Mix and PV-Battery Climate Change Impacts per kWh.	61
Figure 14: Comparison of PV Microgrid, Home Diesel Genset, and Traditional Electrification Impacts.	65
Figure 15: Comparison of PV Microgrid, Home Diesel Genset, and Traditional Electrification Impacts..	66
Figure 16: Comparison of PV Technology Life Cycle Impacts per kWh..	67
Figure 17: CdTe and Mono-Si PV-Battery Impact Comparison per kWh.....	69
Figure 18: Climate Change Comparison per kWh of PV technology in PV Microgrids.	71
Figure 19: Scaling of Life Cycle Climate Change Impacts Based on Total Daily Demand.	72
Figure 20: Contribution of PV-Hybrid Components.	149
Figure 21: Contribution Analysis of Lithium-ion Battery Components.....	150
Figure 22: Contribution Analysis of Battery Cell Components.	151

List of Tables

Table 1: Li-Ion Battery Specifications.	33
Table 2: Operating characteristics of Morningstar TS-MPPT-600v Charge Controller.	38
Table 3: Average Power To Weight Ratio for Diesel Generators	40
Table 4: Recoverable Materials from Li-Ion Battery Recycling.	46
Table 5: Life Cycle Impacts of PV Microgrids per Kwh.	50
Table 6: Category Impacts per kWh of PV-Battery Microgrids and Home Diesel Gensets.	55
Table 7: Category Impacts per kWh of PV-Battery Microgrids and Traditional Electrification.	57
Table 8: Category Impacts per kWh of PV-Battery Microgrids with Different End of Life Scenarios.	62
Table 9: Category Impacts per kWh of PV-Hybrid Microgrids with Different End of Life Scenarios.	63
Table 10: Category Impacts per kWh of PV-Diesel Microgrids with Different End of Life Scenarios.	63
Table 11: Percent Change in Component Impact from Switching CdTe to Mono-Si.	70
Table 12: Savings from 1 MW of PV-Microgrids.	73
Table 13: Benchmarking of Lifecycle GWP Impact for Major Microgrid Components	91

Abstract

Currently over 1.3 billion people worldwide lack access to electricity. Access to a reliable source of electricity creates significant benefits for communities in terms of health, economic development, and quality of life. Smaller versions of electricity grids, known as microgrids, have been developed as an alternative to central grid extension. Using an attributional life cycle assessment, this project evaluated the environmental impacts of PV-Battery, PV-Diesel, and PV-Hybrid microgrids compared to other energy options in Kenya. The systems were sized to meet the total daily electricity demand in a model Kenyan village. Normalized per kWh of electricity production, the PV-Battery system was the least environmentally impactful design in the climate change, particulate matter formation, photochemical oxidant formation, and terrestrial acidification impact categories. When compared to small-scale diesel generators, the PV-Battery system saved 91-98% in the above categories. When compared to the marginal electricity grid in Kenya, the PV-Battery system had savings of 66-81%. Contribution analysis suggested that electricity and primary metal use during component, particularly battery, manufacturing were the largest contributors to overall microgrid impacts. Accordingly, additional savings were seen from changing battery manufacturing location and adding end of life recycling. Overall, this project highlights the potential for PV microgrids to be feasible, adaptable, long term energy access solutions, with health and environmental advantages over the expansion of central grids and existing incumbent energy options.

Executive Summary

Currently over 1.3 billion people (18% of the global population) worldwide lack access to an electrical grid. Without electricity access, rural and suburban communities rely on alternative energy sources such as diesel generators, and kerosene or biomass combustion for cooking and lighting. Unfortunately, the use of these energy sources causes numerous health impacts; combusting kerosene, diesel, and biomass fuels can lead to damages to human and environmental health from accidental ingestion, fires, respiratory illnesses, carcinogenic emissions, and the destruction of local habitat areas.

Access to a reliable source of electricity creates significant benefits for communities in terms of health, economic development, and overall quality of life. Communities receive health benefits through sanitation improvements, clean cooking methods (improved air quality), refrigeration, and propagation of health education through media (i.e. radios and television). Electricity access is also significantly linked to improved productivity, growth, poverty alleviation, household income, employment, new enterprise development, and enterprise productivity. Significant quality of life benefits are also created, most notably in improved educational opportunities like vocational classes and improved educational performance through better teachers and extended study environments.

Traditionally, electrification has been achieved by extending the central electricity grid. However, this extension requires resources for construction, planning and significant funds to be implemented, while incurring negative environmental impacts. Grid extension is also both capital and time intensive, making it a difficult electrification option for many off-grid communities.

An alternative solution is smaller stand-alone versions of electrical grids known as microgrids. Microgrids are an attractive option for off-grid communities because they can be pre-constructed and directly installed in the communities with reduced impacts to the local environment. There are over 3,700 microgrids already in operation around the world with varying energy storage and generation technologies, and a wide range of output capacities. These facilities have proven the potential of microgrids and paved the way for expansion. Studies from the International Energy Agency (IEA) have predicted that over 50% of the connections necessary to electrify the remaining 1.3 billion people in the world will rely on alternative energy sources, such as microgrids.

First Solar, a major solar PV manufacturer, has recognized the potential benefits of PV microgrids and teamed up with Powerhive to install three microgrid pilot projects in Kenya with 10kW, 20kW and 50kW capacities. To expand operations, off-grid developers need to understand the benefits and tradeoffs of microgrid designs. Therefore, the primary objective of this project is to evaluate the life cycle environmental impacts and tradeoffs of three microgrid systems using process based life cycle assessment (LCA) and to determine how these impacts compare to each other, to traditional solutions for electrification, and to small scale energy options in Kenya. In addition to the overall microgrid system design, this project also seeks to

explore the effect of component variation and other factors on the life cycle impacts of these microgrid systems.

This report models the environmental impact of three different solar PV microgrid designs. These include a PV microgrid with a battery backup (PV-battery), a PV and diesel generator microgrid with battery backup (PV-Hybrid), and a PV and diesel generator microgrid with no battery backup (PV-Diesel). All of the microgrids are designed to fully satisfy electricity demand and operate under the same meteorological conditions. The demand and operation conditions are modeled to represent remote communities in Kenya without electricity access.

All of the primary microgrid components including PV modules, batteries, charge controllers, wiring, balance of systems (BOS), diesel generators, and security fencing are included in the relevant microgrid models. For a systematic approach, a model was designed in Excel to properly size each component of the microgrid. Following the sizing, a model for each microgrid component was designed in the LCA software GaBi thinkstep (ts). These models were then combined into separate models for each microgrid system so that life cycle inventories (LCIs) could be developed. Additional models for small-scale diesel generators and the marginal Kenya electricity grid mix were also developed for comparison. An avoided burden approach was utilized when modeling the recycling benefits for each microgrid.

The LCIs for the three microgrids were characterized based on their impact in seven categories from the ReCiPe 2008 characterization factors, namely climate change (kg CO₂e), freshwater eutrophication (kg P eq.), human toxicity (kg 1,4-DB eq.), particulate matter formation (kg PM₁₀ eq.), photochemical oxidant formation (kg NMVOC), terrestrial acidification (kg SO₂ eq.), and terrestrial ecotoxicity (kg 1,4-DB eq.) In the end, the climate change, eutrophication, particulate matter, photochemical oxidant formation, and terrestrial acidification differences between the three microgrid systems were likely to be significant (**Figure 8**). Due to the magnitude of differences and confidence in the categories, the analysis primarily focused on the climate change, particulate matter formation, photochemical oxidant formation, and terrestrial acidification impacts.

Category impacts of the systems were compared to those of a home diesel generator and the marginal electricity grid mix in Kenya (excluding the impact from grid extension) to represent comparisons to small scale energy options and the traditional solution for electrification in Kenya. The analysis suggests that PV microgrids, particularly PV-Battery microgrids, have substantial savings (31-98%) in the climate change, particulate matter formation, photochemical oxidant formation, and terrestrial acidification categories compared to home diesel gensets (**Table 6**). Compared to traditional electrification, the PV-Battery system saves 66-81% per kWh depending on the category, whereas the PV-Hybrid system saves 22-54% in the climate change, particulate matter formation, and terrestrial acidification categories but actually appears to have 34% higher impacts in the photochemical oxidant formation category. Finally, the PV-Diesel appears to have higher impacts per kWh in all four categories compared to the marginal grid mix (**Table 7**).

Looking closer at the PV-Battery system, the majority (72-80%) of the impacts came from the lithium-ion battery (**Figure 11**). In climate change, 50% of the total battery impact and 36% of the total microgrid impact comes from the electricity used in the manufacturing of the battery cell. The battery grid mix also contributed 11-16% of the total impact in the other categories (**Figure 12**). With this in mind, shifting the battery production from the baseline European grid mix to a Chinese grid mix increases the total microgrid climate change impact by over 35%, whereas shifting from a generalized European grid to the grid in France or Switzerland decreases overall impact 18-27% (**Figure 14**).

For the other categories, 47-67% of the total battery impact and 34-53% of the total microgrid impact comes from the cathode and anode production in the battery cell specifically the utilization of copper and other metals like cobalt and manganese. An analysis of elementary flows suggested that these metals were major contributors to the other impact categories as well. With such large impact from metal use, a scenario was run to test the impact of end of life recycling for microgrid components compared to the baseline landfilling process. The PV-Battery and PV-Hybrid systems saw impact savings from recycling on the order of 7-68% largely because of the avoided burden of primary material use. The PV-Diesel system had much smaller savings because the majority of its impacts stemmed from the burning of diesel rather than the use of metals (**Table 8**, **Table 9**, and **Table 10**). Adding recycling at the end of life enhances the PV-Battery benefits and minimizes its potential tradeoffs compared to other microgrid systems, home diesel gensets, and traditional electrification.

Another scenario was run to test the impact of substituting Mono-Si PV panels instead of the baseline CdTe PV modules. Across the seven impact categories, there was only a significant difference in climate change impact where the Mono-Si impact was 19% greater than the CdTe impact (**Figure 18**).

Finally, a scenario was run to apply the savings seen in our 6.31 kW system to a larger application of PV microgrids, namely Powerhive's announcement to install a combined 1 MW installed capacity of PV microgrids in Western Kenya. The savings from this analysis suggested that, when compared to home diesel gensets, developing PV-Battery microgrids to meet this scale could avoid over 65 million kg CO₂e, over 400,000 kg of PM₁₀e, over 1.2 million kg NMVOC, and over 700,000 kg SO₂e over the 25 year lifetime of the microgrids used in this analysis. Compared to the marginal grid mix in Kenya, this model suggests savings of over 23 million kg CO₂e, over 66,000 kg PM₁₀e, over 96,000 kg NMVOC, and over 127,000 kg SO₂e (**Table 12**).

The results of this analysis highlight several major conclusions regarding the development of solar microgrids for energy access solutions. First, compared to the home diesel and traditional electrification solutions, PV-Battery and, to a lesser extent, PV-Hybrid microgrids have significantly less climate change, particulate matter formation, photochemical oxidant formation, and terrestrial acidification impacts. This highlights an important conclusion for solar developers that in terms of the climate change, particulate matter formation, photochemical oxidant formation, and terrestrial acidification impacts, lithium-ion batteries are a better backup option for PV microgrids than diesel generators are in places with high insolation and

low demand like Kenya. This distinction is particularly important for particulate matter formation, photochemical oxidant formation, and terrestrial acidification because of the local nature of the effects. While the PV-Battery design does affect these impact categories, the majority of these impacts happen during the manufacturing stage, rather than during the use phase on site in off-grid communities.

This analysis also identified major hotspots for solar microgrid developers to improve the overall life cycle impacts of PV microgrids. The most notable opportunity is in battery manufacturing. The battery grid mix scenario suggests that the single biggest way to reduce the overall climate change impact of a PV-Battery microgrid is to shift battery production to nations or regions that utilize high levels of renewable energy. The contribution and elementary flow analyses also highlighted the importance of takeback and recycling programs at the end of project life for avoiding the impact of primary metal use in microgrid manufacturing.

While this analysis provides an in depth exploration into the environmental impacts of various scenarios for different microgrids, there were however some limitations associated with the modeled impacts. Most notably this analysis didn't model the socioeconomic considerations of microgrids (i.e. life cycle cost), varying battery chemistries (i.e. lead acid batteries), or the impacts from the inevitable increase in electricity demand. All of these considerations present opportunities for future research.

Despite the limitations, this project advances photovoltaic life cycle assessment research by modeling three complete PV microgrid systems. By performing a system wide comparative assessment of three different PV microgrid designs, and evaluating them in comparison to small-scale diesel generators and the expansion of a traditional grid, this project is able to provide a comprehensive comparison of the environmental impacts across viable electrification options. The analysis of multiple design options and real life development scenarios can help microgrid developers better match solutions to the specific needs and priorities of the off-grid communities they plan to serve. With proper information regarding the environmental impacts of PV microgrids, all stakeholders involved in electrification projects can be confident they are making the most informed and beneficial decisions. Whether it is a decision by citizens and developers on the ground, or decisions by international policy makers trying to meet sustainable development goals, the evaluation of tradeoffs in this analysis can serve as the basis of an informed discussion. More than anything else, this project highlights the potential for PV microgrids to be feasible, adaptable, long term energy access solutions, with health and environmental advantages over the expansion of central grids and existing incumbent energy options.

Background

Access to a reliable energy source is a basic human need that is critical for the development of robust economies (Williams et al., 2015), modern healthcare, and proper sanitation (Mills, 2014). In spite of this, approximately 1.3 billion people worldwide (18% of the global population) lack access to an electrical grid, a baseline commodity present in most developed nations (Mills, 2016) (Williams et al., 2015) (Mills & Jacobson, 2007). More than 95% of people living without access to electricity reside in Asian and sub-Saharan African nations, specifically those that are still in the process of developing (**Figure 1**) (International Energy Agency, 2015) (United Nations Development Programme, 2011). In Africa alone, there are over 600 million people without access to electricity, fostering an environment that hinders economic development and effective healthcare (**Figure 1**) (International Energy Agency, 2015). This population of off-grid communities is projected to increase considerably in the next 30 years, further exacerbating the issue (Lighting Africa, 2011). Within Africa, one of the developing nations of interest is Kenya, which supports less than 10% of its rural population and only 23% of its entire population with access to an electrical grid (World Bank, 2010).

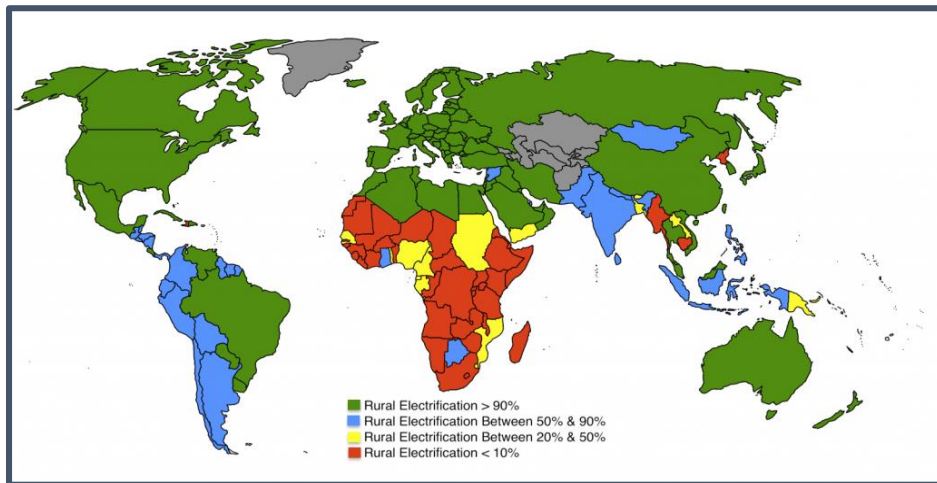


Figure 1: Global Map of Rural Electrification Rates by Country (2013). Information was not available for those countries colored grey. Map taken from (Miret, 2015).

Without access to an electrical grid, rural and suburban communities alike have been forced to use alternative energy sources to sustain their demand for electricity. Common sources of energy in rural communities include diesel combustion in generators to produce electricity, and kerosene and biomass combustion for cooking and lighting (Mills & Jacobson, 2007) (Rao, 2012) (Barnes & Floor, 1996). An unfortunate consequence of these alternatives is that they are inherently hazardous to human health when burned (especially in closed spaces). These alternatives are also more costly, and are a less effective and reliable source of lighting. Research done by Lighting Africa (2011) showed that extremely poor communities spend approximately 10-15% of their household income on lighting alone (Lighting Africa, 2011).

Health effects of the status quo energy sources are numerous. Kerosene use has caused documented injuries in rural South African communities due to accidental ingestion (3.6% of all households), accidental fires (200,000 citizens affected annually), and chemically induced pneumonia (Mills, 2012). These effects are intensified when biomass or kerosene is burned inside, where the chance of fire is increased and quantities of hazardous particles are concentrated (Mills, 2012) (Barnes & Floor, 1996). Diesel generators lack many of the emission controls present in industrial combustion mechanisms, resulting in increased local toxic air emissions (including particulate matter) and greenhouse gas (GHG) emissions to the environment. Burning of biomass incentivizes the destruction of local natural habitats and the release of more potent hazardous emissions. Biomass combustion results in the release of particulates and carcinogens that cause adverse effects on the human body similar to that of tobacco smoking (de Koning, Smith, & Last, 1985). In Kenya, indoor biomass combustion has precipitated acute respiratory infections that can lead to disease and potentially mortality (Ezzati & Kammen, 2001).

In order to offset the local and global health impacts of these traditional sources of energy, it is essential that the benefits of electrification be propagated to influence support of clean alternative sources of energy. Access to a reliable source of electricity creates significant benefits for communities in terms of human health, economic development, and overall quality of life. Access to electricity enables substantial improvements in community health through the sanitation improvements, access to clean water, and a host of other benefits (United Nations Development Programme, 2011). Overall community healthcare systems are significantly improved with access to electricity (World Bank, 2008); case studies have shown electrified health facilities receive and treat more than double the patients when compared with non-electrified areas (United Nations Development Programme, 2011). Electrification not only benefits institutional health care systems, but also improves health within each home. Traditional cooking methods (kerosene and biomass) can also be displaced by electricity access, which can lead to significant reductions in mortality from a reduction in indoor air pollution and accidental fire (Mills, 2012) (Mills, 2016) (World Bank, 2008). Further health benefits can be achieved through improved nutrition from access to refrigeration (World Bank, 2008). Additionally, critical information and communication tools such as radios, television, the Internet, and cell phones become available to electrified communities. Access to these devices help to fight and respond to pandemics such as HIV/AIDS and malaria, and promote improved contraceptive use through education (Kirubi et al., 2009) (Grimm, Sparrow, & Tasciotti, 2015).

For off-grid communities, electricity access is also significantly linked to economic development (Attigah & Mayer-Tasch, 2013) (Kanagawa & Nakata, 2008). A review of literature conducted by Attigah and Mayer-Tasch found that electricity access improved productivity, growth, poverty alleviation, household income, employment, new enterprise development, and enterprise productivity (Attigah & Mayer-Tasch, 2013). A World Bank study on the benefits of rural electrification highlighted an increase in the profitability of both existing and electricity enabled home businesses (World Bank, 2008). Specific to Kenya, a study of microgrid electrification in the village of Mpeketoni in southeastern Kenya found that electrification provided a suite of benefits for small & medium enterprises (SMEs) in agriculture, communication services, and

small-scale manufacturing. The study found that electricity access, particularly access to electric tools and equipment, increases SMEs' productivity per worker by 100-200% and gross revenues by 20-125%, depending on the product (Kirubi et al., 2009).

Significant quality of life benefits are also created for communities through electricity access, most notably in improved educational opportunities and performance. A study of solar electrification in Kenya demonstrated that lighting provides for longer and improved study environments, which significantly contributed to the overall quality of education for children in rural Kenya (Jacobson, 2007) (Kirubi et al., 2009). A World Bank study in the Philippines suggests that, all else being equal, children with access to electricity in their homes gained about two years of educational achievement compared to children from homes without electricity access (World Bank (ESMAP), 2003). Electricity also improves educational opportunities by allowing a wider range of vocational classes that depend on electronic tools such as information technology, carpentry, engineering, metal works, etc. (Kirubi et al., 2009). In addition to improved study environments, educational attainment, and opportunities, electricity also attracts better teachers and professionals. For example, a World Bank study in Ghana found that a lack of electricity access made it difficult for remote facilities (i.e. schools) to attract and retain professional workers (World Bank (IEG), 2004). Better teachers and professionals logically lead to better educational outcomes.

In order to gain a better understanding of why not all communities have access to electricity, it is beneficial to examine how communities become electrified. Traditionally, electrification has been achieved by extending the existing grid to communities without access. Extending the existing grid requires time and resource intensive construction and substantial coordination due to the vast amount of external infrastructure required for distribution and transmission. Extension of the existing grid also requires an increase in generation capacity to meet the increase in demand. Typically, grid extensions are composed of, but not limited to, additional substations, transmission networks, roads, power lines (high and medium voltage), transformers, and meters. Depending on the distance and quantity of electricity being transmitted, grid extension projects can cost hundreds of thousands of dollars (Deichmann et al., 2011).

Extension of transmission and distribution, coupled with generation stations, also account for significant environmental impacts (Weber et al., 2010). Multiple life cycle assessment (LCA) studies have been done to estimate the extent of the environmental impacts of grid expansion, and most studies cited non-negligible carbon dioxide (CO₂) impacts from generation and sulfur oxides (SO_x), nitrogen oxides (NO_x), and particulate matter (PM) impacts from the raw energy extraction (Lee, Lee, & Hur, 2004) (Weber et al., 2010) (Widiyanto et al., 2003) (Turconi et al., 2014) (Jorge, Hawkins, & Hertwich, 2012). Two principal barriers to grid extension as a solution to the lack of energy access are the non-trivial distance between existing grid production and rural off-grid communities, as well as insufficient funds for expansion. There are many rural communities in Kenya that reside long distances from the established grid. Even if they were located next to the grid, the capital to fund the initial cost of connection is nonexistent (Lighting

Africa, 2011). Due to these issues, grid extension is not currently a viable option to electrify rural communities in Africa (Schnitzer, et al., 2014).

Grid extension and traditional sources of energy cannot reasonably supply the demand in a socially and environmentally beneficial fashion to rural communities, however there are new renewable technologies that can. A microgrid is a smaller, standalone version of a traditional grid comprised of an electricity generation source and a transmission system, which can operate autonomously from the traditional grid (Schnitzer, et al., 2014). Microgrids are typically powered through renewable energy sources such as solar photovoltaic (PV), wind, or hydro. The inherent intermittency of renewable resources is often offset by an energy storage system or diesel generator (Wang, Palazoglu, & El-Farra, 2015). A basic microgrid system consists of the energy generation component (e.g. PV modules), an energy back up system (e.g. battery bank or diesel generator), and the other necessary electrical components, including transmission lines, a charge controller, and the balance of systems (BOS). When implemented in small villages, microgrids are intended to power small electronic devices, charging of cell phones, and simple lighting (Schnitzer, et al., 2014).

Compared to traditional grid extension, microgrids have the potential to be cheaper, faster, and more effective solutions for rural electrification (Williams et al., 2015). Because their components can be manufactured and prepared before implementation, on site installation is relatively quick with minimal land degradation. Microgrid implementation in small rural villages can provide communities with a sense of ownership and pride, reducing chances of theft and increasing the probability of long-term virtuous cycles (Schnitzer, et al., 2014). Due to the ability to provide access to sustainable clean energy in remote towns, microgrids are an attractive solution to the lack of electricity access, especially in developing nations. Studies from the International Energy Agency (IEA) have predicted that over 50% of the connections necessary to electrify the remaining 1.3 billion people in the world will rely on alternative energy sources, such as microgrids (Schnitzer, et al., 2014).

Successful installations of diverse microgrids have percolated throughout the globe, totaling over 3,793 MW of installed capacity, of which 754 MW is generated in remote systems (Navigant Consulting, 2013). Projects span from India and Malaysian Borneo to African locations such as Guinea-Bissau, and extend to remote fingers of the globe (Arsenio et al., 2014) (Schnitzer, et al., 2014). Microgrids are often built to power small off-grid villages (1-10 kWh), though larger installations (e.g. 312 kWp) for whole communities have been successfully implemented as well (Arsenio et al., 2014). These microgrids are often equipped with different types of energy storage systems. Technologies currently in use include pumped hydro storage, battery storage, compressed air energy storage, hydrogen based energy storage, flywheel storage, superconducting magnetic storage, and supercapacitor energy storage (Palanisamy & Fathima, 2015). In addition to storage variation, systems often are comprised of multiple power generating sources including, but not limited to, hydro, PV, wind, diesel generators, and biogas. One of the larger microgrid developers is the Chhattisgarh Renewable Energy Development Agency (CREDA) based in India, which has over 575 microgrids implemented and in use.

National utilities such as Electricité d'Haiti have fewer microgrids installed, but more than double CREDA's installed capacity (Schnitzer, et al., 2014).

Government and nonprofit agencies such as CREDA and Electricité d'Haiti have incentive to produce microgrids for their welfare benefits; however for-profit corporations in the United States have found a stake in global microgrid deployment as well. First Solar, one of the largest manufacturers of thin film cadmium telluride (CdTe) solar modules, has teamed up with Powerhive, a technology venture focused on developing energy access solutions, to launch pilot scale PV microgrids in Kenya (First Solar, 2014). These pilot projects involve the installation of 10 kW, 20 kW and 50 kW sets of PV microgrids. Installation of PV microgrids has already taken place in three villages in East Africa, and First Solar has been looking to expand the program to an additional 100 villages in order to assess the scalability of these projects (First Solar, 2014). Eventually, First Solar would like to expand PV microgrid solutions to new regions, communities, and scales. In doing this they are looking to understand the benefits and tradeoffs of different technologies, components, and system designs.

Project Objectives

The primary objective of this project is to evaluate the life cycle environmental impacts and tradeoffs of three microgrid systems using process based life cycle assessment (LCA) and to determine how these impacts compare to each other, to traditional solutions for electrification, and to small scale energy options in Kenya. The three microgrid systems considered are:

- PV-Battery
- PV-Diesel
- PV-Battery-Diesel (PV-Hybrid)

The primary difference between these system designs is the technology employed to back up or complement the electricity generation from the solar modules. Either a battery bank or a diesel generator are used, or a combination of the two in the case of the PV-Hybrid system, to complement the PV electricity generation. In addition to the overall microgrid system design, this project also seeks to explore the impact of other factors on the overall design and life cycle impacts of these microgrid systems. These factors include:

- PV technology
- Manufacturing locations
- End of life (EOL) recycling

Project Significance

This project builds upon existing knowledge to better advise the expansion and success of future energy access projects, particularly the implementation of PV microgrid solutions. By identifying and evaluating the life cycle tradeoffs of different solar microgrid designs, this project can help microgrid developers to design better microgrid solutions that match the specific characteristics and priorities of the off-grid communities and regions they are operating in. In advancing the knowledge base of microgrid impacts and helping developers expand PV microgrids to new communities and regions, this project aims to help expand access to electricity in developing nations. This, as described above, can lead to the achievement of significant global development outcomes such as reduced mortality, local economic development, improved quality of life, and significant environmental improvements such as reduced GHG emissions (Smith, et al., 2015).

This project also advances life cycle assessment research applications. As of the time of this report, other than a single study on the life cycle impacts of a diesel-PV-Wind hybrid microgrid on Koh Jig, an island near Thailand, most of the life cycle assessment (LCA) research at this point has been focused on components of PV microgrids (i.e. modules and batteries) in isolation or in other applications (Smith, et al., 2015). This analysis is novel in that it uses LCA research and models to assess a variety of complete and functioning microgrid options for on the ground developers, providing a much more thorough set of results for informed implementation decisions.

For solar PV modules, one of the most extensive LCA efforts has been the ongoing harmonization study conducted by the National Renewable Energy Laboratory (NREL). This study has worked to review and screen over 400 published estimates for life cycle GHG impacts of PV technologies. From the screening process, thirteen studies with forty-one estimates were reported for mono-Si panels and thirteen studies with twenty-four estimates were reported for thin film CdTe laminates (National Renewable Energy Laboratory, 2016) (Kim et al., 2012) (Hsu, et al., 2012). The International Energy Agency, through its Task 12 research project, has also worked extensively to model life cycle considerations in PV technology, particularly the environmental health and safety aspects of material choices and manufacturing (Frischknecht, et al., 2015). In addition to this, our project client, First Solar, has also conducted several LCAs of the manufacturing and application of CdTe laminate (Sinha, 2013) (Sinha, Cossette, & Menard, 2012) (Sinha & de Wild-Scholten, 2012). Even though these studies were mostly focused on utility scale, rooftop, and other grid connected applications of PV technology, the estimates provide a good benchmark for the microgrid applications modeled in this analysis.

Energy storage systems, specifically batteries in battery electric vehicles (BEVs) have similarly been a recent focus in LCA research. The Argonne National Lab (2010) has compiled a comprehensive literature review and aggregation of previously published battery LCAs, the majority of which were about lead-acid (PbA), nickel metal hydride (NiMH), and lithium-ion (Li-ion) battery banks (Sullivan & Gaines, 2010). In their study, Argonne National Lab noted that

there was information missing for the energy requirements within the manufacturing process for lithium-ion batteries. Similarly, Sullivan and Gaines (2012) published a study examining the current information available for the cradle to gate environmental assessments of five battery chemistries (PbA, NiCd, NiMh, Na/S and Li-ion) (Sullivan & Gaines, 2012). Various other published LCAs, whose results varied by orders of magnitude, were used as benchmarking samples for our model (Notter, et al., 2010) (Rydh & Sanden, 2005) (Ellingsen, et al., 2014) (Zackrisson, Avellan, & Orlenius, 2010) (Majeau-Bettez, Hawkins, & Stromman, 2011). Only few lithium-ion LCAs provided detailed information regarding the specific material components (positive active material) and electrical specifications of the batteries modeled (Ellingsen, et al., 2014).

By building the existing knowledge base to help expand energy access projects and extending the utilization of LCA to new applications and arenas, this project has the potential to significantly impact both development outcomes and future research in life cycle assessment. This research also serves as a first step toward improving the overall impact of microgrids by identifying impact hotspots and opportunities in the manufacturing and procurement of microgrid components.

Methodology

General Methodology

Life cycle assessment (LCA) involves a systematic analysis of the environmental impact of a product during each phase from resource extraction to its end of life (Rebitzer, et al., 2004). ISO 14040:2006 lays out the definition, principles, and the framework for the use of LCA (International Organization for Standardization, 2010). However, each LCA project is unique, and demands careful application of the methodology.

This project performs a mostly attributional LCA, wherein the primary aim is to assess and evaluate the environmental life cycle impacts of solar photovoltaic (PV) microgrids in remote off-grid communities of developing countries. However it also takes, to some extent, a consequential outlook while analyzing the results in later sections. This project considers multiple configurations of PV microgrids to explore and compare different scenarios including a comparison with small scale energy and traditional electrification solutions in Kenya. In each configuration, manufacturing, use, and end of life (EOL) phases of each component within the microgrid systems have been analyzed.

Three different types of microgrids have been modeled (**Figure 2**):

- (a) **PV-Battery:** a PV microgrid system with battery backup
- (b) **PV-Diesel:** a PV microgrid system with a diesel generator back-up
- (c) **PV-Hybrid:** a PV microgrid system with both battery and diesel generator backup

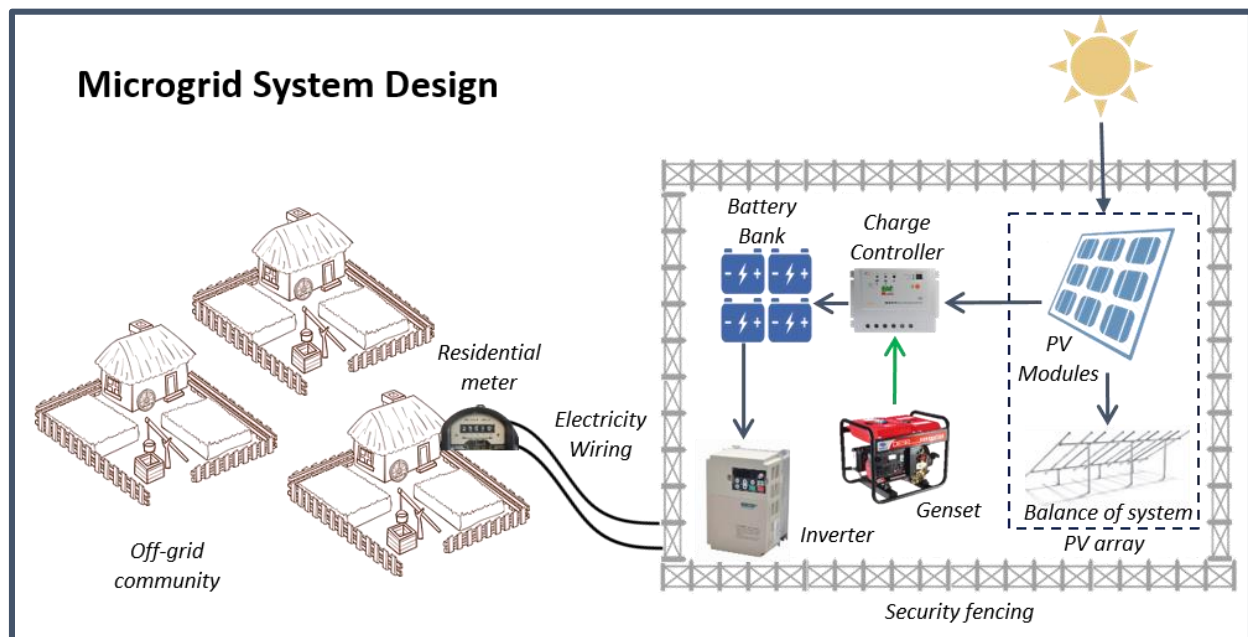


Figure 2: General Setup of a PV Microgrid.

Each system has been modeled to include all necessary components that are part of real world installations. All the systems have been designed to meet the same demand and therefore, have the same functional output. Specifically, all the designed microgrids fully meet the demand of the target community and operate under the same meteorological conditions that persist in the region. Thus, 1 kWh of available electricity produced over the lifetime of the system is chosen to be the functional unit for calculating the impacts. This enables a justified, parallel comparison of the microgrid lifetime impacts across the three types of microgrids as well as with other energy generation options.

For PV modules, two different technologies have been considered: a *mono crystalline silicon (mono-Si)* module and a thin film *cadmium telluride (CdTe)* module. Both types have different manufacturing processes, characteristics and operating efficiency.

The CdTe PV modules have been modeled to estimate First Solar Series 4 FS4110-2 PV modules based on previous module generations and discussions with manufactures (First Solar, 2015). The mono-Si PV modules have been modeled to reflect First Solar Tetra Sun PV modules (First Solar, 2015). Other components in the microgrid systems have been modeled either based on a single existing model available on the market or based on an average of existing models and technology available on the market. The selected models are believed to be suitably representative of all the models in the same category. The life cycle inventory (LCI) data for each of the components were developed using a combination of publicly available data, secondary sources/literature, and conversations with manufacturers. In the light of a lack of data, modifications have been made and supplemented with approximate data when required. These modifications are described in further detail in the individual component sections as well as in the data quality and uncertainty section later in the report.

The first step in system sizing was to make a preliminary assumption of a specific village size. Next, the meteorological conditions, namely the average daily solar insolation, were incorporated. The village electricity demand (in kWh) and the average daily solar insolation (in kWh/m²/day) form the foundation for the modeling of the three microgrid systems. These input parameters are common to all the microgrid models. Any change in the value of these parameters propagates through all the microgrid models. The village electricity demand input itself contains multiple independent parameters including daily demand per household (kWh/day), people per household, and the total population of the village. Each of these values have been populated either directly using available secondary data or through assumptions based on secondary data. For a given average daily demand (kWh/day), the peak load (kW) was estimated by multiplying the average load by a factor of 2.69. This factor was calculated based on the average and peak demand of the village of Marsabit in Northern Kenya in a 2010 report by the Kenya Power and Lighting Company (Mwangangi, et al., 2010). Specific values for the baseline parameters are included later in the methodology.

The data for insolation and other meteorological parameters have been retrieved from the NASA Surface Meteorology and Solar Energy (NASA SSE) database for the specific latitude of 1.2667 degrees South and longitude of 36.8 degrees East, representing Nairobi, Kenya (NASA,

2016). The NASA SSE dataset provides the yearly and monthly averaged meteorological data based on twenty two years of measured data. Therefore, the values of meteorological parameters have been considered to be very robust and reliable for sizing of microgrids.

Baseline Parameters and Scenario Analysis

By changing the model input parameters individually, multiple scenarios were created and explored. The impacts of different scenarios were compared with the baseline model in order to understand the advantages and disadvantages of the specific system modification. The values of the shared model input parameters for the baseline model of each microgrid type were as follows:

- Village population: 100
- Daily demand per household: 1.545 kWh/day (Zeyringer, et al., 2015)
- Number of people per household: 5.7 (Zeyringer, et al., 2015)
- Total daily demand: 27.108 kWh/day
- Average daily solar insolation: 5.925 kWh/m²/day
- PV module type: CdTe
- End of life scenario: Landfill

The scenarios analyzed include changes in manufacturing practices, different PV technologies, and end of life recycling of microgrid components. Lastly, the potential advantages of large scale deployment of the baseline PV-Battery microgrids were also assessed.

Life Cycle Modeling

For the life cycle modeling, this project used the GaBi ts software developed by Thinkstep along with the Ecoinvent database v2.2 already built into GaBi ts. In order to systematically model the microgrids in GaBi, this project developed complete microgrid systems populated with fixed and variable input parameters, in Excel. Village demand, meteorological data, and the technical specifications of the respective components constitute the bulk of the independent parameters used. The Excel model has been used to calculate the size and number of each component required over the lifetime of the system based on these independent parameters.

For each system, this analysis selected and modelled the major microgrid components. For the PV-Battery system, these components include PV modules, balance of systems (BOS), charge controllers, batteries, distribution systems, and a certain land area for the installation of the system and security fencing. The PV-Hybrid system utilized all of the same components, with some components sized differently, along with the addition of diesel generators. The PV-Diesel system contained a diesel generator with no charge controllers or batteries.

This step was followed by modeling the capacity/size of each of these components for each microgrid system type. The calculation of the size/capacity and the number of the components required in each of the three microgrid types were independent from each other except for the common input parameters. The Excel model was built to be flexible, meaning any changes in the common input parameters are propagated throughout each of the three microgrid systems. Each microgrid model was fundamentally designed to meet an equal demand under the same meteorological conditions. The following sections describe the general assumptions and decisions made while modeling each of the three microgrids. The detailed sizing methodology for each component is provided in their respective sections later in the report.

PV-Battery system

The PV-Battery system has a single electricity generation source, PV modules, which have been sized to completely meet the average electricity demand. In order to meet the peak load, a battery backup was included in the microgrid with an autonomy period of 24 hours. Therefore, the average daily demand was used to model the required PV capacity. A derate factor of 0.782 was calculated to account for losses in the electricity production from PV arrays. This factor combines the efficiency of all subsequent components in the system, namely the charge controller and inverters, which can cause loss of power. The daily electricity demand of the village divided by the derate factor equals the total required installed capacity of PV array in kWh/day. The total number of modules to be installed was then calculated using the area of each module and the total required installed capacity of PV arrays. Average energy produced per module has been calculated based on the average yearly solar insolation (kWh/m²/day) for Kenya and the average lifetime efficiency (%) of the PV module.

PV-Diesel system

The PV-Diesel system has been modeled taking into consideration three main factors: the hourly variability in solar insolation, the average daily electricity demand, and the peak electricity demand. The solar insolation variability data was collected from the NASA SSE database in the form of three hourly average insolation values. Hourly electricity demand was calculated based on the 24-hour load profile of the village of Marsabit in Northern Kenya (Lukuyu & Cardell, 2014). By using the above data, it was possible to calculate the contribution of the diesel generator in meeting total daily demand. Details of the system sizing calculations have been elaborated in the diesel generator section of this report.

PV-Hybrid system

The PV-Hybrid system has been modeled similarly to the PV-battery system with one additional factor being considered, the variability in daily solar insolation. Solar insolation variability data was collected from the NASA SSE database in the form of number of monthly equivalent no-sun days or black days. This factor helped to calculate the electricity deficit in the PV-Battery system that can be met by the diesel generator, further helping to determine the total operational

hours for the generator. Details of the system sizing calculations have been elaborated in the diesel generator section of this report.

GaBi modeling

The GaBi ts software package provides a variety of industrial processes which represent a quantified environmental impact associated with a per functional unit quantity of the product/material output. The database covers most of the major industrial sectors and processes that exist in the real world. The methodology and assumptions involved in the data collection of all of the processes are documented in the software to help the users choose the processes most suitable for their LCA modeling purposes.

GaBi ts has a built-in feature called “parameters”, which allows the user to build very flexible models. Parameters are like variables in a model, which also have a value corresponding to them. The value of a parameter can either be independent or calculated based off of another set of parameters. The parameters can be used to set the amount of the various input and output elementary and intermediate flows in a process. GaBi ts also has another object type called “plans”. A plan is a collection of one or more processes/plans connected to each other, representing the combined impact of all of those processes/plans.

For each component, thorough research was conducted to collect the best available life cycle inventory (LCI) data. More details about the LCI data and the data sources are presented in the respective component methodologies below. Based on the already available and collected LCI data, an overall plan representing the impact per unit of component for each component in the microgrids was built. Most of the overall component plans contained multiple processes and plans well connected through parameters. For each component, the specifications of its particular model used were coded into the parameters of the overall component plan. This enabled the modeling of the lifecycle impact for the specific components used in the microgrids. While developing the model for each component, multiple iterations of quality assurance (QA), quality control (QC), and benchmarking were conducted with other secondary sources to verify the data and model quality (**Appendix 1**).

Additionally, for all of the major components (batteries, charge controller, diesel generator, PV modules, and BOS) two different end of life (EOL) models were built. One represented a general landfill process while the other represented a recycling process. In each system, the avoided burden approach of recycling was used to model the impact of recycling. As a result, all of the component manufacturing plans are modeled with only primary materials as their input. In the recycling plan, the old scrap produced during manufacturing is recycled into secondary material, which in turn avoids an equivalent amount of the primary material originally used in manufacturing.

A GaBi plan was created for each type of microgrid design, based on the Excel model described above. Each GaBi system plan included all the relevant components and parameters. The intermediate flows in the models were determined by the parameters calculated in the same

manner as the Excel model. Thus all of our GaBi microgrid models reflect the component sizes in our Excel model giving an equal, fixed value for all the independent parameters in both programs. Ultimately, the model gives life cycle impacts of the microgrid per kWh of electricity produced over the lifetime of the microgrid.

Impact Assessment

LCA utilizes characterization factors to translate life cycle inventories into environmental impacts across a range of impact categories. ReCiPe 1.08 Hierarchical indicators were selected because they are commonly used in other papers and they represent a scientific consensus based perspective. ReCiPe indicators classify the impacts into 18 midpoint and 3 end point indicators. For the impact characterization in this analysis, seven midpoint indicator categories were chosen to illustrate the tradeoffs of microgrid system impacts (Goedkoop et al., 2009):

1. **Climate change (kg CO₂e)** - Characterizes the potential for a given substance to impact global warming also known as a substances global warming potential (GWP). Measurement is in kilograms of CO₂ equivalent (kg CO₂e).
2. **Freshwater eutrophication (kg P eq.)**- Characterizes the potential of a substance to impact eutrophication in freshwater systems. Measurement is in kilograms of phosphorous equivalent (kg P eq.).
3. **Human toxicity (kg 1,4-DB eq.)**- Characterizes the potential toxicity to humans from a given substance. Measurement is in kg of 1,4 dichlorobenzene equivalent (kg 1,4-DB eq.).
4. **Particulate matter formation (kg PM₁₀ eq.)**- Characterizes how a given substance relates to the formation of particulate matter in the air. Measurement is in kilograms of 10-micrometer particulate matter equivalent (kg PM₁₀ eq.).
5. **Photochemical oxidant formation (kg NMVOC)** - Characterizes how a given substance relates to the formation of photochemical oxidants in the air. Measurement is in kilograms of non-methane volatile organic compounds (kg NMVOC).
6. **Terrestrial acidification (kg SO₂ eq.)**- Characterizes the potential of a substance to cause acidification to terrestrial ecosystems. Measurement is in kilograms of sulfur dioxide (kg SO₂ eq.).
7. **Terrestrial ecotoxicity (kg 1,4-DB eq.)**- Characterizes the potential toxicity of a substance to ecosystems and the environment. Measurement is in kilograms of 1,4 dichlorobenzene equivalent (kg 1,4-DB eq.).

While there are other impact categories included in ReCiPe and other sets of factors, these impact categories were chosen because they represent an important mix of impacts to climate, air, water, ecosystems, and human health.

PV Module Methodology

PV Panels

This analysis utilized two different solar technologies in the construction and design of solar microgrids: cadmium telluride (CdTe) and monocrystalline silicon (mono-Si).

Cadmium Telluride (CdTe)

CdTe solar cells, known as a CdTe laminate, are thin film solar cells made by depositing thin layers of photovoltaic (PV) cadmium telluride onto a flat substrate such as solar glass or metal sheets through chemical sheeting processes known as sputtering and physical vapor deposition (Figure 3) (Kim et al., 2014).

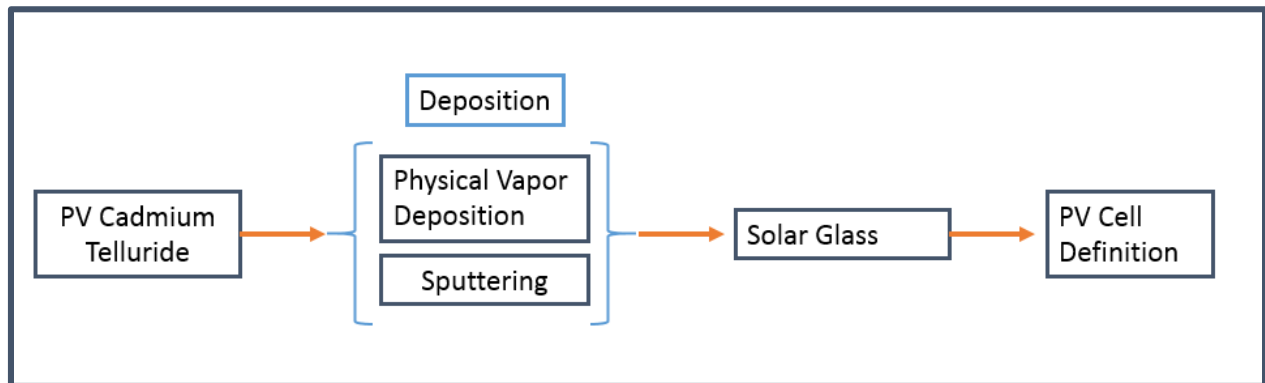


Figure 3: General Manufacturing Process for Thin Film CdTe Laminate

This analysis worked to model a CdTe laminate module based off of First Solar’s Series 4v2 CdTe PV module. To do this, LCI data from sections 5.1.4-5.1.9 of the International Energy Agency’s PVPS Task 12 LCI report for an older CdTe module were adapted to estimate the newer version of the CdTe modules (Frischknecht, et al., 2015). A detailed LCI of the CdTe laminate cannot be published in this report because it contains some proprietary information. Based off of the specifications sheet for First Solar’s Series 4v2, the CdTe module was assumed to have the following characteristics (First Solar, 2015):

- Module area: 0.72 m²
- Nameplate efficiency: 16.3%
- Nominal power output: 0.118 kWp
- Open circuit voltage: 88.2 Voc
- Short circuit current: 1.79 Amps

The specification sheet for the First Solar Series 4 module lists a 25-year warranty with a guaranteed power output of 97% in the first year. With this information, this analysis assumed a 25-year lifetime for the CdTe laminate (First Solar, 2015). The power output of the laminate

was also assumed to decline linearly over the lifetime (0.5% per year) (Strevel et al., 2013). Given this, the lifetime average power output for the CdTe laminate was calculated at 0.104 kW and the average lifetime module efficiency was calculated at 14.4%.

Mono Crystalline Silicon

Monocrystalline silicon (mono-Si) solar panels are among the most common solar cells in the PV industry. These panels are thicker than their thin-film counterparts, but tend to be more efficient. In general, the manufacturing of mono-Si panels occurs in four stages: 1) Silicon crystal forming and processing; 2) mono-Si wafer production and cutting; 3) PV cell manufacturing 4) PV panel production (**Figure 4**).

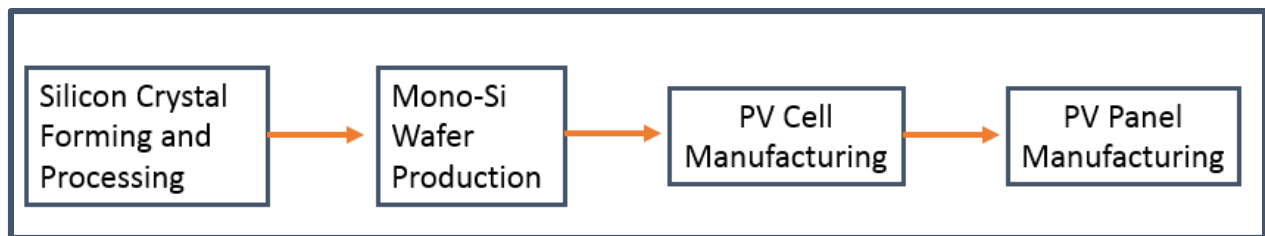


Figure 4: General Manufacturing Process for Mono-Si PV Panels

The mono-Si panel modeled in this analysis primarily utilized LCI data from sections 5.1.4-5.1.9 of the International Energy Agency’s PVPS Task 12 LCI report (Frischknecht, et al., 2015). The processes and materials were altered slightly to try and match LCI estimates for the LCI of First Solar’s Tetra Sun mono-Si module (Sinha & de Wild-Scholten, 2015). The first two stages didn’t deviate from the Asia Pacific module in the Task 12 database other than to use Malaysia’s electricity grid in the wafer process to better match First Solar’s manufacturing process (Sinha & de Wild-Scholten, 2015). Detailed LCIs of the crystalline silicon and mono-Si wafer processes can be seen in **Tables A1** and **A2** in **Appendix 2**.

The cell manufacturing process is where this model deviated from the Task 12 report. In traditional mono-Si manufacturing, screen-printing with a silver paste is used in the metallization process to promote conductivity in the cell. Instead, the Tetra Sun module uses front and back copper plating (Sinha & de Wild-Scholten, 2015). The First Solar specific manufacturing process is proprietary information, so a proxy copper plating process was developed using the Gabi and Ecoinvent databases. This proxy was based off of a review of a nickel-copper plating process in mono-Si cells (Ur Rehman & Hong Lee, 2014). This process starts by depositing a thin layer of nickel onto the cell through a process known as light induced plating. This process uses a bath of nickel chloride (NiCl₂) and sodium hypophosphite to reduce the nickel chloride and deposit nickel onto the cell. A very thin layer of tin is then deposited as a capping layer to prevent the oxidation of the copper. Finally, the cell is immersed in an electrolyte bath of cupric sulfate (CuSO₄·5H₂O) and sulfuric acid (H₂SO₄) to deposit the copper (Ur Rehman & Hong Lee, 2014). With no preexisting process to match this, our proxy used primary nickel and aluminum selective coating process for nickel pigmented aluminum oxide to

estimate the impacts of the nickel light induced plating process. Next, primary tin and a simple tin-plating process were used to model the tin cap. Finally, since cupric sulfate and sulfuric acid are missing in the Gabi and Ecoinvent databases, primary copper was used to represent the copper plating process. While not the exact process outlined, we are confident that this proxy represents a good estimate for the impact embodied by the copper plating process. A detailed LCI of the copper plating proxy can be seen in **Table A4** in **Appendix 2**.

In the panel process, another deviation was modeled, as the back sheet for the Tetra Sun panel only utilizes polyethylene terephthalate (PET) layers rather than the combination of polyvinyl fluoride (PVF) and PET layers seen in the Task 12 report (Sinha & de Wild-Scholten, 2015). This was simply modeled by assuming that the original 0.458 kg combined weight of the PVF and PET in the Task 12 cell was met only by PET in this model. A plastic film extrusion process was also added to the panel process to account for the processing of the PET. A detailed LCI of the panel process can be seen in **Table A5** in **Appendix 2**.

In addition to estimating the Tetra Sun manufacturing process, the mono-Si panel modeled here also assumed the base characteristics of First Solar's Tetra Sun mono-Si panel (First Solar, 2015):

- Module area: 1.64 m²
- Nameplate efficiency: 18.3%
- Nominal power output: 0.3 kWp
- Open circuit voltage: 42 voc
- Short circuit current: 9.35 amps

The Tetra Sun module also assumed a 25-year lifetime based on the warranty offered by First Solar (First Solar, 2015). The power output of the mono-Si panel was also assumed to decline linearly over the lifetime, but at a lower rate (0.36% per year) (Jordan & Kurtz, 2013). Given this, the lifetime average power output for the mono-Si panel was calculated at 0.278 kW and the average lifetime module efficiency was calculated at 16.9%. Detailed LCIs of the four stages of the mono-Si manufacturing can be seen in **Tables A1-A5** in **Appendix 2**.

Module AC/DC Cabling

AC/DC cabling is utilized in both CdTe modules (2.3 meters) and in Mono-Si modules (2 meters) (First Solar, 2015) (First Solar, 2015). This is simple electricity cabling made up of copper wiring encapsulated in an insulation jacket made from equal parts polyvinyl chloride (PVC) and nylon 6 (Frischknecht, et al., 2015) (Socolof et al., 2014). A detailed LCI of the AC/DC cabling can be seen in **Table A6** in **Appendix 2**.

Retaining Clips

The specifications sheet for the First Solar Series 4 CdTe module illustrates the use of four retaining clips per module (First Solar, 2015). The MP-Tec 80mm Pro Laminate Clamps (GPV-01-

0003-43) were selected based on a list of retaining clips approved by First Solar for use with Series 4 modules (First Solar, 2015). These clamps are made of die-casted aluminum and ethylene propylene diene elastomer (EPDE) rubber (MP-Tec, 2013). These clips are not used for the mono-Si modules. A detailed LCI of the retaining clip can be seen in **Table A7** in **Appendix 2**.

Balance of Systems Inventory Modeling

This analysis created a baseline model of the balance of systems (BOS) components in the construction and design of solar microgrids containing CdTe PV modules, with specific additions to the BOS model for solar microgrids that contain mono-Si PV panels.

Baseline CdTe Balance of Systems

The balance of systems of a solar microgrid provides the structural support and physical connection between PV modules. In this analysis, the BOS contains components for mounting, inverters, transformers, construction, operation and maintenance (O&M), transport, and other necessary support structures. Using manufacturing data from a life cycle inventory conducted by First Solar, as well as additional processing of materials not previously accounted for, this analysis worked to model a fixed-tilt ground BOS for CdTe PV panels (Sinha & de Wild-Scholten, 2012). The total area of CdTe fixed-tilt ground BOS is modeled to be the same as the total area of PV modules required for the microgrid.

Mounting

The mounting racks of the CdTe fixed-tilt ground BOS modeled in this analysis are made up of steel, aluminum, zinc coating, and synthetic rubber (Sinha & de Wild-Scholten, 2012). The steel and aluminum are formed into bars using bar rolling processes, and the synthetic rubber is put through a vulcanization process. A detailed LCI of the mounting component for CdTe fixed-tilt ground BOS can be seen in **Table B1** in **Appendix 2**.

Inverter

The inverter component of the CdTe fixed-tilt ground BOS modeled in this analysis utilizes the Ecoinvent “Inverter, 500kW, at plant” process. A very small portion of this inverter (0.0237%) is attributed to each square meter of BOS (Sinha & de Wild-Scholten, 2012).

Transformer

Transformers are commonly built into, or modeled as part of, the BOS of a solar microgrid. In this analysis, the transformer component of the CdTe fixed-tilt ground BOS is comprised of steel, copper, polyethylene granulate, and a lubricant. The steel is flattened using a rolling process and the copper is turned into copper wire with a wire drawing process. The polyethylene granulate is made useable with a plastic extrusion process. The use phase of a

transformer is also modeled using an Ecoinvent process (Sinha & de Wild-Scholten, 2012). A detailed LCI of the transformer component for CdTe fixed-tilt ground BOS can be seen in **Table B1** in **Appendix 2**.

Construction, Operation, and Maintenance

Diesel fuel, petrol fuel, natural gas, and electricity are required in order to construct, operate, and maintain the CdTe fixed-tilt ground BOS (Sinha & de Wild-Scholten, 2012). Burning processes, which were not previously accounted for, were added in order to include the use phase of diesel, petrol, and natural gas in this analysis. A detailed LCI of the construction and O&M components of CdTe fixed-tilt ground BOS can be seen in **Table B1** in **Appendix 2**.

Transport

The transport of BOS components is modeled using two Ecoinvent processes; “Transport, transoceanic freight ship” and “Transport, lorry >16ft, fleet average” (Sinha & de Wild-Scholten, 2012).

Other Support Structures

This component accounts for the foundation needed to support the CdTe fixed-tilt ground BOS, which is not accounted for in the mounting component. The support structures component includes concrete, sawn timber, and polyvinylchloride (Sinha & de Wild-Scholten, 2012). A detailed LCI of the other support structure components of CdTe fixed-tilt ground BOS can be seen in **Table B1** in **Appendix 2**.

Mono-Si Balance of Systems

The components of the BOS for the mono-Si panels modeled in this analysis are identical to the BOS for the CdTe modules, except in the mounting process. The mono-Si mounting in this analysis is based off of the open ground mounting systems detailed in sections 5.1.4-5.1.9 of the International Energy Agency’s PVPS Task 12 LCI report (Frischknecht, et al., 2015). Even though less m² of BOS is needed for the mono-Si panels, the mono-Si panels are heavier, thicker, and bigger than the CdTe laminate which requires the mounting structure to utilize more steel, concrete, and polystyrene than the CdTe mounting. A detailed LCI of the mono-Si mounting can be seen in **Tables B2** and **B3** in **Appendix 2**.

Lithium-ion Battery Methodology

A lithium-ion battery bank has been modeled for the storage component of this microgrid. Lithium ion battery technology was first established in 1991 and is being increasingly utilized in numerous fields of use (Zhu, et al., 2012) (Warner, 2015) (Poullikkas, 2013). This technology is particularly attractive due to its high energy density and reliable performance (Wang, Vest, &

Friedrich, 2011) (Shuva & Kurny, 2013). Lead acid batteries have historically been utilized more often due to the fact that they are cheaper and readily available for purchase. However, lithium-ion battery technology was chosen despite the fact that many current microgrid systems utilize lead acid batteries, as it is an emerging technology whose energy density, lifetime, and charge-discharge efficiencies are typically superior to lead-acid (Sullivan & Gaines, 2010).

Other evidence of increased lithium ion use in renewable energy systems comes from a more recent study by Malhotra et al. (2016), which states that lithium ion battery technology is, "... particularly suited for integration of renewable energy, frequency regulation, and also to serve multiple applications (Sullivan & Gaines, 2010)." Additionally, this study compiled a database spanning 42 countries and 612 battery storage projects whose capacities sum to 1350 MW of installed capacity (Malhotra et al., 2016). Within this study, 62.6% of the projects utilized lithium ion technology. It should be noted that only a small portion of these projects pertained to off grid microgrids, though this database does imply a trend of increased utilization of lithium ion batteries as they continue to become cheaper. Due to its evidence of increased use in conjunction with data availability, lithium ion battery technology was selected for the microgrid energy storage system.

Lithium-ion batteries are typically made up of four primary components: battery cells, packaging, a battery management system (BMS), and a cooling system. Energy is stored in the system through the movement of lithium-ions through the electrolyte between the positive and negative electrodes (Dunn, Kamath, & Tarascon, 2011). For this analysis, the cathode active material modeled is comprised of lithium nickel manganese cobalt oxide ($\text{Li}(\text{Ni}_x \text{Co}_y \text{Mn}_z)\text{O}_2$, nickel-cobalt manganese) and the anode modeled is comprised primarily of graphite. The assumed characteristics for the battery model used in this analysis are listed in **Table 1** below:

Table 1: Li-Ion Battery Specifications. List of battery bank electrical and operating characteristics that the model was based on. Battery bank voltage was calculated by connecting 6.58 cells in series, and battery cell capacity was calculated by connecting 152 strings in parallel. Further calculations are discussed in the battery sizing section. Baseline values were based on (Ellingsen, et al., 2014).

Category	Quantity	Unit
Nominal cell voltage	3.65	V
Cells in series	6.58	No.
Battery bank voltage	24	V
Cell capacity	20	Ah
Cells in parallel	152	No.
Installed battery capacity	3041	Ah
Total cells	1000	No.
Battery bank mass	1231	kg
Battery bank efficiency	95	%
Depth of discharge	50	%
System autonomy	24	hrs.
Lifespan	13.7	yrs.

Nominal cell voltage, cell capacity and battery efficiency were largely based off of the example battery from Ellingson et Al. (2014), which is an accurate representation of common lithium-ion battery specifications (Ellingsen, et al., 2014). Pack voltage was chosen as a common voltage that suits other components of a microgrid system, and calculated by connecting 6.58 cells with a 3.65 nominal cell voltage in series (Table 1). A depth of discharge (DOD) was chosen at only 50% as to maximize the life span of the battery bank, in order to minimize costs. Battery life span is primarily based off of the depth of discharge, and numerous other factors with a lesser impact (ex. temperature and speed of discharge) (Ellingsen, et al., 2014). The usable life of a battery is considered to be over when its active capacity decreases to 80% of its nameplate capacity (Ellingsen, et al., 2014) (Kalhammer et al., 2007). Ellingson et Al. (2014) estimated a total of 5000 discharge cycles would be possible before its capacity reached 80%. As the system autonomy was modeled at 24 hours, one full discharge (to 50% DOD) was assumed to occur every 24 hours. This results in a total lifespan of 5000 days, or 13.7 years (**Table 1**).

Battery Model

The lithium-ion battery bank in our model was based off of a lithium-ion battery intended for original use in a battery electric vehicle (BEV) detailed in (Ellingsen, et al., 2014). The basic battery attributes (cell capacity and voltage) were used to size-up battery capacity in order to meet the demand of a small village (Table 1), which is discussed further in component sizing. The battery coolant system was omitted from the model as it was considered outside the scope of this project and others, due to its minimal environmental impact (Ellingsen, et al., 2014) (Majeau-Bettez, Hawkins, & Stromman, 2011).

While battery manufacturing comprises the majority of impacts in a battery life cycle, the end of life (EOL) was modeled as well. The use phase of the battery was assumed to have no impacts in this model. The baseline EOL method for the battery bank was assumed to be a landfill process, though a recycling scenario was also modeled.

Battery Manufacturing

The modeled lithium-ion battery bank is composed of three main components, battery cell, BMS and packaging (**Figure 5**). Each individual component model is discussed in detail below. The majority of processes modeled are based off of the inventories listed in Ellingson et Al. (2014). All of the precise processes in battery manufacturing were not present, thus proxy processes were frequently used as substitutes.

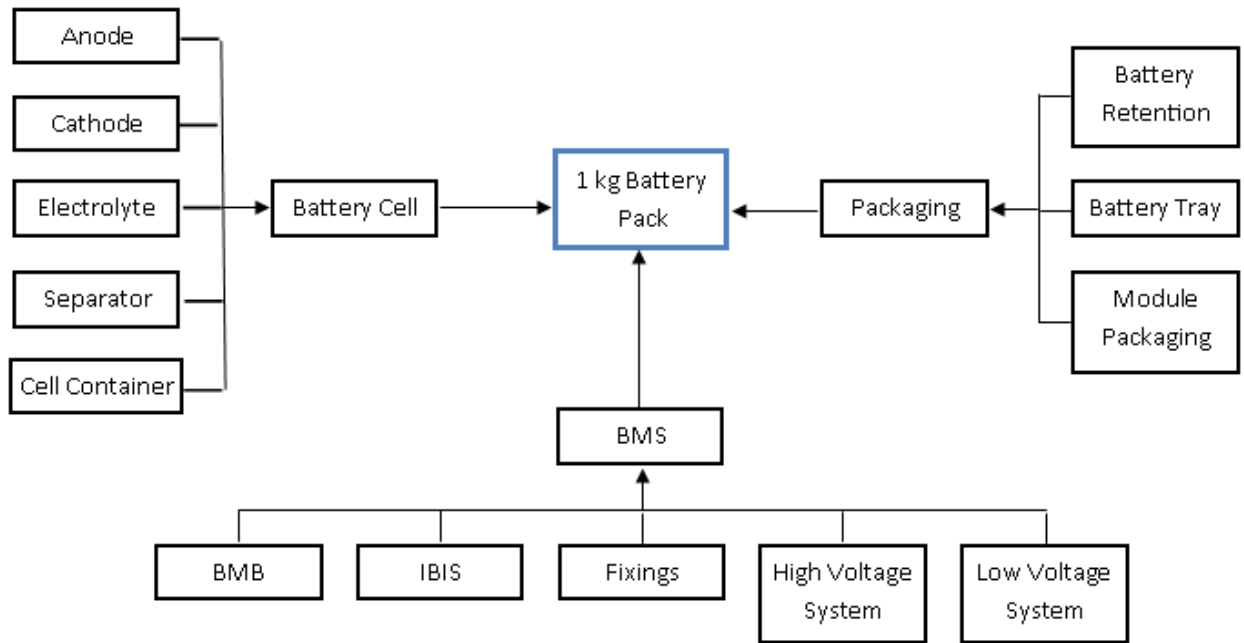


Figure 5: Manufacturing of a Lithium-ion Battery Pack. Manufacturing flow chart for one kilogram of lithium-ion battery pack used in this model. Specific production of each process is discussed further below and detailed in **Tables C1-C27 Appendix 2**. BMS = Battery Management System; BMB = Battery management board; IBIS = Integrated Battery Interface System. General design of the system was adapted from Ellingson et Al. (2014).

Areas where this model deviated from Ellingson et al. are described in the sections below. One overall change to the battery plan is that inputs to the battery model are set to use primary material flows, which do not include any secondary material (**Tables C1-C27, Appendix 2**). This is because recycling is modeled using the avoided burden approach, and recycling secondary inputs would result in double counting of recycling benefits.

Battery Cell

The battery cell of the lithium-ion battery is comprised of a cathode, anode, separator, electrolyte and cell container (**Figure 5**). The modeled cathode is made of an aluminum current collector that is coated in a positive electrode paste ($\text{Li}(\text{Ni}_x \text{Co}_y \text{Mn}_z)\text{O}_2$). The positive electrode paste was based on a 1:1:1 ratio of Ni, Co and Mn, combined with carbon black. While processes exist in Ecoinvent and GaBi ts to represent the majority of the process necessary to create a cell cathode, several processes needed to be created in order to represent the formation of CoSO_4 , NiSO_4 and MnSO_4 for the positive electrode paste. These were approximated based off of Majeau-Bettez et Al. (2011) and are detailed in (**Tables C4-C8 Appendix 2**) (Majeau-Bettez, Hawkins, & Stromman, 2011).

The cell anode is made of a copper current collector covered in a graphite based negative electrode paste. The electrolyte is lithium hexafluorophosphate (LiPF_6) combined with ethylene carbonate as a binder. The remaining separator is made of polypropylene and the cell container is made of aluminum, copper, and a multilayer pouch with numerous plastics. The

manufacturing of the battery cell is very energy intensive, as it requires multiple mechanical processes. The most energy intensive step is the operation of dry rooms that are essential to the quality of the lithium-ion battery (Ellingsen, et al., 2014). The total energy required for this step varies and is difficult to measure; with this in mind, the energy required for the manufacture of one kg of battery cell was modeled at 101 MJ. This number is representative of the most energy efficient month from Miljøbil Grenland, a lithium-ion battery manufacturer in Norway (Ellingsen, et al., 2014) (Nordic Green, 2010). The grid mix used for cell manufacture was an average European grid mix from GaBi ts (**Tables C5-C7 Appendix 2**).

Packaging

Battery packaging was comprised of battery retention, module packaging and a battery tray. Battery retention is primarily made of steel and modeled to match (Ellingsen, et al., 2014). A cutoff criterion of 10% was used in the model of module packaging. Based on this criterion, module fasteners, bimetallic busbars and washer, end busbar (aluminum), end busbar (copper), and module lid was omitted from the model. The resulting lack of mass from this omission was distributed evenly to the inner and outer frames. Using the same cutoff criteria, the tray lid was omitted from the battery tray plan.

Battery Management System

The BMS is comprised of battery module boards, integrated battery interface systems, fasteners, high voltage system, and a low voltage system. The BMS was modeled exactly as the model presented in Ellingson et al (2014).

Battery Sizing

An important component of a microgrid LCA is the sizing of the system, as that will significantly affect the environmental impacts. In order to calculate installed capacity the required capacity was divided by the depth of discharge and the battery efficiency listed in Table 1.

$$\text{Installed Capacity} = \text{Required Capacity} * (\text{Battery Efficiency} * \text{DOD})^{-1}$$

Knowing the installed capacity, the nominal cell voltage and installed capacity were used to calculate the total number of cells in parallel and series. Cells connected in series increase voltage and cells connected in parallel increase capacity. Total cells connected in each fashion were calculated as follows:

$$\begin{aligned} \text{Cells in Series} &= \text{Pack Voltage} * \text{Cell Voltage}^{-1} \\ \text{Cells in Parallel} &= \text{Installed Capacity} * \text{Cell Capacity}^{-1} \end{aligned}$$

The total cells in parallel were multiplied by the total cells in series to obtain the total cells necessary to fulfill the listed demand. To calculate the total cells needed over the lifetime of

the microgrid, the ratio of microgrid lifetime to battery life was multiplied by the total necessary cells:

$$\text{Total lifetime cells} = \text{total cells} * (\text{Microgrid lifetime} * \text{Battery lifetime}^{-1})$$

Once the total lifetime cells necessary were calculated, the mass of the battery bank was calculated based on the example from Ellingson et al. (2014), they had included 360 cells in their pack, with a cumulative mass of 150 kg. Therefore we assumed an individual cell mass of 0.42 kg. To calculate total cell mass, individual cell mass was multiplied by the total cells necessary over the lifetime.

$$\text{Total cell mass} = \text{individual cell mass} * \text{total lifetime cells}$$

The mass calculated above only represents the battery cells. To calculate the total mass of the entire pack, a ratio of cell mass to pack mass was calculated from Ellingson et al. (2014). Based on a total pack mass of 243 kg (10 kg were omitted because the coolant system was not modeled), and a total cell mass of 150, relative pack mass was calculated at 61.73%. To get total kg of the battery bank the total cell mass was divided by 0.6173. Total pack mass was then entered into the GaBi model which was set for an output of 1 kg of battery pack.

Charge Controller Methodology

In off-grid PV generation systems with battery storage, the batteries are connected to the PV array through a maximum power point tracking (MPPT) charge controller to optimize the power transfer from the PV array to batteries (Chen et al., 2007). Adding a charge controller is more useful for the systems where the PV array voltage is much higher than the battery nominal voltage, as is the case with many new generation PV modules. The charge controllers efficiently manage the state-of-charge of batteries and regulate the charging voltage of the batteries, thus prolonging battery life (Dunlop & Farhi, 2001). The current and voltage output of a PV module is a function of temperature and insolation and can vary very significantly, giving rise to a characteristic current-voltage (I-V) curve specific to that solar PV cell/module (Aranda et al., 2009). Thus, extracting power from a solar PV array at lower than optimum voltage can cause power losses over 40%; out of which 30% is because of voltage mismatch (Chen et al., 2007). MPPT charge controllers trace the I-V curve of the PV array and automatically adjust their AC/DC voltage conversion, reducing the mismatch loss to 15% and delivering up to 90% of the input power in optimal conditions (Grzesiak, 2006).

Morningstar's Tristar 600v MPPT charge controller was chosen for modeling as it is a high capacity charge controller suitable for system with PV modules with high open circuit voltage (V_{oc}) and short circuit current (I_{sc}).

Modeling

For modeling purposes, the charge controller is divided into three parts; printed wiring board (PWB), PWB enclosure, and a passive heat sink. Certain specific information about the relative weights, material composition, and manufacturing location of the charge controller was collected from the manufacturer (Marcellino, 2015). The specific components of the charge controller and other details about the PWB were proprietary and thus approximated from other secondary sources (Dutta, 2015) (Morningstar Corporation, 2013).

The pre-existing Ecoinvent processes in the GaBi software were scaled to match the information collected. The collected information revealed the likely use of copper weighted PWB instead of regular PWB. A standard 6oz/m² copper weighting was assumed and added on to the pre-existing PWB manufacturing and mounting processes. The enclosure is made of steel while the passive heat sink is composed of casted aluminum. The suitable processes to represent steel bending, stamping, and aluminum casting were modeled. The electricity mix of China was used to represent the actual manufacturing input. Certain small components apparent from the charge controller specification sheets, such as a small plastic knob, wiring, and paint/coating were ignored due to lack of data and a likely minor impact. The three major parts, PWB, enclosure, and heat sink, were then combined to represent a single, complete unit of the charge controller, which was later sized appropriately according to other system parameters. The detailed life cycle inventories are listed in **Table C27** in **Appendix 2**.

Sizing

The charge controller is a very crucial component that needs to be sized carefully. A charge controller is limited by its capability to accommodate a certain maximum level of the incoming I_{sc} and V_{oc} . It is also limited by the output current at which it can deliver the peak power from the PV array to the battery at a certain battery bank voltage. Thus, the charge controller is separately sized based on two sets of parameters. The specification of the modeled charge controller is given below (**Table 2**).

Table 2: Operating characteristics of Morningstar TS-MPPT-600v Charge Controller. Values were based off of the specification sheet (Morningstar Corporation, 2015).

Parameter	Value	Unit
Peak Efficiency	97.9	%
Maximum Battery Current	60	A
Maximum Input Operating Current	15 (self-limiting)	A
PV Input Operating Voltage Range	100-525	V
Unit Weight	9	Kg.
Life expectancy	15	yrs.

The first parameter is the input I_{sc} from the PV array. For this, it was assumed that the number of PV modules in each string of the array is based on the maximum V_{oc} that the charge

controller can accept. Given the total number of modules, the number of strings and thus the incoming I_{sc} were calculated. This way, it is ensured that both the V_{oc} and I_{sc} requirements of the charge controller are met.

$$\begin{aligned} & \text{Number of Modules in each string (in series)} \\ &= \frac{V_{oc} \text{ of Module}}{\text{Maximum input } V_{oc} \text{ of charge controller}} \end{aligned}$$

$$\text{Total Input short circuit current} = \text{Number of strings} * I_{sc} \text{ of module}$$

$$\text{Number of charge controllers required} = \frac{\text{Total } I_{sc}}{\text{maximum input operating current}}$$

Secondly, the controller was sized such that it can deliver the peak power of the PV array at Standard test conditions (STC; 1000 W/m², relative air mass 1.5, 25°C) at its maximum output current given a certain battery bank voltage. In this particular method, a safety factor of 1.25 was also included as recommended by the manufacturer in the operation manual. The life expectancy of the charge controller is assumed to be 15 years based on similar Morningstar products (RV Solar Connection, 2008). The average efficiency of the charge controller was assumed to be 85% to accommodate for variation in the operational conditions of PV array.

$$\begin{aligned} & \text{Required Amperage for charge controller} \\ &= \frac{\text{power of PV array at STC} * \text{Average Controller efficiency} * \text{Safety factor}}{\text{Battery Pack Voltage}} \end{aligned}$$

$$\text{Required number of charge controllers} = \frac{\text{Required Amperage}}{\text{Maximum Battery Current}}$$

This efficiency was also used in the system derate factor to suitably inflate the installed capacity (in kWh/day, daily demand divided by the derate factor) to meet the daily demand (kWh/day). The power of the PV array at STC (in kW_p) is the power that the PV array can deliver at the standard operational conditions. This power is based on the number of PV modules corresponding to the calculated installed capacity.

The larger of the two numbers as calculated by both methods is then used as the number of charge controllers required in the system. Finally, the number of charge controllers required over the lifetime was calculated using the above number and the life expectancy of each charge controller.

Diesel Generator Methodology

In the context of this analysis a diesel generator refers to a diesel genset, which is a combination of a diesel engine and an electric generator (or alternator). Diesel generators are

analyzed in two different microgrid configurations; the PV-Diesel system and the PV-Hybrid system. Depending on the system, the generator capacity and operational hours vary.

Generator Production

Using secondary data from similar life cycle assessment studies and an existing diesel generator manufacturing process from GaBi, this analysis modeled the manufacturing process of a diesel generator (Smith, et al., 2015). The plan was structured such that the diesel generator’s total mass was linked to its nameplate capacity, using a calculated average power to weight ratio of 0.024 (Table 3).

Table 3: Average Power to Weight Ratio for Diesel Generators Calculation of average power to weight ratio for a diesel generator (Aurora) (Cummins Onan, 2007) (FG Wilson) (Kohler).

Genset Nameplate Capacity (KW)	Weight (kg)	Power to Weight Ratio
2.5	347	0.036
6.8	303	0.022
5.5	280	0.020
4	222	0.018
Average Power Factor		0.024

This link provided the flexibility to assess various generator capacities (that change based on system requirements) using the same production process. The production process assumed the following mass mix of raw materials:

- Aluminum : 35%
- Steel : 30%
- Casted steel : 30%
- Copper: 3%
- Plastic: 2%

The lifetime of one diesel generator was assumed to be 10 years (Cummins Onan, 2007). Considering a 25-year lifetime for both cadmium telluride (CdTe) and monocrystalline silicon modules, the reference flow of the diesel generator over the system lifetime was calculated as 2.5. Therefore, the lifecycle production impacts of generator were calculated for 2.5 generators over a span of 25 years. A detailed LCI of the generator production can be seen in **Table D1** in **Appendix 2**.

Generator Use Phase

This analysis modeled the burning of diesel to produce electricity using a general process for diesel burned in an electric generating set from GaBi. The plan was scaled off of the total electricity output required from the diesel generator over the system lifetime (25 years).

One of the major components of designing the generator use phase was estimating its total operational hours. This was directly linked to the electricity demand and the nameplate capacity of generator. The total electricity to be supplied from the generator varied based on the microgrid system being considered. A detailed LCI of the generator use phase can be seen in **Table D2** in **Appendix 2**.

The total operational hours and electricity output calculation for each system has been explained below.

PV-Diesel Generator System

In order to identify the hourly peak demands per day, a 24-hour load profile of a village in Northern Kenya (Marsabit) was used (Lukuyu & Cardell, 2014).

The load profile gives a breakdown of hourly electricity demand that has to be met by the microgrid system. In order to identify the solar potential within each hour, three hour averages for annual insolation from the NASA Surface Meteorology and Solar Energy Database were used. This gives the total electricity that can be produced from the PV modules within each hour of the day. Although due to the variation in solar irradiation and a fixed demand during sunlight hours, the amount of electricity produced by the PV and the amount of electricity used were not always equal. Therefore, if during an hour the electricity produced by the PV was more than the demand, the extra electricity did not get used and thus got wasted. On the other hand, if during an hour the electricity produced by PV was not sufficient to meet the demand, the deficit was be met by the diesel generator. Overall, the PV electricity used and the electricity produced by the diesel generator together completely met the demand during each the hour of the day (**Figure 6**).

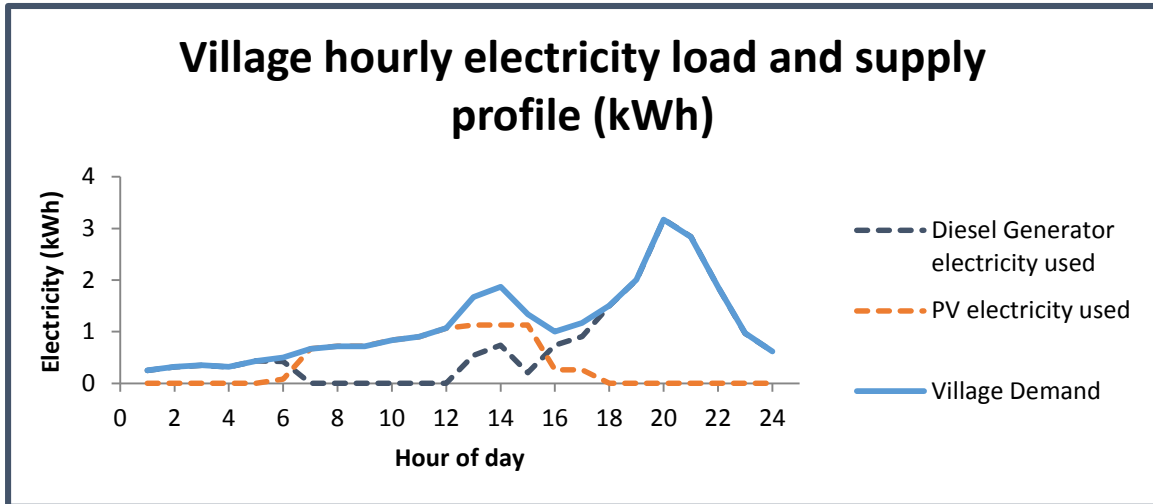


Figure 6: Hourly Electricity Load and Supply Profile for village. The total electricity demand of the village (blue solid line, kWh), the demand met by PV electricity (orange dashed line, kWh), and the demand met by generator (navy dashed line, kWh) during each hour of the day.

As the size of the generator was dependent on the PV capacity, a certain installed capacity of PV was first decided. This installed capacity was based on a defined independent parameter, PV demand contribution threshold, which represented the percent of the daily demand intended to be met by the PV. A higher value of the threshold represented more dependence on PV and less on the diesel generator. As PV contribution threshold value was increased from 0% to 100%, the required installed PV capacity increased linearly but the rate of increase in the PV electricity used decreased (**Figure 7**). At the threshold value of 32.87%, the amount of daily demand met by the PV was observed to be exactly equal to the intended percent of the demand to be met by PV. This means that at 32.87% value of the threshold, PV electricity met 32.87% of the total daily demand of the village. This threshold percentage was selected to size the PV and consequently the other microgrid components. The remaining 67.13% of demand was then met by the diesel generator.

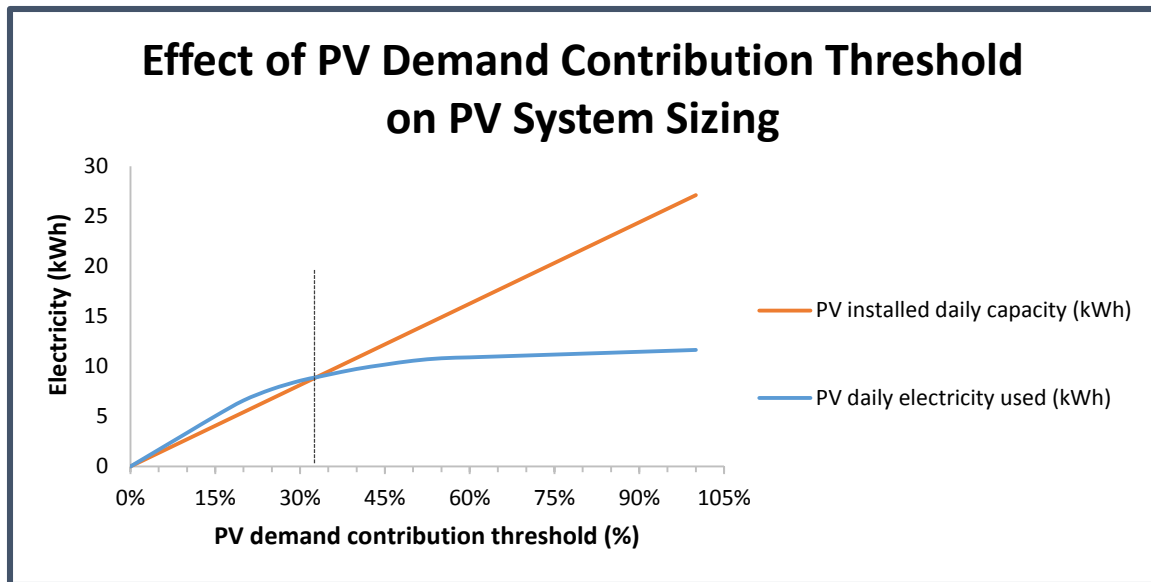


Figure 7: Variation of PV Installed Capacity and PV Electricity Use with PV Demand Contribution Threshold. Change in the installed daily capacity of PV (Orange line, kWh) and the daily amount of the electricity used (blue line, kWh) with increasing value of the PV demand contribution threshold.

The use of a variable speed, prime rated diesel generator was assumed for this system, since power has to be continuously supplied at variable loads for long durations each day. From the 24-hour load profile, peak and off-peak demand hours were identified in order to set load factors for the operation of the diesel generator. Operation at each load factor gives rise to a specific fuel consumption efficiency, which in turn dictates a specific electricity production efficiency (or, fuel to electricity conversion efficiency). The different efficiencies arising from varying load factors were used to calculate a single weighted operational efficiency for a diesel generator of this particular nameplate capacity. Using this weighted efficiency and total operational hours over the system’s lifetime, the total electricity output from the diesel generator was calculated.

PV- Hybrid Generator System

The PV modules across all systems were sized based on the average solar insolation of 5.92 kWh/m²/day over all 12 months of the year. In order to identify the deficit in electricity output that has to be met by the generator, a parameter from the NASA Surface meteorology and Solar Energy Database (equivalent number of monthly black days, 22-year average) for Kenya was used. This parameter gives the consecutive number of “black days” or no-sun days within each month where the insolation was much below the average resulting in minimal or no PV electricity production. It is assumed that the PV-battery system does not provide electricity on the no-sun days (assuming the battery bank has been depleted), whereas the PV-hybrid system can, using the diesel generator. The total electricity deficit was calculated over the lifetime of the PV microgrid system and was used to obtain the total diesel generator operational hours

and electricity output. The PV module and battery sizes remain consistent between the PV-battery and PV-hybrid microgrid systems.

Distribution System Methodology

Residential Electricity Meters

For the distribution system, the microgrid models assume that each household will be equipped with a household electricity meter to monitor and report electricity use. The meter modeled for this analysis was based off the Centron II residential meter (CENTRON C12.19) (Itron, 2014).

This meter, while potentially not the specific meter used in off-grid contexts, is however representative of the materials and impacts that electricity meters use and embody. The meter is made up of a polycarbonate plastic casing, an aluminum die-cast counting part, general electronic control units, and an LCD glass display (Marshall, 2009). A detailed LCI of the electricity meter can be seen in **Table E1** in **Appendix 2**.

Residential Electricity Wiring

This model also assumes that each household will install two electricity wires to connect the household with a centrally located PV array. An average distance of 20 meters between households and the array is used. Like the module AC/DC cabling, the residential wiring is made up of copper wire and a PVC/nylon 6 insulation sheath (Socolof et al., 2014). A detailed LCI of the electricity wiring can be seen in **Table E2** in **Appendix 2**.

Security Fencing Methodology

This model also assumes a chain link fence will be installed surrounding the microgrid system to provide a basic level of security from people and the environment. To accomplish this we assumed a 10 ft. high, 1 and $\frac{3}{4}$ inch diameter fence with posts every three meters (Chain Link Manufacturers Institute, 2011) (Wheatland Tube, 2014). The fence was modeled using steel wire rod for the chain link and steel piping for the fence posts. A detailed LCI of the security fencing can be seen in **Table E3** in **Appendix 2**.

End of Life Methodology

Baseline Landfilling of Microgrid Systems

The baseline end of life for the microgrid systems was assumed to be a generic landfilling process. To model this, the major inert material flows from our microgrid (steel, aluminum, glass, ferro metals, and plastic) were sent to a landfill. While there are other materials that would be a part of the microgrid components, these five were chosen because of the significance of their mass contribution to the total microgrid mass. The breakdown of individual material masses sent to landfill came from estimates of the material's proportion of total microgrid mass based on the amount of the given material used throughout the manufacturing and use of the microgrid components. For the PV-Battery (~2500 kg), PV-Hybrid

(~2900 kg), and the PV-Diesel (~1100 kg.) the proportions were assumed to be 50% steel, 25% aluminum, 10% glass, 10% Ferro metals, and 5% plastic. The exact landfilling proportions are difficult to determine, but this process is representative of the magnitude of impacts for the landfilling of PV microgrids. A detailed LCI can be seen in **Table F1** in **Appendix 2**.

Recycling of CdTe Modules

As an alternative to the baseline landfill process at the end of life (EOL), a recycling process for the individual components of a microgrid was also modeled for this analysis. The recycling of CdTe PV modules at the end of the system's usable lifetime is modeled using an avoided burden approach. Secondary materials from the CdTe PV modules that can be recycled are recycled and a credit is given to account for the avoided use of primary materials required to create the modules. The materials that cannot be recycled are treated and disposed. This model also accounts for the transport of these materials to a recycling facility. The avoided products from this recycling process are cadmium sludge, copper telluride cement, silica sand, soda powder, limestone, natural gas, heavy fuel oil, and primary copper. This model takes into account the emissions of cadmium to air and water during the recycling process, and also accounts for the avoided emissions of carbon dioxide to the air due to avoided primary production. A detailed LCI of the CdTe module recycling process can be seen in **Table F2** in **Appendix 2**.

Recycling of BOS

An avoided burden approach to EOL recycling of BOS components was used in this analysis. This means that secondary or scrap materials from the BOS are recycled after the system's useable lifetime and a credit is given to account for the avoided use of the primary materials required to create the BOS. The recycling process for the BOS uses inputs of secondary aluminum, steel, and copper. This model also accounts for the transport of these materials to a recycling facility. The avoided products from this recycling process are primary aluminum, steel, and copper, which match the inputs needed to make the BOS components used in our analysis. The amount of secondary material inputs and avoided primary materials are the same, because losses from recycling were already taken into account before being modeled in this analysis (Bergesen et al., 2014). These losses are 21% for aluminum, 10% for steel, and 24% for copper. A detailed LCI of the BOS recycling process can be seen in **Table F3** in **Appendix 2**.

Recycling of Charge Controllers

For material inputs, only primary metals were used following the avoided burden method of modeling end of life recycling. For recycling considerations, a scrap reclamation factor of 0.9 was assumed. The existing Ecoinvent process dictated the recycling efficiency of 95.2%. The amount of the secondary material produced was used as a credit to avoid the burden of the primary materials used originally as inputs.

Battery End of Life

The EOL for the battery has been modeled to either be sent to landfill, or recycled with pyrometallurgical or hydrometallurgical processes. There are lithium-recycling facilities in use around the world, despite the difficulty and economic burden of recycling these batteries (Warner, 2015). Because there is incentive for recycling, its potential impact was modeled using the avoided burden method (Arsenio, 2015).

Both recycling processes modeled were based off of a study done by Fisher et al. (2006), who provided sample models for hydrometallurgical and pyrometallurgical recycling processes based on industry contacts (Fisher et al., 2006). Hydrometallurgical processing was modeled based on the technology utilized by Recupyl, a French battery recycling company. Pyrometallurgical recycling processes were based off of the technology used by Batrec, a Swiss recycling corporation. The energy mixes used in each process are representative of their geographical grid average. However both of these processes were generalized for a host of varying sizes and chemistries of lithium-ion batteries. The models in Fisher et al. (2006) were adapted for this analysis to be more specific to the battery bank used in this model. Material inputs to each recycling process were not altered from Fisher et al. (2006).

To properly alter the outputs, battery bank material mass (**Table 4**) was used to determine how many grams of each recoverable material were present in one kilogram of battery bank. Recoverable materials for each process and their mass per kilogram of battery pack are listed below (**Table 4**). Recoverable materials were determined by listed outputs from these processes in Fisher et Al. (2006).

Table 4: Recoverable Materials from Li-Ion Battery Recycling. List of the recoverable materials and their representative masses in 1 kilogram of lithium-ion battery bank modeled in this analysis. Data under the scrap recovery columns represent the amount of recovered material for each recycling process per kg of spent battery pack, assuming a 95% recovery rate. 'N/A' means that the listed material is not recovered in the specified recycling process. Materials with a '*' go through a secondary process before they are fully recovered for use.

Material	Mass in 1 kg of battery pack [kg]	Hydrometallurgical scrap recovery [kg]	Pyrometallurgical scrap recovery [kg]
<i>Aluminum*</i>	0.19	0.18	0.18
<i>Copper*</i>	0.14	0.13	0.13
<i>Steel*</i>	0.13	0.12	0.12
<i>Lithium</i>	5E-4	4.7E-4	N/A
<i>Cobalt</i>	4.5E-2	4.3E-2	4.3E-2
<i>Manganese</i>	4.3E-2	N/A	4.1E-2

Specific recovery rates for each material were not available for this battery chemistry, thus a scrap recovery rate of 95% was assumed for all recoverable materials (**Table 4**). Additionally, aluminum, copper and steel scrap were sent through secondary metal production processes to

accurately model the energy required for secondary production (**Tables F4 and F5 Appendix 2**). Recycling efficiencies were assumed to be 95% in each of these additional secondary scrap processes. It should be noted that secondary cobalt, lithium and manganese were not modeled through secondary material production processes as there were no representative processes in our database. Therefore, the energy burden from recovering these three usable secondary elements is likely underestimated.

Generator Recycling

Three main inputs (aluminum, steel and copper) that constitute a major portion of the generator manufacturing inputs were assumed to undergo recycling. A total of 90% of the input mass was assumed to enter the recycling process (Smith, et al., 2015). A detailed LCI of the generator recycling can be seen in **Table F6 in Appendix 2**. The following recycling efficiencies were assumed for each material, based on existing processes from the Ecoinvent database:

- Aluminum: 96%
- Steel: 95%
- Copper: 96%

Traditional Electrification Solution

Average Kenya Electricity Grid Mix

The Kenya electricity grid was modeled in order to compare the life cycle impacts from the PV microgrid systems to the existing electricity grid where the pilot projects are focused. It is important to note that this comparison doesn't include the impact from the extension of the central electricity grid in Kenya. This means that the impacts from activities like the construction of roads, power plants, substations, and power lines are excluded. The baseline comparison, therefore, becomes just the production of electricity from the existing grid in Kenya which was modeled as follows: 31% from oil, 2% from biomass, 44% from hydro, 23% from geothermal, 0.2% from wind, and 0.01% from solar. The Kenya specific energy processes flows were unavailable in GaBi and Ecoinvent so they were estimated using energy processes from other countries as a proxy. A detailed LCI of the Kenya electricity grid can be seen in **Table G1 in Appendix 2**.

Marginal Kenya Electricity Grid Mix

The current grid mix in Kenya represents the average impacts from the production of one kWh with existing power plants and resources. This, however, is unlikely to represent the impacts from future electricity development. With this in mind, a marginal electricity grid was also developed to better represent the energy resources that will be developed to provide electricity access in these communities. This marginal grid was modelled based on the Ten Year Power Sector Expansion Plan in Kenya (Republic of Kenya, 2014). It includes the following resource mix: 3% from oil, 6% from imported hydro, 31% from coal, 33% from geothermal, 10%

from wind, and 17% from natural gas. Once again, the Kenya energy processes were unavailable so they were estimated using energy flows from other countries as a proxy. A detailed LCI of the marginal Kenyan electricity grid can be seen in **Table G2** in **Appendix 2**.

Small-scale Diesel Comparison

Home Diesel Genset

The combustion of diesel fuel in a home diesel genset was modeled to compare microgrids to small-scale energy options that may be available in some communities or households. The home diesel-electric genset was modelled the same as the use phase of the generator set as used in the PV-Diesel microgrid. A detailed LCI of the diesel burning process can be seen in **Table D2** in **Appendix 2**.

Manufacturing Electricity Grid Mixes

The manufacturing of the microgrid components, most notably the PV modules, occurs in countries that do not have preexisting electricity grid mixes in Gabi or Ecoinvent. With this in mind, individual grid mixes for these countries were developed to improve the geographic precision of this analysis.

Malaysia

Malaysia was the site of many of the PV module manufacturing processes, including the CdTe PV laminate and the wafer, cell, and laminate for the mono-Si modules. The electricity mix for Malaysia was modeled to contain the following mix of generation: 26.68% from hard coal, 1.89% from fuel oil, 63.52% from natural gas, and 7.72% from hydro (International Energy Agency, 2010). Since individual energy flows (i.e. electricity from natural gas) for Malaysia are absent from the Gabi and Ecoinvent databases, they were estimated using the existing electricity unit processes from the electricity grid in Japan. A detailed LCI of the Malaysian electricity grid can be seen in **Table G3** in **Appendix 2**.

South Korea

The refining, processing, and growing of the CZ crystalline silicon was assumed to take place in South Korea based off of the IEA Task 12 LCI data (Frischknecht, et al., 2015). The South Korean electricity mix was built to have the following mix of generation sources: 39.71% from hard coal, 3.39% from industrial gases, 3.45% from fuel oil, 18.28% from natural gas, 1.3% from hydro, 33.54% from nuclear, 0.06% from solar, 0.1% from wind, 0.01% from wood, and 0.14% from waste incineration (International Energy Agency, 2011). Just like Malaysia's grid, individual energy flows for South Korea were not available in the Gabi and Ecoinvent databases, so these flows were estimated using flows from the electricity grid in Japan and other neighboring countries. A detailed LCI of the South Korean electricity grid can be seen in **Table G4** in **Appendix 2**.

Data Quality and Uncertainties

In order to understand the degree of uncertainty associated with this study, the life cycle analysis was split into three stages; input, processing and output.

Input Uncertainties

Input uncertainties are the uncertainties associated with raw material selection, assumptions related to local environmental conditions and demography. The plans in this analysis primarily assume global or European raw materials for most processes while in reality, manufacturing of individual components (apart from the solar PV modules, which are manufactured in Malaysia and have been modeled to reflect that) can occur in multiple nations across the world and be imported to Kenya. This model has certain fixed input parameters reflecting local environmental conditions that affect electricity production and demand such as solar insolation, average number of people per household and electricity demand per household (KWh). These values are either average for the entire nation or are location specific values that have been assumed to be true for the entire nation of Kenya for the purpose of this project. Despite this section having an overall medium uncertainty and affecting the granularity of our study, the implications of these uncertainties aren't major since the project itself is a comparative environmental assessment of different microgrid system designs, and these assumptions have been maintained consistently throughout all the systems.

Processing uncertainties

Process uncertainties refer to uncertainties and assumptions associated with the processes used as part of the lifecycle modeling. The range of uncertainties varies from low to medium, depending on the quality of data utilized for the individual component plans. Solar modules and the BOS (manufacturing, takeback, and recycling) utilize data from previous manufacturer LCAs and therefore have low uncertainty. The modeling of batteries under different grid mixes and the modeling of charge controller uses established secondary data and hence, has low uncertainty. Whereas, the modeling of the diesel generator and inverter assumes a general manufacturing and use process available in Ecoinvent, resulting in medium uncertainty. Overall, considering the combination of process related data and assumptions that were made, this section has low uncertainty associated with it.

Output Uncertainties

The reference flows, or total output, for each component is based on their industry average lifetime and the overall microgrid system lifetime (solar module's lifetime). Since this is mostly based off of primary data of high quality, this section has low uncertainty. See **Appendix 3** for flow chart of uncertainties and assumptions.

Results

Overall Microgrid Impacts

The three microgrid systems were modelled and normalized based on their lifetime electricity production. The system’s normalized life cycle inventories were characterized based on their impacts in seven different impact categories: climate change (kg CO₂e), freshwater eutrophication (kg P eq.), human toxicity (kg 1,4-DB eq.), particulate matter formation (kg PM₁₀ eq.), photochemical oxidant formation (kg NMVOC), terrestrial acidification (kg SO₂ eq.), and terrestrial ecotoxicity (kg 1,4-DB eq.). The results of this characterization can be seen in **Table 5**.

Table 5: Life Cycle Impacts of PV Microgrids per Kwh. Comparison of the life cycle climate change (kg CO₂e), freshwater eutrophication (kg P eq.), human toxicity (kg 1,4-DB eq.), particulate matter formation (kg PM₁₀ eq.), photochemical oxidant formation (kg NMVOC), terrestrial acidification (kg SO₂ eq.), and terrestrial ecotoxicity (kg 1,4-DB eq.) impacts of PV-Battery, PV-Diesel, and PV-Hybrid microgrids. Red highlights indicate the max value in a category, while green and yellow highlights indicate the lowest and the middle values, respectively.

Category	PV-Battery	PV-Diesel	PV-Hybrid
Climate change [kg CO ₂ -Equiv.]	1.10E-01	9.71E-01	2.67E-01
Freshwater Eutrophication [kg P eq.]	2.03E-04	4.13E-05	2.04E-04
Human toxicity [kg 1,4-DB eq.]	4.46E-01	7.65E-02	4.44E-01
Particulate matter formation [kg PM ₁₀ eq.]	4.25E-04	5.74E-03	1.34E-03
Photochemical Oxidant Formation [kg NMVOC]	5.13E-04	1.75E-02	3.26E-03
Terrestrial Acidification [kg SO ₂ eq.]	1.34E-03	1.06E-02	3.02E-03
Terrestrial Ecotoxicity [kg 1,4-DB eq.]	1.27E-04	3.43E-04	1.82E-04

The initial characterizations suggest there are substantial differences between the three microgrid systems. These results, however, should be tempered because of the inherent uncertainty associated with the characterization factors themselves. The generally accepted default rules for the impact categories chosen are as follows (Jolliet et al., 2015):

- For CO₂, any difference less than 10% can be considered insignificant at first glance.
- For respiratory inorganic effects or acidification and eutrophication, the difference between two scenarios should typically be greater than 30% to be significant.

- For toxicity characterization, the calculation of impacts often involves more uncertainty, requiring a difference of at least one to two orders of magnitude (Ecotoxicity one to three) between scenarios to be considered significant.

Applying these rules to the life cycle impacts above, it can be seen that, on the surface, the differences in climate change impact between the three systems are very likely to be significant. For eutrophication, the difference between the PV-Diesel and the other systems is also likely to be significant, but the difference between the PV-Battery and PV-Hybrid is not. In human toxicity, the difference isn't likely to be significant in the three systems. Acidification differences are likely to be significant between all three systems. While there are no established rules for particulate matter and photochemical oxidant formation, the magnitude of the system differences suggests that they are likely to be significant. This conclusion is further supported because of significant differences in the likely highly correlated impact categories of climate change and terrestrial acidification. Finally, the ecotoxicity results are not likely to be significant. A graph of percent impact in relation to the PV-Battery baseline can be seen below (**Figure 8**).

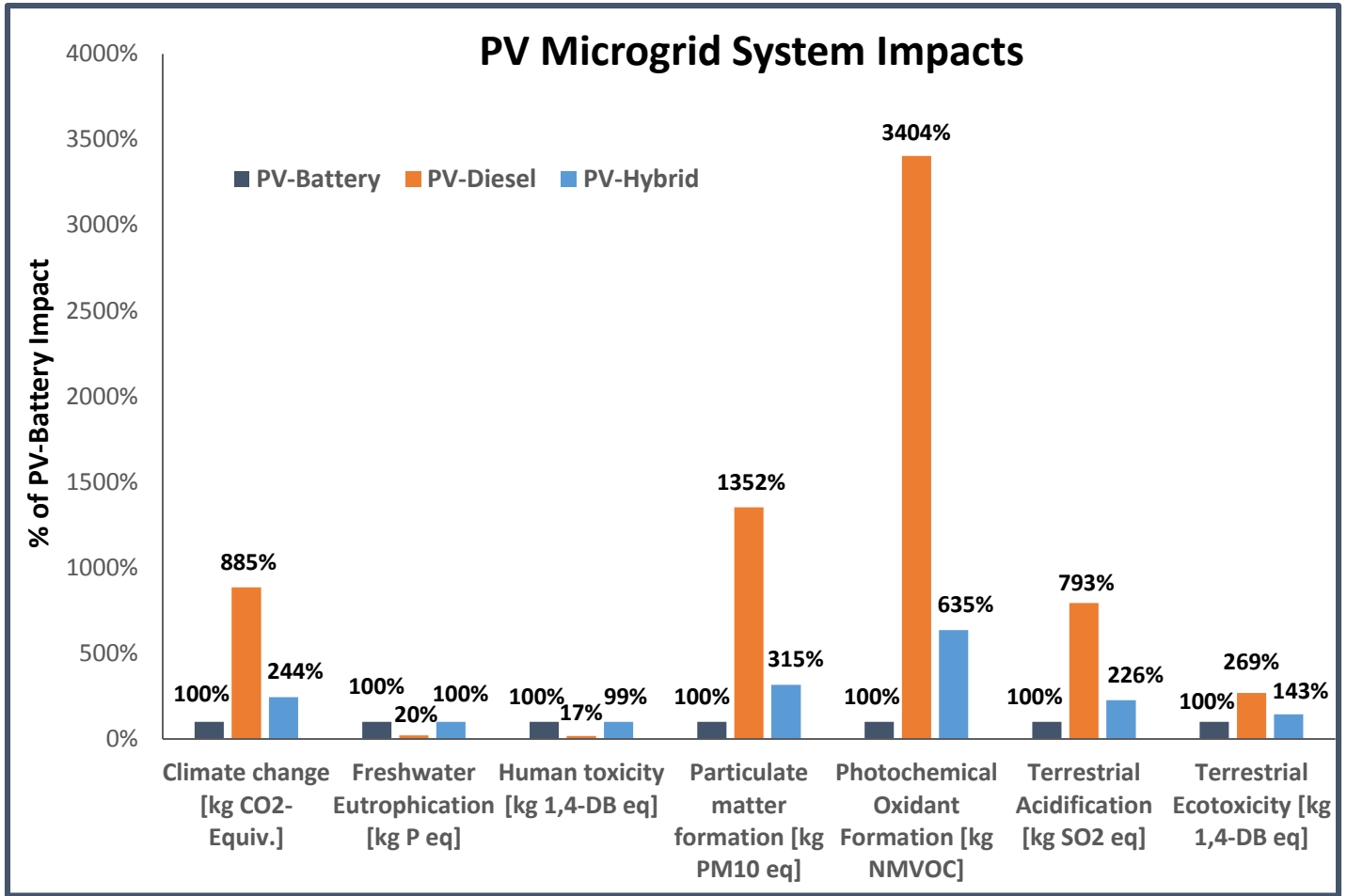


Figure 8: Comparison of PV Microgrid Life Cycle Impacts. Comparison of the life cycle climate change (kg CO₂e), freshwater eutrophication (kg P eq.), human toxicity (kg 1,4-DB eq.), particulate matter formation (kg PM₁₀ eq.), photochemical oxidant formation (kg NMVOC), terrestrial acidification (kg SO₂ eq.), and terrestrial ecotoxicity (kg 1,4-DB eq.) impacts of PV-Battery (dark blue), PV-Diesel (orange), and PV-Hybrid (light blue) microgrids. All impacts are presented as a percent of the PV-Battery impact.

Elementary Flow Analysis

To better assess the significance of the impact differences between categories, an analysis of elementary flows was conducted to compare the microgrid systems. The elementary flow analysis focused on the PV-Battery and PV-Diesel systems in order to understand the impact differences between a battery backup and a diesel generator backup.

As might be expected, carbon dioxide emissions to air contributed 92.6% and 96.4% of the climate change impacts for the PV-Battery and PV-Diesel systems, respectively. In both systems, methane was the next largest contributor at 4.9% and 1.4%, respectively. In the PV-Diesel system, 97% of the impacts came from the production and burning of diesel fuel. The burning of diesel in the PV-Diesel microgrid alone was more than 3 times the impact from the entire PV-

Hybrid system and more than eight times the impact of the entire PV-Battery system. Given this, it is highly likely that the climate change differences are significant.

In the eutrophication category, the flow of phosphate to freshwater accounted for the vast majority (99%) of the eutrophication impacts in both systems. In the PV-Battery system, the copper production process for copper used in the production of the battery anode accounted for 58.8% of the total phosphate flows. The PV-Diesel system had 60% of its impact from the production of diesel fuels. This supports the conclusion that the eutrophication differences between the PV-Battery/PV-Hybrid and the PV-Diesel systems are likely to be significant since the PV-Battery and PV-Hybrid systems have the same impacts from the module and BOS, as well as the substantive additional impact from the battery.

For human toxicity, the majority of the impacts in both systems came from the emission of Manganese (+II) to fresh water. In total, the emission of manganese (+II) caused 51.4% of the PV-Battery impact and 38.4% of the PV-Diesel impact. In the PV-Battery system, 60% of these manganese emissions (31% of the total human toxicity impact) came from the copper in the battery anode. On the other hand, the diesel production accounted for the largest portion (~40%) of the manganese (+II) emissions from the PV-Diesel system. The next largest contributors to the PV-Battery and PV-Diesel systems were arsenic (+V) to fresh water (14.6%, 8.9%, respectively), arsenic to air (12.1%, 6.2%), and lead to air (8.9%, 7.2%). Similar to the Manganese (+II), the copper in the battery and the production of diesel fuels were the largest contributors. The PV-Diesel system also had 7% of its impact come from chlorine emissions to industrial soil, mostly from the burning of diesel. The additional impacts from the battery are a little under one order of magnitude in each of the top four emissions. With this in mind, the differences in human toxicity are not likely to be significant.

Particulate matter impacts varied substantially between the microgrid systems. In the PV-Battery system, 52.2% of the PM impacts came from sulfur dioxides, 18.3% from nitrogen dioxides, 16.2% from dust $PM_{2.5}$, and 10.8% from dust $PM_{2.5-10}$. For the sulfur dioxides, the nickel, cobalt, and manganese in the cathode were the largest contributors, while the nitrogen dioxides largely came from the electricity consumption during battery cell manufacturing. For the dust emissions, the copper in the battery anode was the largest contributor. As a result of the burning of diesel fuels, the PV-Diesel system had 59.7% of the total PM impacts come from nitrogen oxides, 33% from dust $PM_{2.5}$, and just 6.5% from sulfur dioxides. In total over 99% of the PM impacts came from the production and burning of diesel fuels. With no established rules for PM formation it is difficult to fully determine the significance of the PM differences, but based on the magnitude of the differences it is likely that the PM impacts are significant, particularly on the ground in the off-grid communities where the impacts from the diesel burning are seen.

The photochemical oxidant category followed a similar story. For the PV-Battery system, 69.2% of the impacts came from nitrogen oxides, 17.4% came from sulfur dioxide, and 8.8% came from unspecified NMVOCs. The copper in the battery anode as well as the nickel, manganese, and cobalt in the battery cathode combined for over 26% of the total POCP impact. For the PV-

Diesel system, the POCP impacts were dominated by nitrogen oxides (89.2%). The next largest contributor was unspecified NMVOCs at 7.5% of the total impact. In total, over 99% of the POCP impacts for the PV-Diesel system are attributed to the production and burning of diesel fuels (94.2% burning, 5.2% production). Like PM, there was no general rule for photochemical oxidants, but given the magnitude of the impact differences and the likelihood that the impacts from the PV-Diesel will occur locally, it is likely that the POCP differences are significant.

In the terrestrial acidification category, the PV-Battery system saw the majority of its impacts come from emissions of sulfur dioxide (82.2%). 56% of these sulfur dioxide emissions came from the nickel, manganese, and cobalt in the battery cathode and the copper in the battery anode. Nitrogen oxides were the next largest elementary flow at 14.8% with the metals again causing the majority of these emissions. In total, just those four metals in the cathode and anode processes caused 50.1% of the acidification impact for the PV-Battery system. For the PV-Diesel system, the elementary contributions flipped with 82.3% of the impacts coming from nitrogen oxides and 17.7% coming from sulfur dioxide. As was seen in other categories, the burning and production of diesel fuels accounted for over 98% of these impacts. Given the suggested margin of 30% and the difference in elementary flows it is highly likely that the differences in the acidification category are significant.

Finally, in the ecotoxicity impact category, the largest elementary flow contributions for the PV-Battery system came from the emission of chlorine to industrial soil (42.1%) and copper (+II) to air (37.6%). Most of these emissions came from the copper used in the battery anode process as well as the metal working factory. Whereas in the PV-Diesel system, over 74% of the total ecotoxicity impact came from chlorine emissions to industrial soil of which over 97% was from the burning of diesel fuel. Since the overall differences are not even one order of magnitude, and the impacts are coming from different flows, it is difficult to conclude whether any of the ecotoxicity differences are significant or just the result of errors in the characterization factors.

As a result of the uncertainties in these impact categories, the remaining results explore the climate change, particulate matter, photochemical oxidant formation, and terrestrial acidification impact categories because our results are well within the suggested margin of error for those categories and they are likely highly correlated with each other. The remaining impact categories are revisited in the recycling and tradeoffs section.

Microgrid Comparisons

Microgrids versus Small-scale Diesel Gensets

Compared to the potentially available electricity generation technologies in these off-grid communities, namely small scale diesel generators, all three microgrid systems have substantial climate change, particulate matter, photochemical oxidant formation, and acidification savings per kilowatt hour of electricity produced in the model village. Of the three microgrid systems, the PV-Battery system had the lowest impact across the four categories (**Figure 9**). Overall this analysis suggests that PV microgrids save 31-92% in climate change, 32-95% in particulate

matter, 32-98% in photochemical oxidant formation, and 32-91% in acidification impacts compared to small scale diesel generators (Table 6).

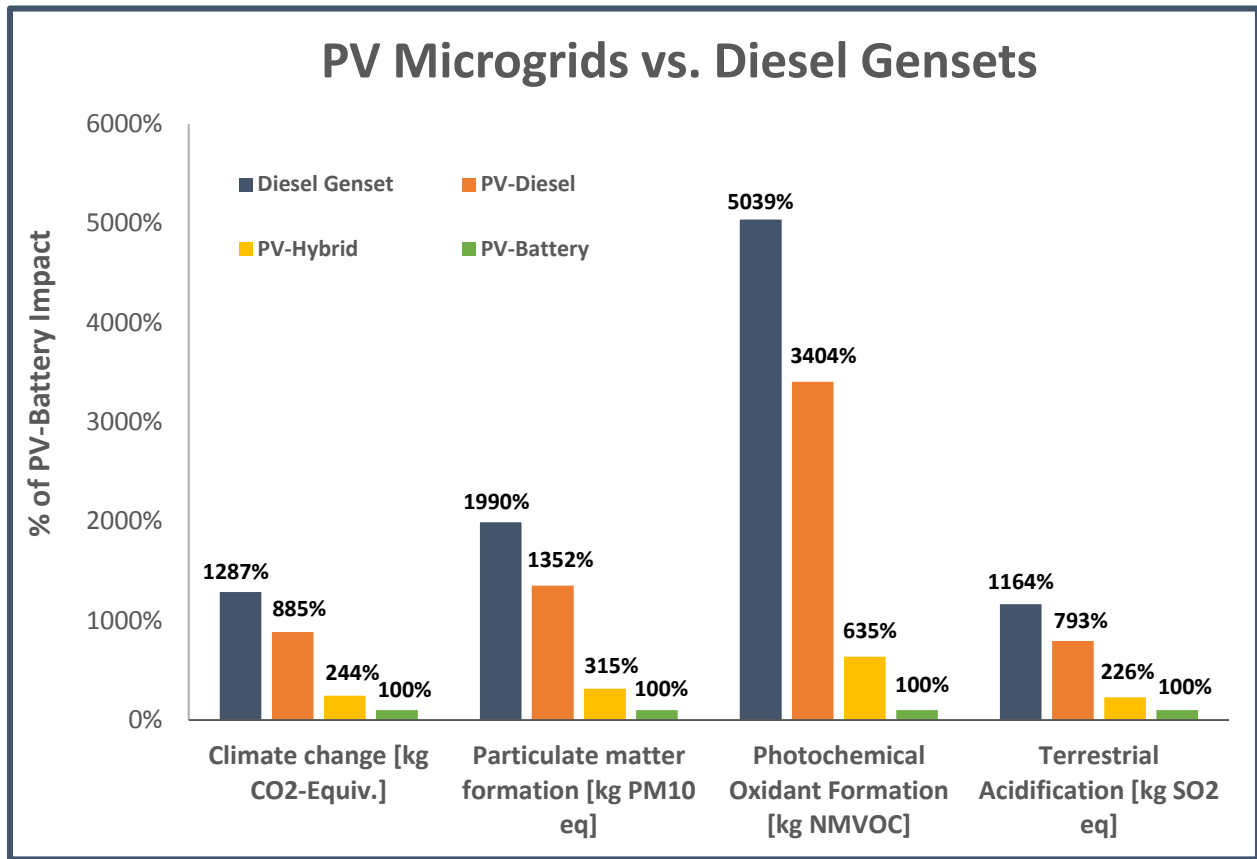


Figure 9: Category Impacts per kWh of PV Microgrids and Home Diesel Gensets. Comparison of per kWh climate change (kg CO₂e), particulate matter formation (kg PM₁₀ eq.), photochemical oxidant formation (kg NMVOC), and terrestrial acidification (kg SO₂ eq.) impacts of home diesel gensets (dark blue), PV-Diesel (orange), PV-Hybrid (yellow), and PV-Battery (green) systems. All impacts are presented as a percent of the PV-Battery impact.

Table 6: Category Impacts per kWh of PV-Battery Microgrids and Home Diesel Gensets. Comparison of per kWh climate change (kg CO₂e), particulate matter formation (kg PM₁₀ eq.), photochemical oxidant formation (kg NMVOC), and terrestrial acidification (kg SO₂ eq.) impacts of PV microgrid systems and home diesel gensets.

Impact Category	Diesel Genset	PV-Diesel	PV-Hybrid	PV-Battery
Climate Change [kg CO ₂ -Equiv.]	1.41E+00	9.71E-01	2.67E-01	1.10E-01
Particulate matter formation [kg PM ₁₀ eq.]	8.45E-03	5.74E-03	1.34E-03	4.25E-04
Photochemical Oxidant Formation [kg NMVOC]	2.59E-02	1.75E-02	3.26E-03	5.13E-04
Terrestrial Acidification [kg SO ₂ eq.]	1.56E-02	1.06E-02	3.02E-03	1.34E-03

Microgrids versus Traditional Electrification

This analysis modelled two grid mixes in Kenya, average and marginal, in order to compare the impacts of different electrification solutions. The marginal grid mix had higher impacts in the climate change (59% higher), particulate matter (57%), and photochemical oxidant (55%) categories, but lower impacts (8% lower) in the acidification category due to less heavy fuel oil utilization. Compared to this marginal electricity grid mix in Kenya, the PV-Battery system saves 66-81% per kWh depending on the impact category. The PV-Hybrid system saves 22-54% in the climate change, particulate matter, and acidification categories but actually appears to have 34% higher impacts in the photochemical oxidants category. Finally, the PV-Diesel appears to have higher impacts per kWh in all four categories compared to the marginal grid mix (**Figure 10**) (**Table 7**). However, it should be noted that the impact estimates for the Kenya electricity grids don't include the impacts of extending the central grid to the off-grid community. For example, a life cycle analysis of electricity infrastructure found that these impacts could range from 12.6-52.1 tons of CO₂e/km for low voltage transmission lines (1 kv), 18.4-56.7 tons of CO₂e/km for medium voltage (1kv-24kv), 43.1-178 tons of CO₂e/km for high voltage (>24 kv), and 336 tons of CO₂e/km for long distance lines (Itten, Frischknecht, & Stucki, 2014). While not all of this impact can be attributed to a single kWh from the Kenya grid, it does suggest that the real impacts from grid extension are likely much higher.

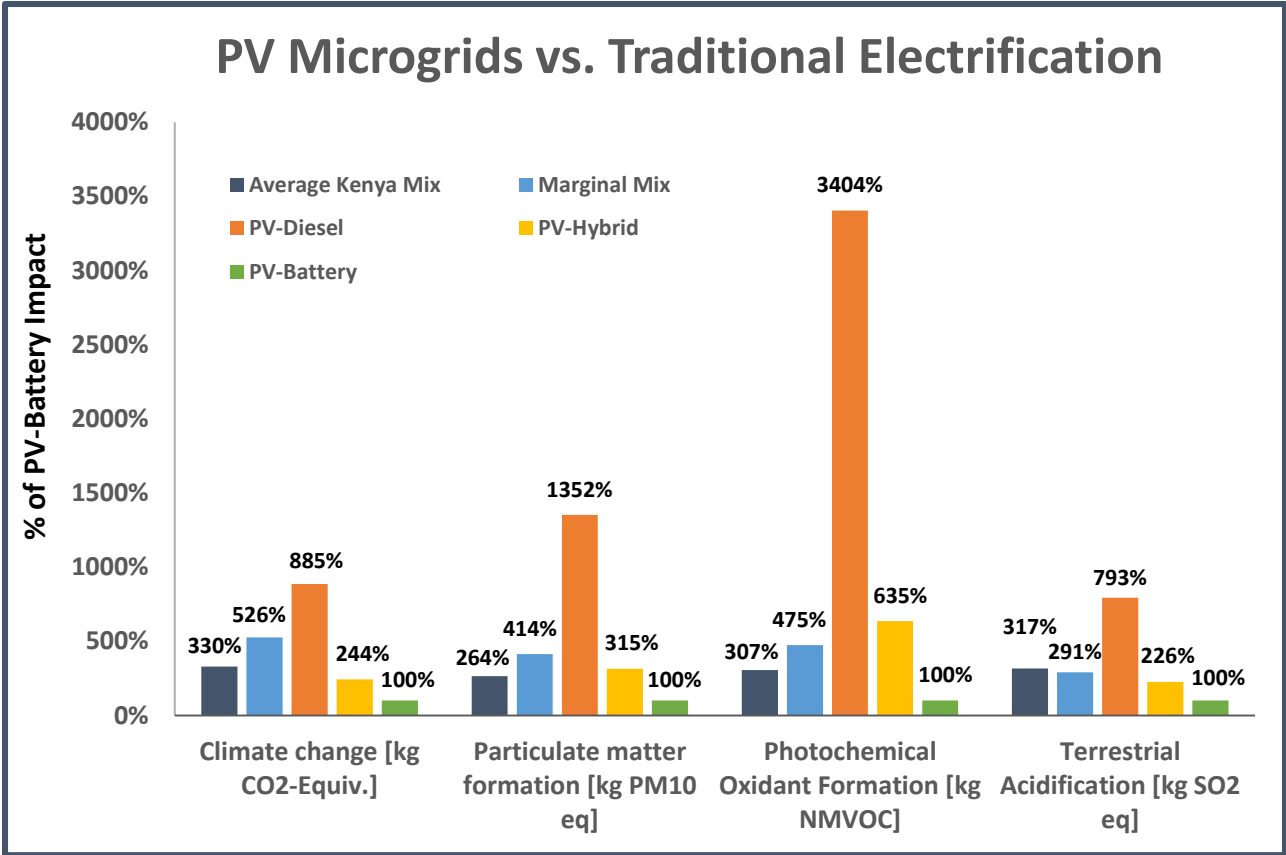


Figure 10: Category Impacts per kWh of PV Microgrids and Traditional Electrification. Comparison of per kWh climate change (kg CO₂e), particulate matter formation (kg PM₁₀ eq.), photochemical oxidant formation (kg NMVOC), and terrestrial acidification (kg SO₂ eq.) impacts of the average Kenya grid mix (dark blue), marginal Kenya mix (light blue), PV-Diesel (orange), PV-Hybrid (yellow), and PV-Battery (green) systems. All impacts are presented as a percent of the PV-Battery impact.

Table 7: Category Impacts per kWh of PV-Battery Microgrids and Traditional Electrification. Comparison of per kWh climate change (kg CO₂e), particulate matter formation (kg PM₁₀ eq.), photochemical oxidant formation (kg NMVOC), and terrestrial acidification (kg SO₂ eq.) impacts of PV microgrid systems and traditional electrification solutions.

Impact Category	Average Grid Mix Kenya	Marginal Grid Mix Kenya	PV-Diesel	PV-Hybrid	PV-Battery
Climate Change [kg CO ₂ -Equiv.]	3.62E-01	5.77E-01	9.71E-01	2.67E-01	1.10E-01
Particulate Matter Formation [kg PM ₁₀ eq.]	1.12E-03	1.76E-03	5.74E-03	1.34E-03	4.25E-04
Photochemical Oxidant Formation [kg NMVOC]	1.57E-03	2.44E-03	1.75E-02	3.26E-03	5.13E-04
Terrestrial Acidification [kg SO ₂ eq.]	4.24E-03	3.88E-03	1.06E-02	3.02E-03	1.34E-03

PV-Battery Contribution Analysis

With clear particulate matter, photochemical oxidant formation, and acidification benefits compared to the small scale and traditional electrification solutions, this analysis looked closer at the individual contributions of the microgrid components in the baseline PV-Battery system (contribution analysis for the other two systems can be seen in **Appendix 4**). For the baseline PV-Battery system, 72-80% of the climate change, particulate matter, photochemical oxidant, and acidification impacts come from the lithium-ion batteries. The next largest contributors were the CdTe module at 10-12%, and the balance of systems at 5-10% of the total impact (**Figure 11**).

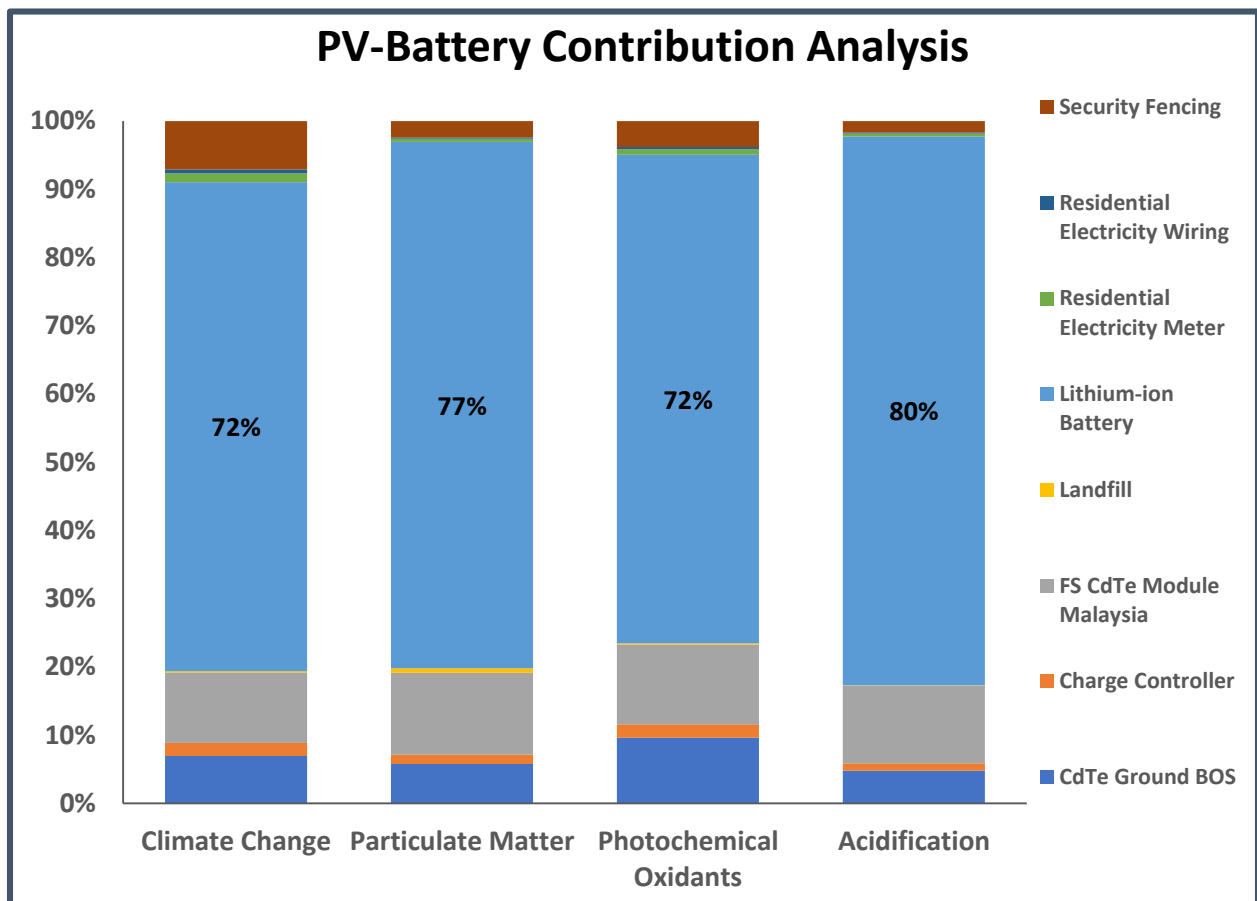


Figure 11: Contribution Analysis of PV-Battery Components. Contribution of individual PV-Battery microgrid components to overall microgrid climate change (kg CO₂e), PM (kg PM₁₀ eq.), photochemical oxidant formation (kg NMVOC), and terrestrial acidification (kg SO₂ eq.) impacts.

For climate change, the battery contributions amount to 78.6 grams of CO₂e, 3.28e⁻⁰⁴ kg PM₁₀, 3.67e⁻⁰⁴ kg NMVOC, and 1.08e⁻⁰³ kg SO₂ per kWh. A closer look at the battery components reveals that 73-86% of the battery impacts come from the manufacturing of the battery cell (**Figure 12**).

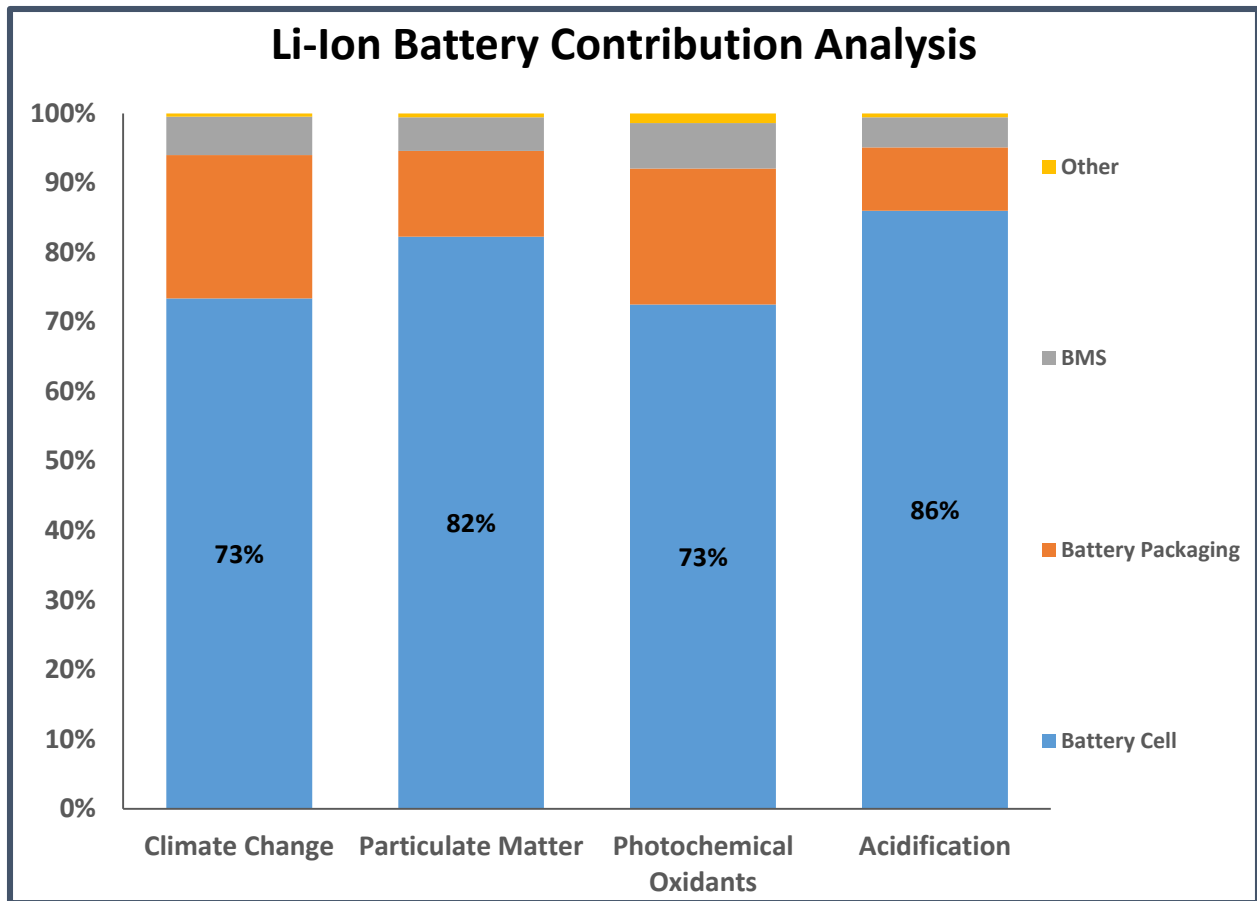


Figure 12: Contribution Analysis of Lithium-ion Battery Components. Contribution of individual lithium-ion battery components to overall Li-ion battery climate change (kg CO₂e), PM (kg PM₁₀ eq.), photochemical oxidant formation (kg NMVOC), and terrestrial acidification (kg SO₂ eq.) impact in the PV-Battery system.

Within the battery cell process, 69% of the climate change impact comes from the electricity utilized in the manufacturing process. The battery cell impacts for the other three categories are more evenly distributed, particularly for the POCP category where the cathode, anode, and electricity grid each accounted for approximately one third of the impact. In the PM and acidification categories, the battery cathode and anode accounted for approximately 40% of the impacts while the electricity grid mix contribution was just under 20% (Figure 13).

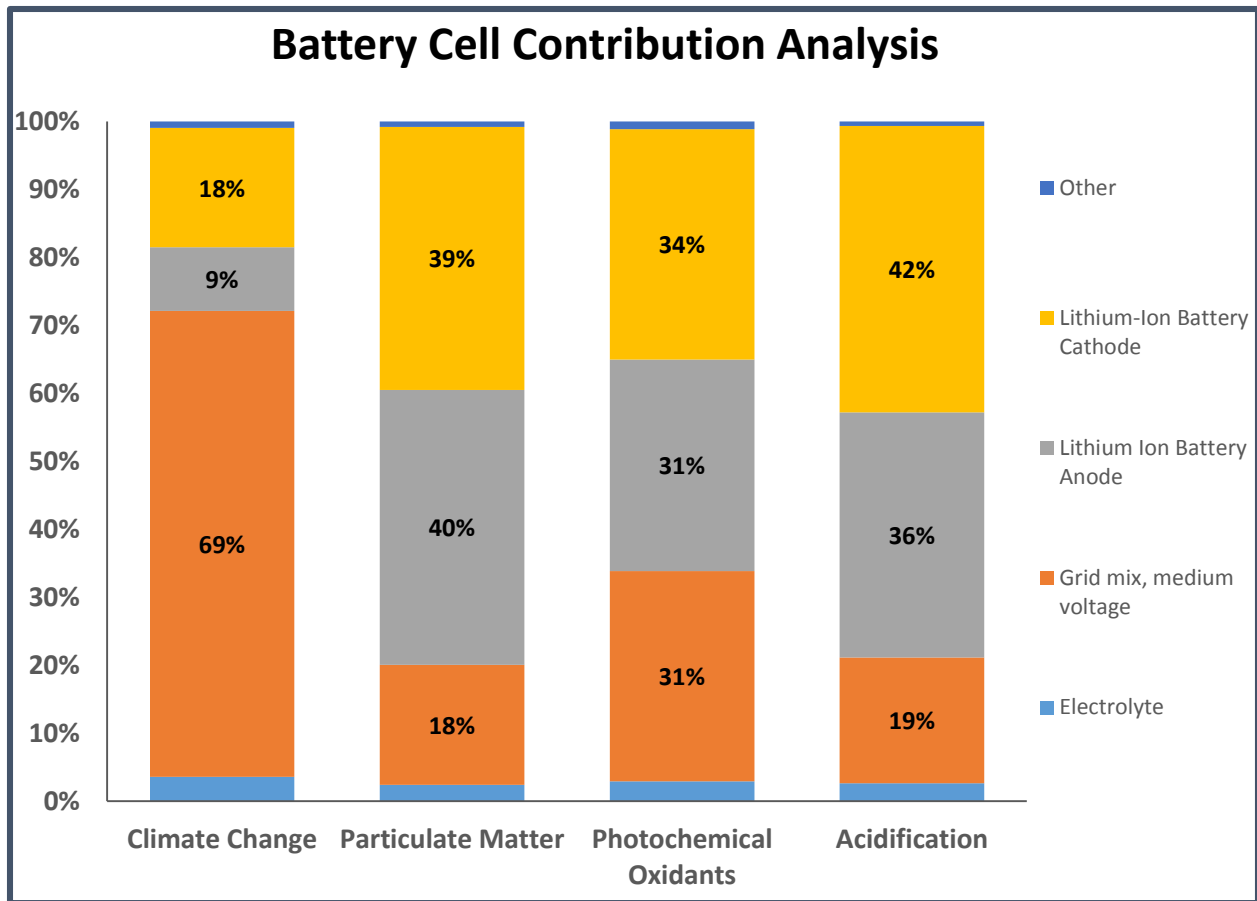


Figure 13: Contribution Analysis of Battery Cell Components. Contribution of individual battery cell components to overall Li-ion battery climate change (kg CO_{2e}), PM (kg PM₁₀ eq.), photochemical oxidant formation (kg NMVOC), and terrestrial acidification (kg SO₂ eq.) impact in the PV-Battery system.

This indicates that about 50% of the total battery climate change impact and 36% of the total microgrid climate change impact comes from the electricity used in the manufacturing of the battery cell. The battery grid mix also contributed 11-16% of the total impacts in the other categories. This suggests an opportunity to significantly lower the climate change impact of PV-Battery microgrids by utilizing lower carbon electricity sources in battery cell manufacturing (**Scenario 1**).

For the other categories, 47-67% of the total battery impact and 34-53% of the total microgrid impacts come from the cathode and anode production in the battery cell. The elementary analysis in this study suggests that most of these impacts result from the utilization of copper and other metals like cobalt and manganese in the cathode and anode processes. The impacts of this primary material use are explored further in **Scenario 2**.

Scenario 1: Electricity Grid Mix for Battery Manufacturing

To explore the impact of battery electricity use on the overall microgrid impact, a scenario was run, which substitutes five electricity mixes for the baseline European grid mix in the battery production process. The electricity mixes used represent regions where lithium-ion battery manufacturing occurs, as well as an entirely photovoltaic grid mix to represent a zero emissions process. The results illustrate a large difference in climate change impacts depending on which electricity mix is used for battery manufacturing. For example, shifting the battery production from the baseline European grid mix to China increases the total microgrid impact by over 35%, whereas shifting from a generalized European grid to the grid in France or Switzerland decreases the overall impact by 18-27% (Figure 14).

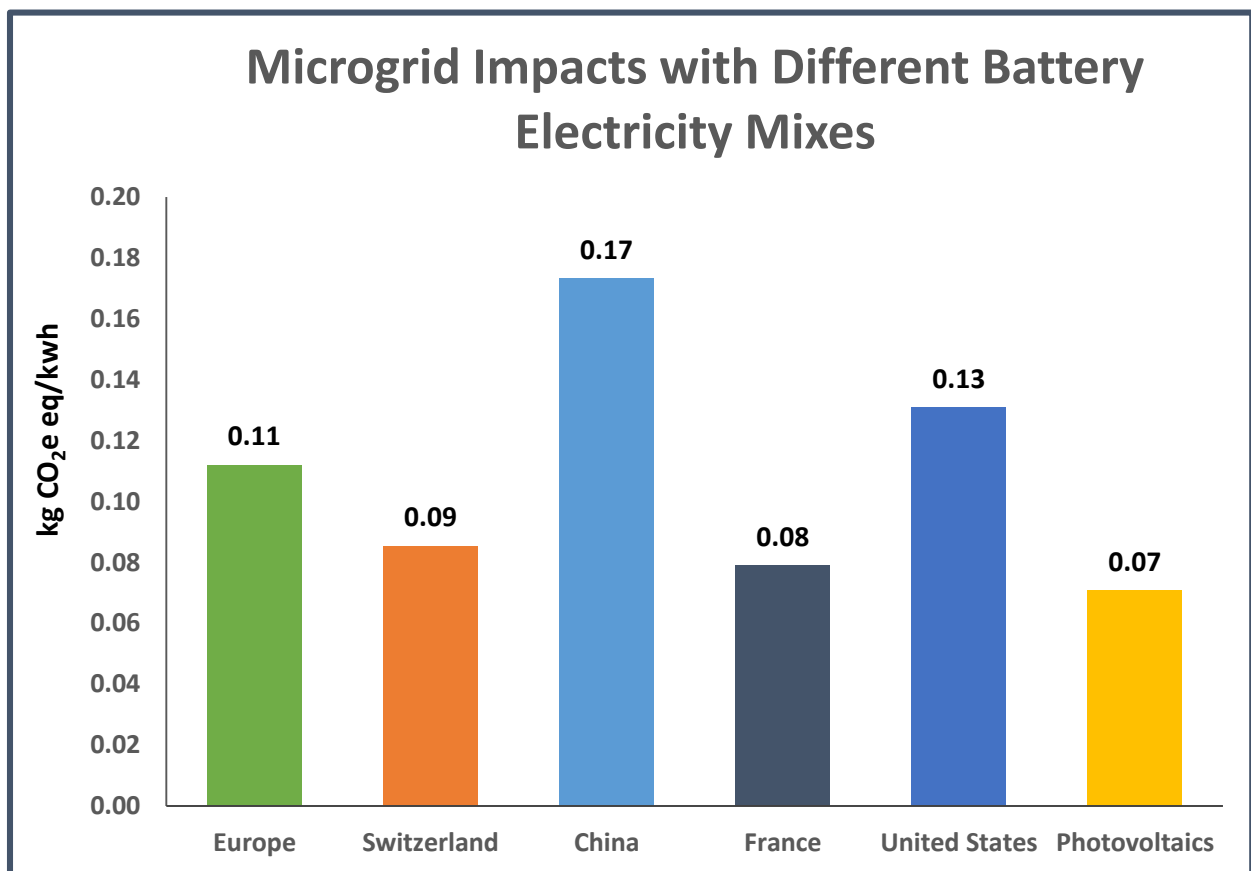


Figure 14: Battery Electricity Mix and PV-Battery Climate Change Impacts per kWh. Climate change impact of PV-Battery microgrids utilizing different electricity grid mixes for battery manufacturing. The baseline mix is Europe's electricity grid mix shown in green. The Photovoltaics category (yellow) represents using only PV electricity for battery manufacturing.

Since the battery grid mix accounted for a much smaller proportion of the particulate matter, photochemical oxidants, and acidification impacts, changing the grid mix didn't have as pronounced an impact as it did for the climate change category. The only differences of note

are seen if battery production is shifted to China. This shift results in approximately 30% higher impacts for the particulate matter, photochemical oxidants, and acidification categories.

Scenario 2: Microgrid End of Life Recycling

Recycling: PV-Microgrid Impacts

A scenario was also developed to test the impact of recycling the microgrids at the end of their usable lifetime rather than sending them to a landfill as was modelled in the baseline. For the PV-Battery baseline, substituting recycling for the landfill at end of life reduced the overall microgrid impacts 18-69% depending on the impact category. The largest savings were seen in the human toxicity and eutrophication categories in large part because of the avoided copper (Table 8).

Table 8: Category Impacts per kWh of PV-Battery Microgrids with Different End of Life Scenarios. Comparison of impacts across seven impact categories for PV-Battery microgrids with landfill versus recycling at end of life.

Impact Category	PV-Battery with Landfill	PV-Battery with Recycling	Impact/kWh Avoided	Impact Savings from Recycling
Climate change [kg CO ₂ -Equiv.]	1.10E-01	9.03E-02	1.94E-02	18%
Freshwater Eutrophication [kg P eq.]	2.03E-04	7.02E-05	1.33E-04	65%
Human toxicity [kg 1,4-DB eq.]	4.46E-01	1.40E-01	3.06E-01	69%
Particulate matter formation [kg PM ₁₀ eq.]	4.25E-04	2.52E-04	1.72E-04	41%
Photochemical Oxidant Formation [kg NMVOC]	5.13E-04	3.39E-04	1.74E-04	34%
Terrestrial Acidification [kg SO ₂ eq.]	1.34E-03	8.53E-04	4.84E-04	36%
Terrestrial Ecotoxicity [kg 1,4-DB eq.]	1.27E-04	8.24E-05	4.50E-05	35%

The PV-Hybrid system saw lower savings from landfill substitution (7-68%). The largest savings again came from the eutrophication and human toxicity categories (Table 9).

Table 9: Category Impacts per kWh of PV-Hybrid Microgrids with Different End of Life Scenarios. Comparison of impacts across seven impact categories for PV-Hybrid microgrids with landfill versus recycling at end of life.

Impact Category	PV-Hybrid with Landfill	PV-Hybrid with Recycling	Impact/kWh Avoided	Impact Savings from Recycling
Climate change [kg CO ₂ -Equiv.]	2.67E-01	2.39E-01	2.83E-02	11%
Freshwater Eutrophication [kg P eq.]	2.04E-04	7.32E-05	1.31E-04	64%
Human toxicity [kg 1,4-DB eq.]	4.44E-01	1.43E-01	3.00E-01	68%
Particulate matter formation [kg PM ₁₀ eq.]	1.34E-03	1.14E-03	2.02E-04	15%
Photochemical Oxidant Formation [kg NMVOC]	3.26E-03	3.04E-03	2.19E-04	7%
Terrestrial Acidification [kg SO ₂ eq.]	3.02E-03	2.48E-03	5.40E-04	18%
Terrestrial Ecotoxicity [kg 1,4-DB eq.]	1.82E-04	1.37E-04	4.58E-05	25%

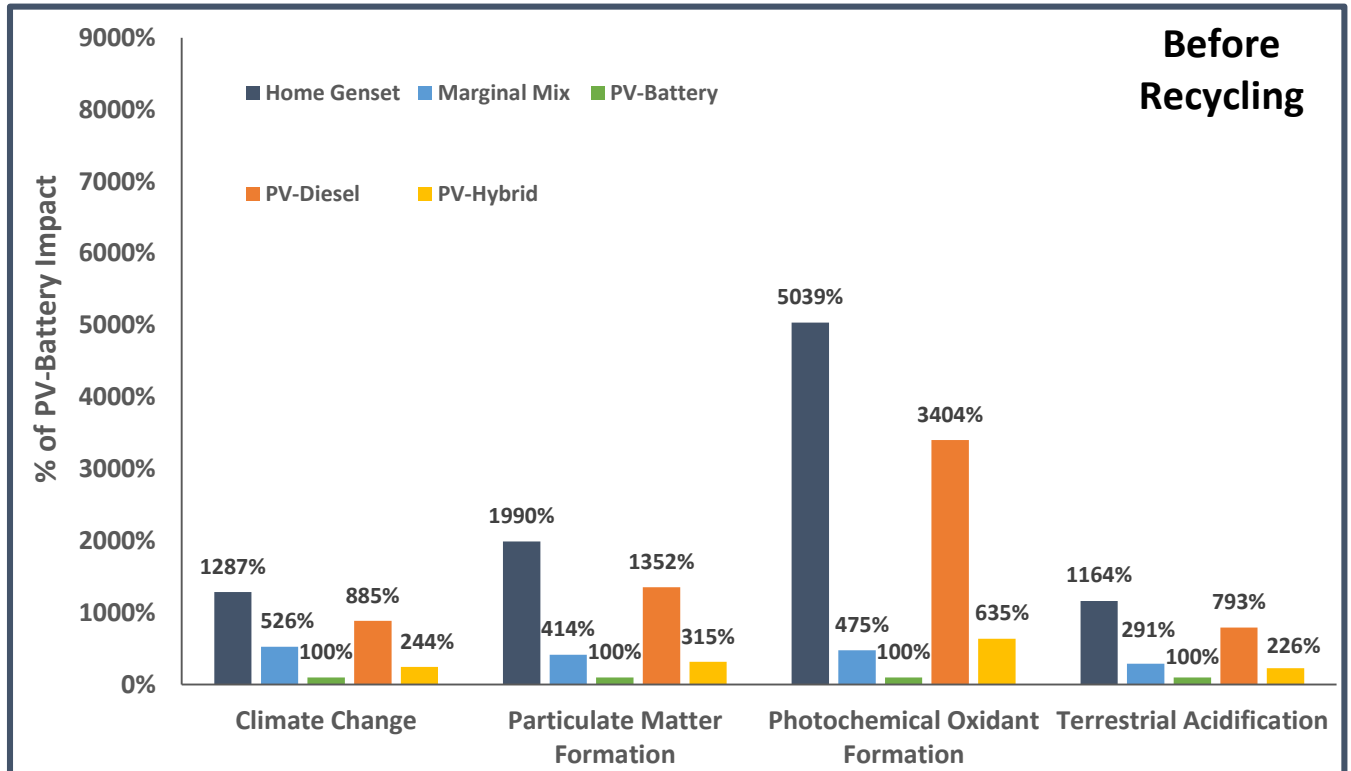
In contrast to the other two systems, recycling of the PV-Diesel system only had savings in the freshwater eutrophication and human toxicity categories. In both of those categories, recycling savings were 19-24%, whereas with climate change, particulate matter, photochemical oxidants, acidification, and ecotoxicity, the savings were in the 0-1% range (**Table 10**).

Table 10: Category Impacts per kWh of PV-Diesel Microgrids with Different End of Life Scenarios. Comparison of impacts across seven impact categories for PV-Diesel microgrids with landfill versus recycling at end of life.

Impact Category	PV-Diesel with Landfill	PV-Diesel with Recycling	Impact/kWh Avoided	Impact Savings from Recycling
Climate change [kg CO ₂ -Equiv.]	9.71E-01	9.63E-01	8.89E-03	1%
Freshwater Eutrophication [kg P eq.]	4.13E-05	3.33E-05	7.99E-06	19%
Human toxicity [kg 1,4-DB eq.]	7.65E-02	5.82E-02	1.83E-02	24%
Particulate matter formation [kg PM ₁₀ eq.]	5.74E-03	5.71E-03	3.60E-05	1%
Photochemical Oxidant Formation [kg NMVOC]	1.75E-02	1.74E-02	4.72E-05	0%
Terrestrial Acidification [kg SO ₂ eq.]	1.06E-02	1.05E-02	8.01E-05	1%
Terrestrial Ecotoxicity [kg 1,4-DB eq.]	3.43E-04	3.40E-04	3.31E-06	1%

Recycling: System Comparisons and Tradeoffs

Adding takeback and recycling to the end of life for these microgrid systems substantially affects the overall comparison of PV-microgrids to each other, to home diesel gensets and to traditional electrification solutions. Initially, PV-Battery microgrids showed significant savings in the climate change, particulate matter, photochemical oxidant, and acidification categories compared to home diesel gensets and traditional electrification as well as the other two PV microgrid systems. When recycling was added, the comparative benefits of the PV-Battery system were enhanced in these categories (**Figure 15**).



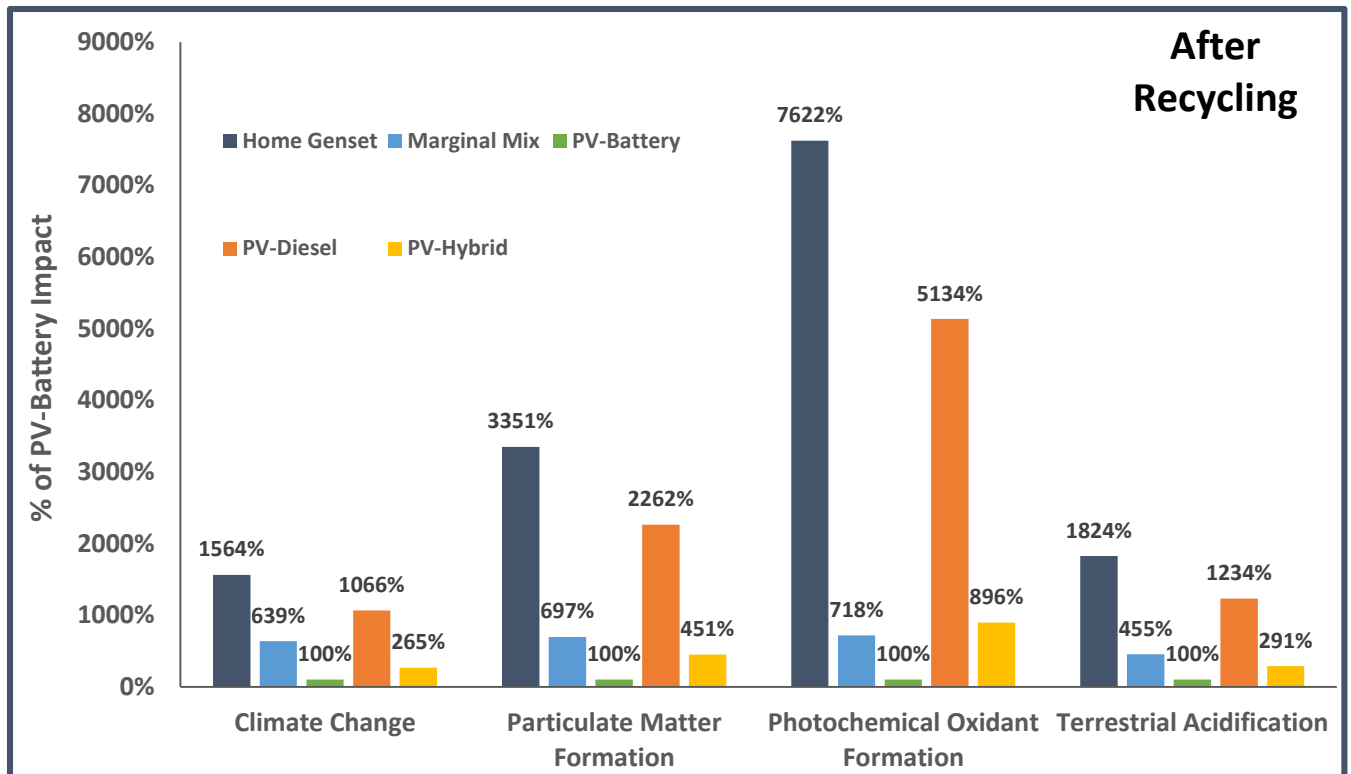


Figure 15: Comparison of PV Microgrid, Home Diesel Genset, and Traditional Electrification Impacts. Comparison of per kWh climate change (kg CO₂e), particulate matter formation (kg PM₁₀ eq.), photochemical oxidant formation (kg NMVOC), and terrestrial acidification (kg SO₂ eq.) impacts of home diesel gensets (dark blue), marginal Kenya mix (light blue), PV-Diesel (orange), PV-Hybrid (yellow), and PV-Battery (green) systems before (top graph) and after (bottom graph) recycling. All impacts are presented as a percent of the PV-Battery impact.

In the eutrophication, human toxicity, and ecotoxicity categories there initially were potential tradeoffs between PV microgrids and the home gensets and traditional electrification solutions, particularly in the eutrophication category (significant differences are 30% rather than 1 to 3 orders of magnitude). While it doesn't eliminate the tradeoffs seen in these categories, adding recycling does dampen these tradeoffs for the PV-Battery, and to a lesser extent the PV-Hybrid, systems (**Figure 16**).

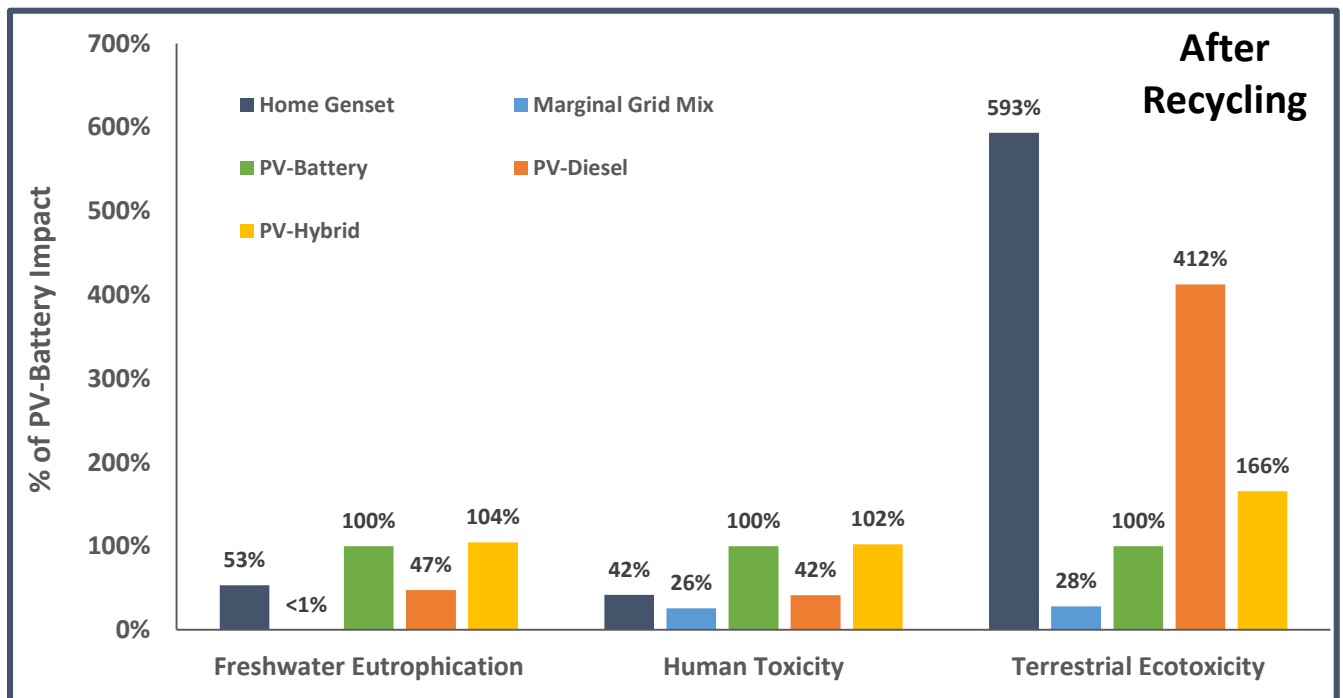
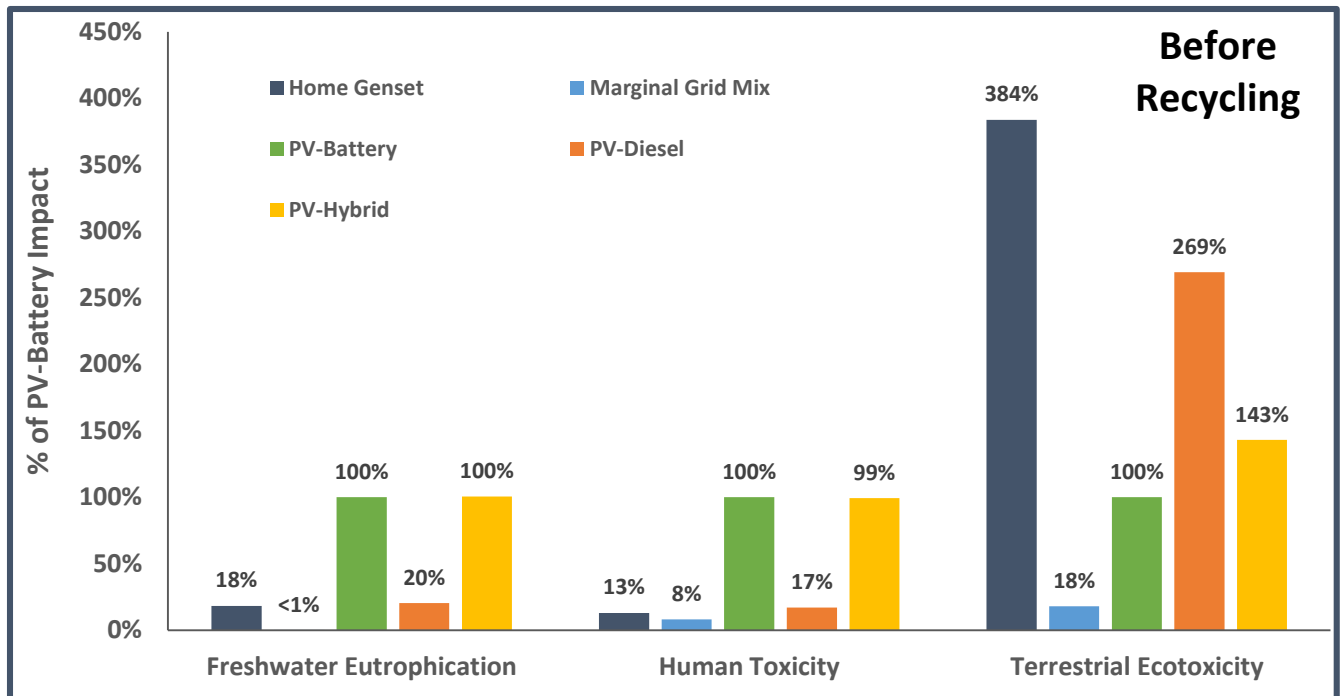


Figure 16: Comparison of PV Microgrid, Home Diesel Genset, and Traditional Electrification Impacts. Comparison of per kWh freshwater eutrophication (kg P eq.), human toxicity (kg 1,4-DB eq.), and terrestrial ecotoxicity (kg 1,4-DB eq.) impacts of home diesel gensets (dark blue), marginal Kenya mix (light blue), PV-Diesel (orange), PV-Hybrid (yellow), and PV-Battery (green) systems before (top graph) and after (bottom graph) recycling. All impacts are presented as a percent of the PV-Battery impact.

Scenario 3: Choice of PV Technology- CdTe vs. Mono-Si

Comparing the two PV modules across impact categories highlights some interesting tradeoffs. On the surface, it appears that using CdTe modules has lower impact in climate change, human toxicity, and terrestrial ecotoxicity, but higher impacts in eutrophication and particulate matter formation. Using the characterization rules outlined earlier, only the climate change difference is likely to be significant (**Figure 17**).

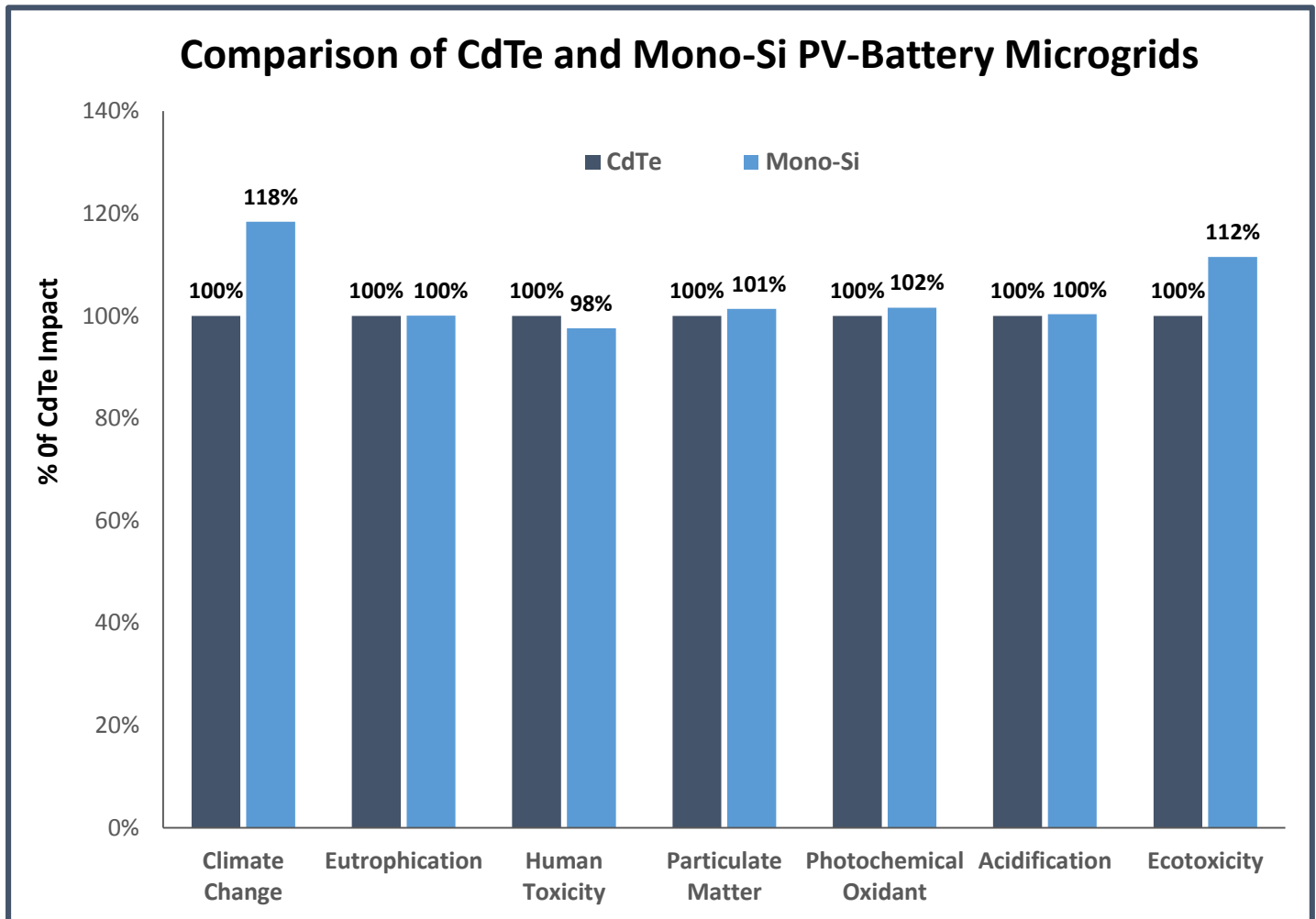
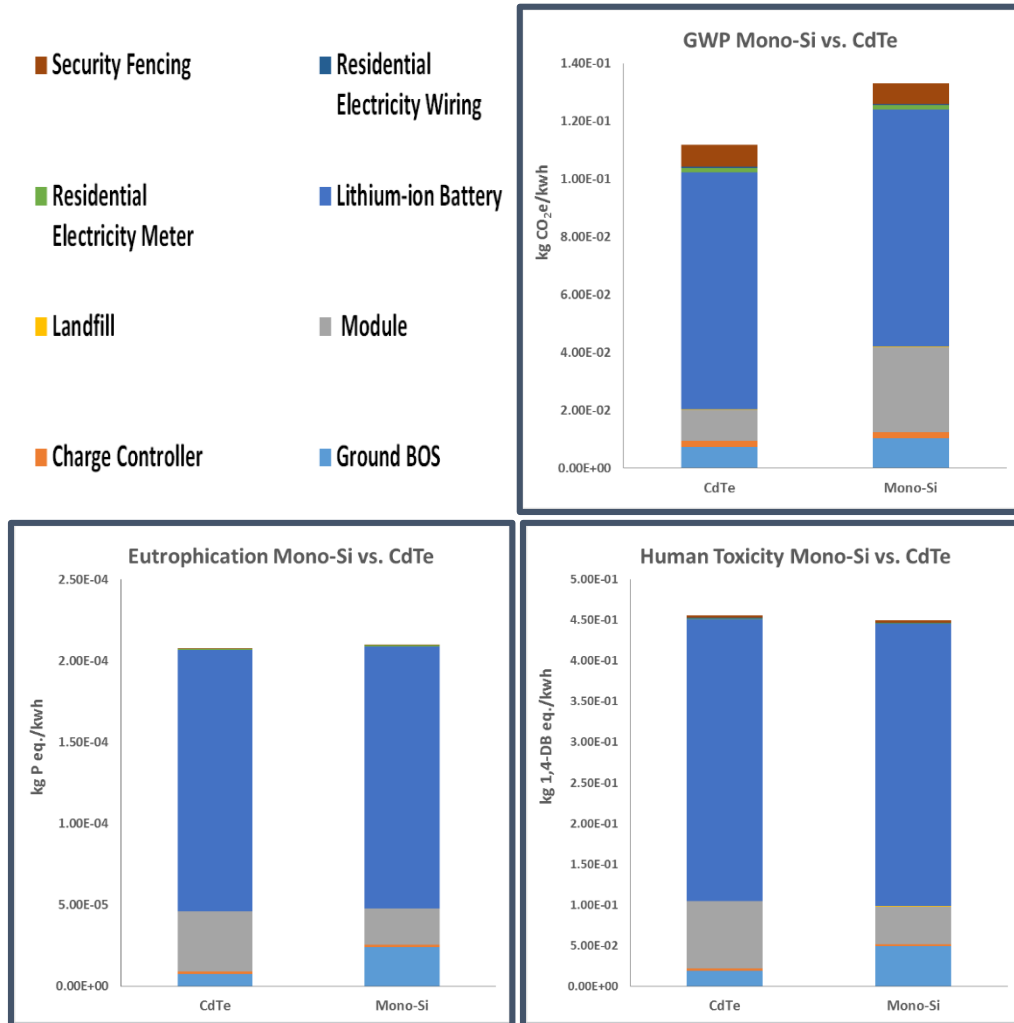


Figure 17: Comparison of PV Technology Life Cycle Impacts per kWh. Comparison of the life cycle climate change (kg CO₂e), freshwater eutrophication (kg P eq.), human toxicity (kg 1,4-DB eq.), particulate matter formation (kg PM₁₀ eq.), photochemical oxidant formation (kg NMVOC), terrestrial acidification (kg SO₂ eq.), and terrestrial ecotoxicity (kg 1,4-DB eq.) impacts of PV-Battery microgrids with CdTe (dark blue) and Mono-Si (light blue) modules. All impacts are presented as a percent of the CdTe impact.

As the graph above suggests, whether or not a savings benefit was realized by the switch of module technology varied by impact category. The differences between the two systems are largely accounted for by the differences in the individual module and BOS impacts. The difference in module impacts was the largest contributor to the overall impact difference in the climate change category. In total, the module climate change impacts increased 172% when

mono-Si was used instead of CdTe. The BOS differences were the largest contributor for the other categories. This is due in large part to the increase in size of the BOS needed for mono-Si panels. For the landfill impacts, the mono-Si modules were consistently 12% higher than the CdTe modules. The security fencing impacts, on the other hand, were consistently 8% lower using the mono-Si modules because there was less area used for the microgrid. Finally, the impacts of the charge controller, battery, electricity meter, and electricity wiring remained constant because the sizing of the components isn't contingent on module area or efficiency (Figure 18 and Table 11).



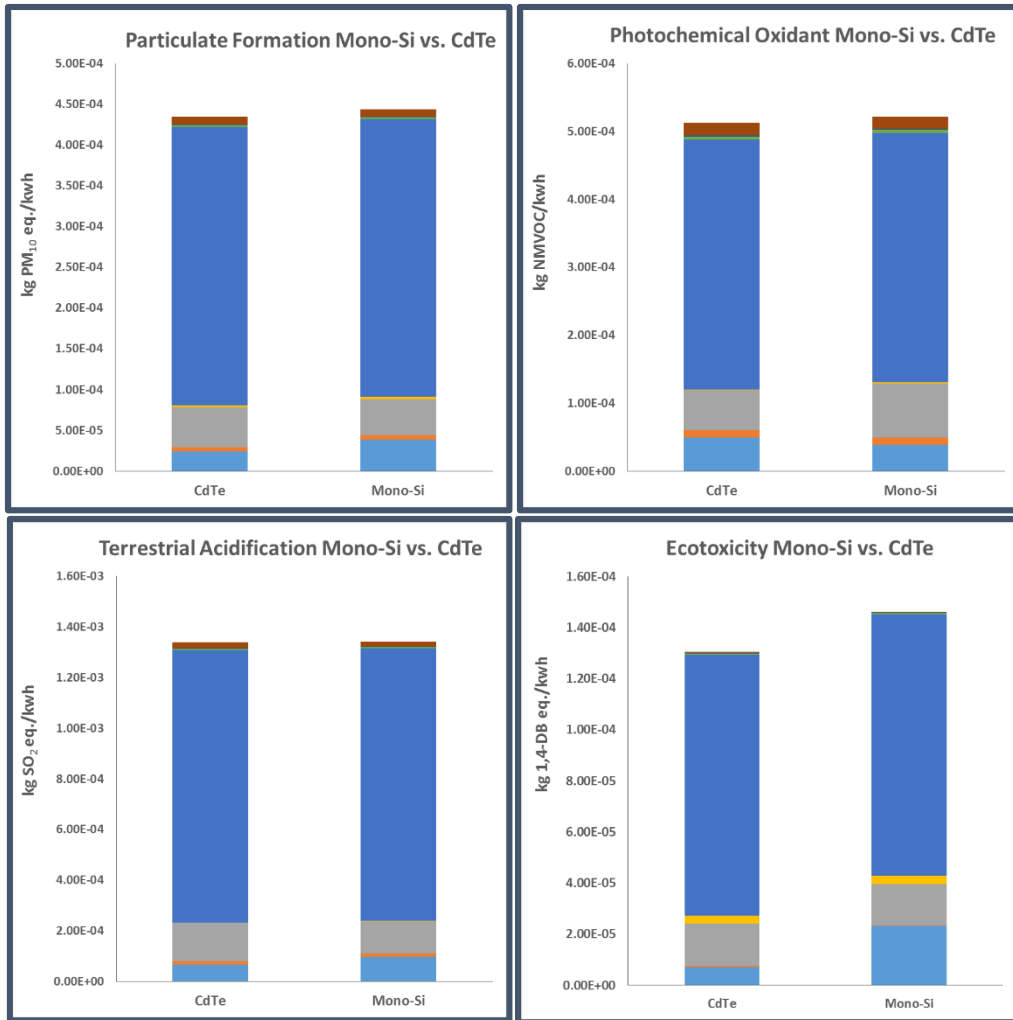


Figure 18: CdTe and Mono-Si PV-Battery Impact Comparison per kWh. Comparison of impacts for PV-Battery microgrid systems utilizing CdTe and mono-Si PV modules. From top to bottom and left to right, climate change (kg CO₂e), freshwater eutrophication (kg P eq.), human toxicity (kg 1,4-DB eq.), particulate matter formation (kg PM₁₀ eq.), photochemical oxidant formation (kg NMVOC), terrestrial acidification (kg SO₂ eq.), and terrestrial ecotoxicity (kg 1,4-DB eq.)

Table 11: Percent Change in Component Impact from Switching CdTe to Mono-Si. Change in component impact when if a Mono-Si PV-Battery microgrid was used instead of the baseline CdTe PV-Battery microgrid. Negative values indicate a decrease in impact when Mono-Si is used instead of CdTe. Orange highlights indicate the largest percent change in a given impact category.

Category	Ground BOS	Module	Landfill	Security Fencing
Climate change [kg CO2-Equiv.]	35%	161%	12%	-10%
Freshwater Eutrophication [kg P eq.]	199%	-41%	12%	-10%
Human toxicity [kg 1,4-DB eq.]	148%	-46%	12%	-10%
Particulate matter formation [kg PM10 eq.]	55%	-14%	12%	-10%
Photochemical Oxidant Formation [kg NMVOC]	-21%	34%	12%	-10%
Terrestrial Acidification [kg SO2 eq.]	47%	-16%	12%	-10%
Terrestrial Ecotoxicity [kg 1,4-DB eq.]	210%	-8%	12%	-10%

Since climate change is the only impact category that is likely to be significant for this scenario, the impact of CdTe and mono-Si modules on the overall climate change impact of the three microgrid systems was tested. The CdTe modules had lower impact for all three microgrid designs saving between 6 and 20 grams of CO₂e per kWh compared to the mono-Si modules (Figure 19).

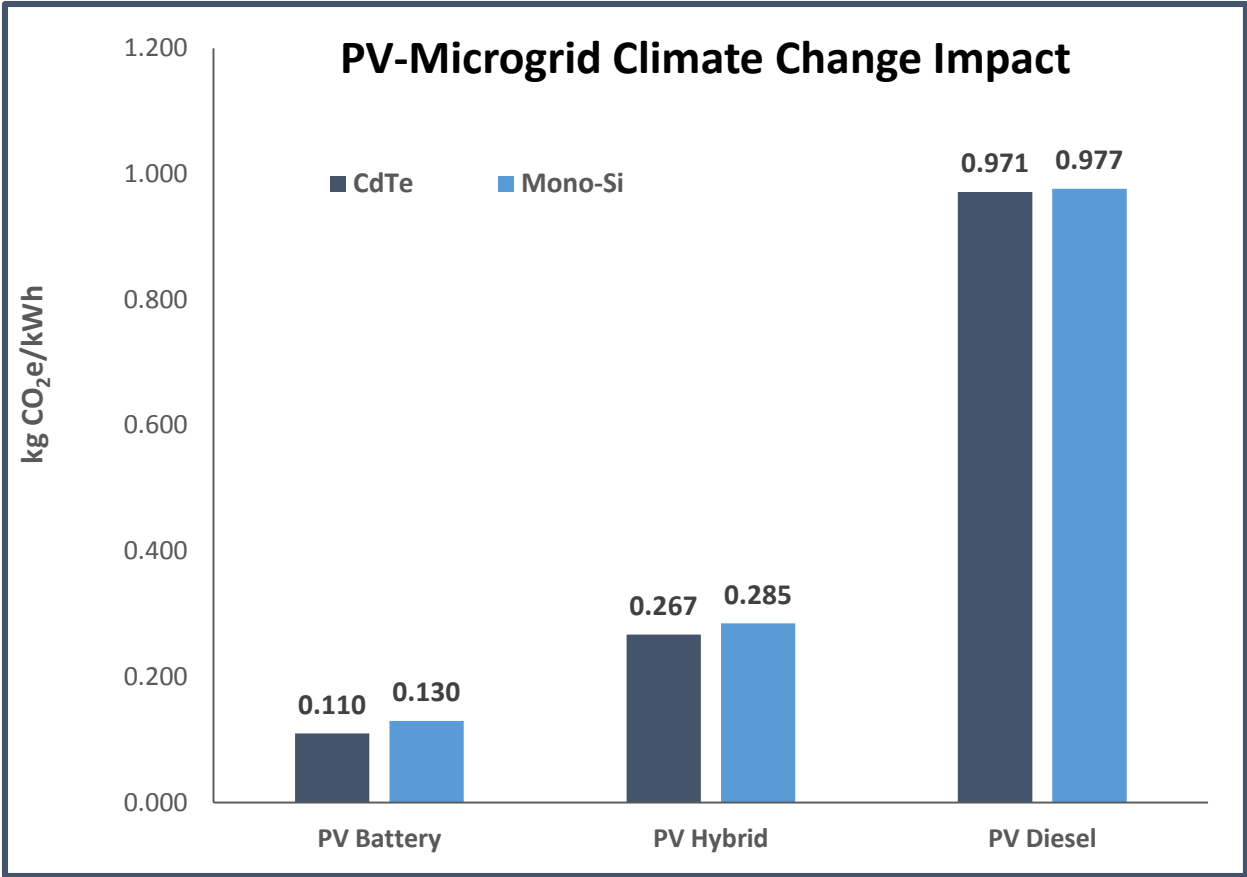


Figure 19: Climate Change Comparison per kWh of PV technology in PV Microgrids. Climate change impact per kWh of PV microgrids using CdTe (dark blue) and Mono-Si (light blue) PV modules.

Scenario 4: Application to Larger Scales - Powerhive’s Planned Expansion

A recent announcement from microgrid developers, Powerhive and ENEL, unveiled a portfolio of solar microgrids totaling 1 MW of installed capacity, proposing to power almost 90,000 people in Western Kenya (Van Gerven, 2015). Due to the structure of this model, almost all the components of microgrids scale linearly with the total daily demand. The only exception to this linearity is the security fencing length, which changes proportionally to the square root of the change in the total daily demand. Therefore, the environmental impact of the microgrid remains almost the same when calculated per unit kWh of electricity produced. Only a nominal change is observed in the system impact per kWh from varying the total daily demand, attributed to the non-linearity of the security fencing length (Figure 20).

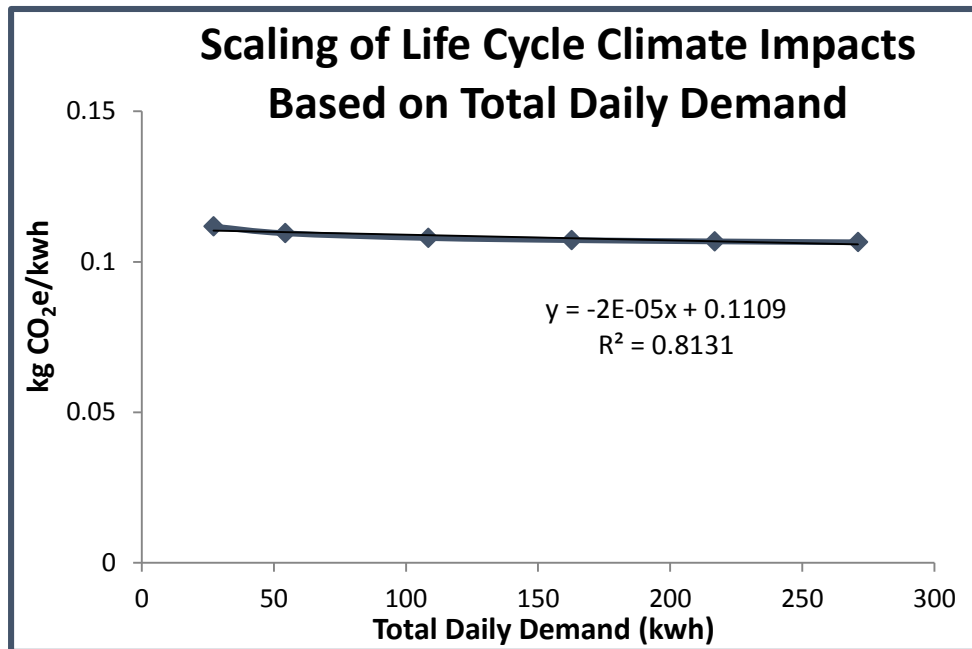


Figure 20: Scaling of Life Cycle Climate Change Impacts Based on Total Daily Demand. Linear model of life cycle climate change impacts per kWh (kg CO₂e/kwh) scaled based off of growing total daily demand (R²= .813).

As a result of this, the climate change and PM savings seen from the 6.31 kW PV-Battery microgrid modelled in this analysis can be applied to the 1 MW planned by Powerhive and ENEL. The savings from this model suggest that, when compared to the home diesel generators, developing PV-Battery microgrids to meet this scale could avoid over 65 million kg CO₂e, over 400,000 kg of PM₁₀e, over 1.2 million kg NMVOC, and over 700,000 kg SO₂e over the 25 year lifetime of the microgrids used in this analysis. Compared to the marginal grid mix in Kenya, this model suggests savings of over 23 million kg CO₂e, over 66,000 kg PM₁₀e, over 96,000 kg NMVOC, and over 127,000 kg SO₂e (**Table 12**).

Table 12: Savings from 1 MW of PV-Microgrids. Model PV-Battery microgrid savings in climate change (kg CO₂e), particulate matter formation (kg PM₁₀ eq.), photochemical oxidant formation (kg NMVOC), and terrestrial acidification (kg SO₂ eq.) compared to home gensets and grid extension applied to the 1 MW of planned microgrid capacity.

Impact Savings	PV-Battery Compared to Diesel Gensets	PV-Battery Compared to Marginal Electricity Grid Mix
Climate Change [kg CO₂-Equiv.]	65,314,536	23,430,199
Particulate Matter Formation [kg PM₁₀ eq.]	402,425	66,794
Photochemical Oxidant Formation [kg NMVOC]	1,270,471	96,418
Terrestrial Acidification [kg SO₂ eq.]	713,227	127,730

Discussion

To build upon existing knowledge and better advise the expansion and success of future energy access projects in the developing world, it is imperative to analyze the tradeoffs of all options available to citizens, developers, and the energy industry. This project advances life cycle assessment research by modeling three complete PV microgrid systems. This analysis of multiple design options and real life development scenarios can support microgrid developers to better match solutions to the specific needs and priorities of the off-grid communities they plan to serve. With the proper information regarding social and environmental impacts of PV microgrids, all stakeholders involved in electrification projects can be confident they are making the most informed and beneficial decisions. Whether it is a decision by citizens and developers on the ground, or decisions by international policy makers trying to meet sustainable development goals, the discussion of tradeoffs should serve as the basis of an informed discussion (United Nations Development Programme, 2015).

Overall Comparison of Microgrid System Designs

In order to provide appropriate and useful information regarding solar PV microgrids and their various design options, this analysis highlights several impact categories within this life cycle assessment that are important for all stakeholders involved. These categories are climate change, freshwater eutrophication, human toxicity, particulate matter (PM) formation, photochemical oxidant formation, terrestrial acidification, and terrestrial ecotoxicity.

Climate change is the most significant impact category for this analysis. PV microgrids can greatly reduce global carbon dioxide equivalent (CO₂e) emissions from electricity production while increasing global electricity supply (Williams et al., 2015). Additionally, PV microgrids can provide an environmentally friendly alternative compared other energy access options in developing nations. Therefore, numerical measurements of CO₂e emissions from the life cycle of a solar PV microgrid are very useful in analyzing the real reduction in GHG emissions from the use of microgrids.

Freshwater eutrophication is also likely a significant impact category in this analysis, and is important to explore as it is a useful indicator of aquatic environmental health impacts. This category is important for developers, manufacturers, and citizens alike when considering the impact of a microgrid project on the health of both humans and wildlife that rely on freshwater resources.

Human toxicity is likely not a significant impact category in this analysis because of the margin of error in the characterization factors. Additionally, the local human health impacts in the off grid communities from particulates and the supply chain global impacts are not distinguished within this category. However, it is inherently important, as the goal of microgrids is to improve quality of human life. An energy access project

would not be successful if local and global human health were to be degraded significantly because of the project.

Particulate Matter formation, while there is no established threshold for significance, the magnitude of the differences and its correlation with the climate change and acidification impact categories likely makes this a significant impact category. Several methods to supply energy access in off-grid communities have drastic human health impacts from the local accumulation and inhalation of PM, specifically the burning of diesel and kerosene in homes for cooking and heating (Mills & Jacobson, 2007). PV microgrids with battery backup options produce very little local PM impact but do have PM formation impacts during manufacturing.

Photochemical Oxidant Formation is very similar to particulate matter formation in that there is no established threshold for significance but due to the magnitude and correlation to the climate change and acidification impact categories it is also likely a significant impact category. Photochemical oxidant formation also has the potential to cause strong human health impacts from local accumulation; therefore it is important for developers and local communities to consider this category when designing a PV microgrid system. PV microgrids have the potential to greatly reduce local photochemical oxidant formation compared to other energy access options in developing countries, when designed properly.

Terrestrial Acidification is a significant impact category for this analysis. Terrestrial acidification can cause damage to agriculture through acidification of the soil, damage to buildings and crops, as well as human health impacts. This is an important category for developers and local communities, in order to prevent local damages to important economic sectors and to human health. With the proper design, PV microgrids can have important reductions in terrestrial acidification compared to other energy access options in developing countries.

Terrestrial ecotoxicity is not likely to be a significant impact category for this analysis, but is nonetheless important as an indicator of impacts on the terrestrial ecosystem.

When these impact categories are explored in more detail between the three microgrid design options highlighted in this project, it is evident that the PV-Battery design encompasses significantly lower impacts in the climate change, particulate matter formation, photochemical oxidant formation, and terrestrial acidification categories (**Figure 8**). This result is due almost exclusively to the burning of diesel fuel in the diesel generator component of the PV-Diesel and PV-Hybrid microgrid designs during the use phase. While the PV-Battery design does impact climate change, particulate matter formation, photochemical oxidant formation, and terrestrial acidification, the majority of these impacts happen during the manufacturing stage, rather than during the use phase on site in off-grid communities. The impacts that are seen from manufacturing are encompassed in all three microgrid designs and are similar across the board, with the overwhelming majority of elevated impacts in the PV-Diesel and PV-Hybrid designs

coming from diesel combustion in the use phase. Due to this result, one of the most important findings of this project is that, in terms of climate change, particulate matter formation, photochemical oxidant formation, and terrestrial acidification, lithium-ion batteries are a better backup option for PV microgrids than diesel generators are. If a project requires a diesel generator backup due to location specific meteorological conditions, it should also be complemented by a battery energy storage system.

Climate change impacts have a global effect regardless of where the emission occurs. Particulate matter formation, photochemical oxidant formation, and terrestrial acidification however, can have significantly different social and environmental impacts depending on where the emissions occur. Particulate matter formation, photochemical oxidant formation, and terrestrial acidification from the burning of diesel fuels in the diesel generator component will have large local impacts, as the combustion in the diesel generator will occur at the site of the microgrid. However, the results relating to climate change impacts should not be ignored simply because the effects are global. In fact, because the effects are global, the impacts on climate change should be relevant and of the utmost importance, for local developers, citizens, and international policy makers alike.

It should be noted that there is a potentially significant tradeoff for the PV-Battery system in the freshwater eutrophication impact category, compared to the other microgrid system designs in this analysis. Tradeoffs in human toxicity and terrestrial ecotoxicity are likely insignificant due to the margin of error in the characterization factors associated with these impact categories. These potential tradeoffs will be explored further in the end of life recycling scenario analysis.

Microgrids versus Small-Scale Diesel Generators

In order to provide the best recommendations for all stakeholders, this analysis delved deeper into the climate change, particulate matter formation, photochemical oxidant formation, and terrestrial acidification impacts from the three microgrid designs and the small-scale diesel generators. Within the three microgrid designs, the PV-Battery design had by far the lowest climate change, particulate matter formation, photochemical oxidant formation, and terrestrial acidification impacts, followed by the PV-Hybrid and PV-Diesel systems, with the PV-Diesel design embodying far more impacts than the other two options (**Figure 9**).

As discussed in the background section of this report, particulate matter formation, photochemical oxidant formation, and terrestrial acidification from small-scale diesel combustion can have many negative impacts on human health including respiratory infections and cancer (Mills, 2016) (de Koning, Smith, & Last, 1985). With the goal of improving the quality of life for people living in off-grid communities, it is important to recognize the immediate local effects of microgrid designs with a diesel generator backup on the local community. It should also be noted that all three microgrid designs exhibited climate change, particulate matter formation, photochemical oxidant formation, and terrestrial acidification impact savings when compared to the option of a single home diesel generator. Therefore, burning diesel as part of a

microgrid is still better than the option of small-scale diesel generator use for electricity access. This is due in part to the efficiency gains from larger scale generators.

Additionally, single home diesel generators used for energy access are generally located much closer to, and sometimes even inside, households. The diesel generator component of a microgrid on the other hand is located at the site of the microgrid, which is typically not in the immediate proximity of a home. The issue of proximity to diesel combustion is relevant because the negative effects of particulate matter formation, photochemical oxidant formation, and terrestrial acidification on human health get substantially worse as the proximity to the source increases (Mills & Jacobson, 2007). PV-Diesel and PV-Hybrid microgrids have lesser local health impacts compared to small-scale diesel generators due to their proximity of combustion to households, but there is also the considerable benefit that comes from supplying a portion of the electrical demand from solar PV. With solar PV meeting part of the demand, diesel combustion levels are reduced overall, further reducing climate change, particulate matter formation, photochemical oxidant formation, and terrestrial acidification impacts when compared to the single home diesel generator option.

From this analysis it is clear that the PV-Battery design is the most beneficial microgrid design option for off-grid communities in Kenya. The savings in climate change (92%), particulate matter formation (95%), photochemical oxidant formation (98%), and terrestrial acidification (91%) impacts from the PV-Battery design compared to the option of small-scale diesel generator use are substantial (**Figure 9**).

Microgrids versus Traditional Electrification Solution

This analysis models two different Kenya grid mixes, one for the average Kenya grid mix, and one that represents the marginal Kenya grid mix, or the grid mix that would likely be used to reach off-grid communities. The marginal grid mix includes power generation from heavy fuel oil, coal, and natural gas, and has less renewable sources than the average Kenya grid mix (Republic of Kenya, 2014). Due to an increase in the use of carbon intensive fuels, and a decrease in the share of renewables, the marginal grid mix embodied higher impacts in the climate change (59% higher), particulate matter (57% higher), and photochemical oxidant (55% higher) categories, but lower impacts (8% lower) in the acidification category (**Figure 10**).

It is important to point out that the Kenya electricity grid model in this analysis does not include any impacts related to the expansion of the conventional grid to off-grid communities. The only impacts modeled are those directly associated with the production of the Kenya electricity grid mix and don't include the manufacturing and construction of new power plants, transmission infrastructure, or transmission losses. Therefore, the estimate of climate change, particulate matter formation, photochemical oxidant formation, and terrestrial acidification impacts from the Kenya electricity grid are conservative, and impacts are likely much higher than what is modeled in this analysis (Republic of Kenya, 2014).

Although the PV-Diesel microgrid design is better than the option of single home diesel generator use, it is actually worse than the traditional grid extension solution for rural electrification in off-grid communities for both grid mixes. This holds true for climate change, particulate matter formation, photochemical oxidant formation, and terrestrial acidification impacts. The PV-Hybrid design shows more promise. When compared to the marginal grid mix, there are savings in the climate change (64%), particulate matter formation (24%), and terrestrial acidification (22%) impacts from the PV-Hybrid design. However, when compared to the average grid mix the only savings that can be seen are in the climate change (26%) and terrestrial acidification (29%) impacts. Particulate matter and photochemical oxidant formation impacts from the PV-Hybrid microgrid are actually worse than the average grid mix. Again, these results should be tempered due to the fact that impacts from extension of either grid mix are not accounted for in this model, and impacts will be higher than seen in the results of this analysis. The savings in climate change impacts from the PV-Battery design compared to the average Kenya electricity grid and the marginal grid (69% and 81%, respectively) are both substantial. The same is true when comparing particulate matter formation, photochemical oxidant formation, and terrestrial acidification impacts of the PV-Battery design to the extension of the average Kenya electricity grid with savings ranging from 62-68%, and the marginal grid with savings ranging from 66-79%, depending on the impact category. For both comparisons the largest savings from the PV-Battery design can be seen in the climate change impact category, followed by the terrestrial acidification category (**Figure 10**).

Overall, the PV-Diesel and PV-Hybrid designs are not nearly as beneficial as a PV-Battery design with regards to climate change, particulate matter formation, photochemical oxidant formation, and terrestrial acidification impacts when compared to traditional grid extension. The PV-Battery design has a significantly lower total particulate matter impact and a negligible local particulate matter impact. The PV-Battery design also encompasses significantly lower climate change impacts, which affects both local and global communities. Due to these findings the PV-Battery design is the most favorable microgrid design option for off-grid communities in Kenya.

PV-Battery Contribution Analysis

Due to the clear benefits of a PV-Battery design, a contribution analysis was performed. This analysis explored the relative proportions of impacts from different components within the baseline PV-Battery microgrid design, in order to determine where the greatest improvements can be made. For the baseline PV-Battery design, the component with the largest contribution to climate change, particulate matter formation, photochemical oxidant formation, and terrestrial acidification impacts was the lithium-ion battery. Impacts from the lithium-ion battery accounted for 72% of the climate change, 77% of the particulate matter, 72% of the photochemical oxidant formation, and 80% of the terrestrial acidification impacts for the entire PV-Battery microgrid. The next largest contributors were the CdTe module at 10-12%, and the BOS at 5-10% of the total PV-Battery impact, depending on impact category (**Figure 11**). The lithium-ion battery contribution will be explored below. The contribution from the other major components is likely due to electricity, copper, and other primary metals utilized in the manufacturing processes.

With the lithium-ion batteries being the largest contributor to climate change, particulate matter formation, photochemical oxidant formation, and terrestrial acidification impacts, this analysis went further and explored what components within the lithium-ion battery are contributing the most to these impact categories. The analysis revealed that 73% of the climate change, 82% of the particulate matter, 73% of the photochemical oxidant, and 86% of the terrestrial acidification impacts from lithium-ion batteries come from the manufacturing of the battery cell (**Figure 12**).

Upon further review and another contribution analysis, it was discovered that 69% of the climate change impact from the battery cell manufacturing process was coming from the electricity utilized in the manufacturing process (**Figure 13**). This indicates that 50% of the lithium-ion battery climate change impact, and 36% of the entire PV-Battery microgrid climate change impact, are coming from the electricity required in the manufacturing of the battery cell. Ellingson et al. (2013) lists the processes included in cell manufacturing to include, “coating of electrode pastes to metallic foils used as current collectors, welding of current collectors to tabs, filling of electrolyte, and initial charging of the finished cell (Ellingsen, et al., 2014).” However, the majority of the energy usage comes from the operation of dry rooms that are necessary for high quality battery production. All of these requirements for cell production necessitate the usage of 101MJ per kg of battery cell produced.

Particulate matter formation, photochemical oxidant formation, and terrestrial acidification formation impacts from the battery cell manufacturing process however do not come primarily from electricity use. Electricity utilized only accounts for 18-31% of the particulate matter, photochemical oxidant formation, and acidification impacts in the battery cell manufacturing process. The majority of the particulate matter formation, photochemical oxidant formation, and terrestrial acidification impacts in battery cell manufacturing come from the battery anode or cathode production. This clarifies that 47-67% of the lithium-ion battery impact and 34-53% of the total PV-Battery microgrid impact comes from the cathode and anode production in the battery cell (**Figure 13**). These impacts are due in large part to the copper and other metals like cobalt and manganese that are utilized in the anode and cathode processes. Lithium-ion battery cells require an aluminum positive current collector and a copper negative current collector. The copper negative current collector in the anode represents 14% and the aluminum positive current collector in the cathode represents 3.1% of the battery pack mass. Given that the microgrids in this model require very large battery banks, a high mass of each of these metals is required for manufacturing.

Even though lithium-ion batteries contribute significantly to the total climate change, particulate matter formation, photochemical oxidant formation, and terrestrial acidification impacts of the PV-Battery microgrid design, it should be made clear that this design has significantly higher savings compared to the microgrid designs that utilize a diesel generator. When considering the geographic location of Kenya and the above impact categories, lithium-ion batteries are a better option than diesel generator when it comes to storage within a solar PV microgrid. For off-grid communities in Kenya, the use of a PV-Battery microgrid is the most

beneficial microgrid design in terms of the climate change, particulate matter formation, photochemical oxidant formation, and terrestrial acidification impact categories.

Impact Hotspots

This analysis also identifies impact hotspots and opportunities for developers to reduce the life cycle impact of PV-Microgrids. The most notable opportunity is in battery manufacturing. For all seven impact categories, the battery, particularly the battery cell manufacturing, contributed the majority of the impact of the PV-Battery system. Within the battery cell the largest contributor depended on the impact category. From the contribution analysis and the elementary flow analysis it is clear that the electricity grid mix in the battery cell production is largely responsible for the battery impact in the climate change category. Conversely, the copper used in the battery anode, and the cobalt, manganese, and nickel used in the battery cathode were largely responsible for the battery impact in the particulate matter formation, photochemical oxidant formation, and terrestrial acidification categories.

Scenario 1: Electricity Grid Mix for Battery Manufacturing

Due to the significant effect of electricity use in battery manufacturing on the overall impact of the PV-Battery microgrid design, a scenario test was run in order to determine how different electricity mixes could alter this impact. Electricity mixes for the United States (US), France (FR), Switzerland (CN), China (CH), and an electricity mix made up entirely of solar PV production were all modeled as substitutes to the baseline European grid mix. The US mix was chosen because the US is a major lithium ion battery producer. Switzerland, France, and China grid mixes were similarly selected because there are lithium-ion manufacturers and recycling companies in operation there. The China grid mix represents a high impact scenario and conversely a grid mix with entirely PV production was chosen to represent a clean energy mix. This scenario explores the effect that changing the battery manufacturing grid mix has on the overall climate change impact category.

The Chinese electricity mix represents an extreme high impact substitute, due to the large portion of electricity production from coal in China (Di et al., 2007). Shifting battery production from the European baseline to China increases the total PV-Battery microgrid climate change impact by over 35%. The opposite end of the spectrum is an electricity mix supplied entirely from solar PV, which represents a comparatively low impact substitute. By manufacturing batteries with entirely renewable solar PV electricity mix, the total PV-Battery microgrid climate change impact can be reduced by 36%. France and Switzerland electricity mixes represent low impact substitutes, as a large portion of electricity production is from renewable sources (nuclear in France and hydro in Switzerland) (Swiss Federal Office of Energy, 2015) (International Atomic Energy Agency, 2014). Shifting battery production to France or Switzerland would decrease the overall PV-Battery microgrid impact by 27% and 18%, respectively. The electricity mix of the United States is more impactful than the baseline European electricity mix, but not as impactful as the Chinese electricity mix. Shifting battery

production from the European baseline to the United States would increase the total PV-Battery microgrid climate change impact by 15% (**Figure 14**). These results suggest that the single biggest way to reduce the overall climate change impact of a PV-Battery microgrid is to shift battery production to nations or regions that utilize high levels of low-carbon energy.

There are slight savings seen in the particulate matter formation, photochemical oxidant formation, and terrestrial acidification impact categories when switching from the baseline European grid mix to a grid mix from France or Switzerland. However, the only substantial difference seen in these three impact categories is when switching from the European baseline to the grid mix in China, which causes over a 30% increase in each category.

Another hotspot for microgrid impacts comes from the metals used in the cathode and anode production within the battery cell. The copper used in the production of the battery anode accounted for 58.8% of the total eutrophication impact, over 61.1% of the human toxicity impact, over 33.9% of the ecotoxicity impact. Metals used in the production of the battery cathode like nickel, manganese, and cobalt similarly had large contributions to the overall microgrid impact. The copper used for module AC/DC cabling was also a substantial contributor to overall system impacts most notably in the PV-Diesel system where it accounted for 42.8% of the total eutrophication impact and 47.3% of the human toxicity impact. This presents an opportunity for developers to work not only in their own operations, but also with battery manufacturers to lessen the impact of microgrids substantially by both using less of these metals in manufacturing and by sourcing them from lower impact suppliers.

Since metals and their processing are so important to the overall microgrid system impacts, and for the potential tradeoffs seen in the PV-Battery system, it is critical for microgrid developers to ensure effective takeback and recycling programs for microgrid components at the end of life. **Scenario 2** explores the impact of recycling components at the end of life instead of landfilling them.

Scenario 2: Microgrid End of Life Recycling

With the goal of reducing the overall impacts of the microgrid designs, particularly the impacts from the metals used in the manufacturing of system components, a scenario was developed to analyze the effect of recycling the microgrid components at the end of their usable life. Recycling of the microgrid components had different effects for all three microgrid designs, with the largest overall savings seen from the recycling of the PV-Battery and PV-Hybrid designs. This was due to the difference in contribution breakdown for the microgrid systems. For the most part, the recycling savings in all systems were not due to the avoided landfilling impact as that only accounted for 0-2% of the total impact in the categories. Instead, the recycling savings were due in large part to the avoided primary material use in microgrid manufacturing.

For the PV-Battery microgrid, substantial savings from substituting recycling for landfill are seen in all seven impact categories, with a range of 18-69% savings depending on the impact

category (**Table 8**). The largest savings from recycling at the end of life were seen in freshwater eutrophication (65%) and human toxicity (69%). The PV-Hybrid saw lower savings from recycling particularly in the climate change, particulate matter formation, photochemical oxidant formation, and terrestrial acidification impact categories because the diesel use accounted for the majority of the impact rather than the battery manufacturing. Freshwater eutrophication and human toxicity again had the largest savings (**Table 9**). As discussed earlier, the contribution and elementary analyses suggest that the battery alone accounts for over 70% of the total impact in all categories, and that that impact is primarily caused by metals used in the battery cell. The savings from these two systems, therefore, are largely attributable to the avoided burden of primary metals and other material from the manufacturing and use of the lithium-ion battery.

In contrast to the other two systems, recycling of the PV-Diesel system only had savings in the freshwater eutrophication and human toxicity categories. In both of those categories, recycling savings were on the order of 19-24%, whereas with climate change, particulate matter formation, photochemical oxidant formation, terrestrial acidification, and ecotoxicity categories, the savings were in the 0-1% range (**Table 10**). These differences in impact savings are a result of the impacts from the PV-Diesel system being mostly tied to the burning of diesel fuels rather than the metals used in the manufacturing.

Overall, this scenario highlights the importance of takeback and recycling programs at the end of a project's life. The effect on the potential tradeoffs of the PV-Battery system with regards to the freshwater eutrophication impact category is of great importance when discussing the implications of takeback and recycling programs. After implementing recycling, the potential tradeoff in freshwater eutrophication is minimized, and the potential tradeoffs in human toxicity and terrestrial ecotoxicity remain insignificant. While the freshwater eutrophication tradeoff is not eliminated, when compared to the notable benefits in climate change, particulate matter formation, photochemical oxidant formation, and terrestrial acidification impact categories, this tradeoff is dampened (**Figure 15** and **Figure 16**).

These findings on the importance of takeback and recycling programs corroborates the existing knowledge of the potential negative toxicological implications from leaving behind microgrid system components, and also the potential economic and ecological benefits of recycling. In the case of lithium-ion batteries considered in this study, as part of the PV-Battery and PV-Hybrid systems, the need for recycling is demonstrated by multiple factors. The battery manufacturing process is both energy and material intensive and is one of the largest contributors across multiple impact categories. This can chiefly be traced back to primary metal extraction and electricity used in different manufacturing processes. Recycling can help significantly reduce material and energy demand (through the use of secondary recovered materials, especially in the case of scarce metal resources such as Cobalt used in these batteries) (Simon & Weil, 2013). Lithium-ion batteries also contain potentially toxic materials such as copper, nickel, and lead. In particular, cobalt, copper and nickel are the main contributors to the total hazard potential of lithium-ion batteries in the categories of human toxicity, terrestrial ecotoxicity and freshwater ecotoxicity. Studies that used simulated landfill conditions showed the potential for human exposure to these substances through groundwater leaching, further providing a compelling

reason to establish takeback and recycling programs at end of life (Kang, Chen, & Ogunseitan, 2013).

In the case of PV modules, although there is an information deficit with regards to their environmental and health impacts from end of life stages, they have been considered potentially dangerous and classified akin to e-waste by the European Union and are subject to the European Directive WEEE (Waste Electrical and Electronic Equipment) (Bakhiyi, Labreche, & Zayed, 2014). Recycling helps limit this potential for harmful exposure and also helps extract secondary materials of economic value. Therefore, through active end of life management plans and assuming responsibility for the entire life cycle of these modules, solar developers can reduce system wide environmental impacts, risk of adverse ecological impacts and human toxicity due to potentially harmful chemical exposure, and also potentially help reduce financial and operational burden for off-grid communities.

Other impact hotspots for microgrids identified by this analysis were the emissions of inorganic material and heavy metals to water, soil, and the air. Of particular concern are the emissions of phosphate to fresh water, chlorine to industrial soil, copper (+II) to air, and manganese (+II) to fresh water. These emission flows were the dominant contributors to the eutrophication, human toxicity, and ecotoxicity categories. The emissions largely came during the manufacturing stages of the microgrid life cycle. Hopefully, by identifying these areas of concern, this analysis can help developers and their suppliers to implement better control technologies and mitigation practices to lessen the impact from specific emission flows.

Scenario 3: Choice of PV Technology- CdTe vs. Mono-Si

This analysis also compared different PV technologies (mono-Si and CdTe) for applications within solar microgrid systems (Scenario 3). CdTe laminate and mono-Si panels represent the vast majority of the solar panel market, so understanding the benefits and tradeoffs between the two technologies in the context of solar microgrids is important. This comparison is particularly valuable for PV developers like First Solar who manufacture both technologies. As demonstrates, for the baseline PV-Battery microgrid system, the two technologies have very similar impacts across all impact categories with the exception of the climate change category, where the mono-Si panels have significantly more impact (approximately 18%). The total GWP savings from the CdTe modules in the PV-Battery system is 20 grams of CO_{2e} per kWh. In the PV-Hybrid and PV-Diesel systems, the savings are lower at 18 and 6 grams of CO_{2e} per kWh, respectively (**Figure 19**).

In the climate change category, the difference in module impact accounted for the largest portion of the increase seen with the mono-Si panels. This is largely because mono-Si manufacturing is a multi-stage process that uses approximately five times the amount of electricity than the single integrated CdTe process uses. In total, utilizing mono-Si panels in a PV-Battery system increases the module impact by over 172% (**Figure 18** and **Table 11**). This suggests that if limiting climate change impacts is a goal for developers, communities, and policy makers alike, CdTe laminate modules should be used instead of traditional mono-Si

panels in future PV microgrid systems. For the other impact categories, the majority of the impact shifts come from the BOS (**Figure 18** and **Table 11: Percent Change in Component Impact from Switching CdTe to Mono-Si**. Change in component impact when if a Mono-Si PV-Battery microgrid was used instead of the baseline CdTe PV-Battery microgrid. Negative values indicate a decrease in impact when Mono-Si is used instead of CdTe. Orange highlights indicate the largest percent change in a given impact category.). Even though less area of BOS is needed for the mono-Si panels, the mono-Si panels are heavier, thicker, and bigger than the CdTe laminate which requires the mounting structure to utilize more steel, concrete, and polystyrene than the CdTe mounting.

Scenario 4: Application to Larger Scales - Powerhive's Planned Expansion

A recent announcement from microgrid developers Powerhive and ENEL, unveils a proposal for the installation of numerous solar PV microgrids in rural off-grid communities in Kenya (Van Gerven, 2015). The proposal describes the plan to implement a portfolio of microgrids, with a combined installed capacity of 1 MW, to provide electricity access to 90,000 people in western Kenya. This announcement is an exciting development for the region, and provides an opportunity for the solar industry and microgrid developers to examine broader solar microgrid use for energy access in off-grid communities. Due to the linear scalability of the model built for this analysis, which is based off of installed capacity, the model can be used to develop a baseline estimate of the potential savings in climate change, particulate matter formation, photochemical oxidant formation, and terrestrial acidification impact categories for a combined capacity of 1 MW of PV microgrid systems. This is assuming that the system design for all of the microgrids developed by Powerhive and ENEL would be the PV-Battery baseline design used in this analysis.

When compared to the option of small-scale diesel generators, PV-Battery microgrids sized to meet a combined 1 MW could provide large savings in the climate change (over 65 million kg CO₂e), particulate matter formation (over 400,000 kg of PM₁₀e), photochemical oxidant formation (over 1.2 million kg NMVOC), and terrestrial acidification (over 700,000 kg SO₂e) impact categories over the 25 year system lifetime. Savings from PV-Battery systems compared to the marginal Kenya grid mix are not as large, but still provide major savings in these four impact categories (**Table 12**). The savings calculated with the model from this analysis are an estimate that provides information on the order of magnitude of savings, not exact values. These results, although a rough estimate, do provide developers and policymakers with enough information to be confident that large scale use of PV microgrids in Kenya can provide energy access with large savings in climate change, particulate matter formation, photochemical oxidant formation, and terrestrial acidification impact categories, compared to the single home diesel generator option and marginal grid mix option for energy access.

Limitations

This analysis provides an in depth exploration into the environmental impacts of various scenarios for different microgrids, however there were some limitations associated with the modeled impacts. First, this analysis didn't take into account the impacts from the inevitable

increase in electricity demand. An important quality of microgrids that makes them attractive to off-grid communities is their ability to increase in capacity with an increase in customer demand. Once off-grid communities get access to a steady source of electricity, it is highly likely that demand will increase due to local economic development (Arsenio, 2015).

Ideally, a socioeconomic analysis would have also been included to determine not only the environmental considerations of PV microgrids but also the impacts on social structure and local economies. To model these impacts properly, surveys of the change in each respective category would need to be done on site in communities with microgrids. Accurate information regarding these categories was not readily available in the modeling software (GaBi ts) utilized in this model. Additionally, life cycle costing analysis (LCC) would be valuable to assess the difference in cost between the microgrid systems over their lifetime. The component and system costs drive the levelized cost of electricity which is important to both developers and the communities in the deployment and operation of the microgrid systems.

A final limitation of our study is that it would have been ideal to model different battery chemistries for our electricity storage system. As mentioned previously, Li-ion batteries were chosen because of data availability and their expanding role in the energy storage market. However, lead acid batteries have historically been utilized more often, particularly in microgrid systems, due to the fact that they are cheaper and readily available for purchase (Arsenio et al., 2014) (Schnitzer, et al., 2014). Since batteries accounted for a large portion of the category impacts in the PV-Hybrid, and particularly the PV-Battery systems, it would be beneficial to compare these results with other battery technologies.

Suggestions for Future Research

Due to the limitations of this analysis, there are several suggestions for future research that would be beneficial to developers, the solar industry, policy makers, and off-grid communities. In this report, the environmental impact of multiple PV microgrid systems has been analyzed and presented. However, in the real world, cost considerations are critical for any decision-making. Just as tradeoffs exist in the environmental impacts across different system configurations and scenarios, important tradeoffs might also exist in terms of the life cycle cost (LCC) of the system. To properly inform decision-making, it is important to include the cost implications of the decision. Thus more research is required on the economics of microgrids and their components. The results of this study in conjunction with LCC studies can provide all the information necessary to make an optimal, sustainable choice most suitable for the off-grid communities.

With a large variety of available and emerging technologies in the energy sector, it is important to understand and compare the environmental impacts across technologies. For example as identified previously, the utilization of different battery technologies in these microgrid systems should be a focus for future research. Additionally, this report only analyzed PV microgrids, whereas, in reality there are other energy technologies such as micro-wind, micro-hydro, and

hybrid systems. Future research should work to incorporate life cycle assessments of other microgrid technologies so that comparisons can be further illustrated across system designs.

Along the same lines, microgrid systems are designed based on the specific geographic and socioeconomic contexts of the implementation region. In this study, off-grid communities in Kenya were the focus, so PV-microgrids were an effective solution, but in places with limited insolation or different electricity demand profiles, other microgrid solutions could be more effective options. Future research, therefore, should explore microgrid designs for different geographies and community situations.

Additionally, this report primarily focuses on microgrid systems that are suitable for small-scale villages. Deployment of microgrid systems at larger scales may experience certain scaling effects such as economies of scale which could influence the overall environmental impacts. Although this report attempts to tease out implications of wider implementation of microgrids, their sustainability on larger scales should be investigated with more precision.

Impacts to Stakeholders

Our study focusing on solar PV microgrids translates into key implications for different stakeholders involved in the renewable energy access market.

Solar Developers

Energy access developers, in particular solar developers, which include the solar industry (research, development, and manufacturing), independent power providers, and energy investors, can benefit from the research insights offered by this study. This study's overarching takeaway for solar developers is to focus on a system wide comparative assessment rather than individual components of microgrids. The life cycle approach adopted by this study not only considers the impacts of individual microgrid components such as PV modules, but also the microgrid systems as a whole. Viewed in isolation, changes in individual components might suggest improvements in environmental impact, but the consequences of that change over the entire system can lead to more impact in other components. For example, improvements in module efficiency can be offset by a more environmentally impactful manufacturing processes or larger support systems. A system wide life cycle assessment, as adopted by this study, can prove to be highly valuable to overcome such discrepancies and to ensure a thorough analysis.

In comparing different energy backup technologies (i.e. batteries and diesel generators), our results highlight the potential for energy storage systems to substantially lower the environmental impacts of microgrid systems. Despite accounting for the environmental impacts of battery manufacturing, it is seen that microgrid systems using battery storage resulted in significantly lower environmental impacts, especially across the climate change, particulate matter formation, photochemical oxidant formation, and terrestrial acidification impact categories, in comparison to systems that used diesel generators as an energy backup. This

project made clear that substituting fossil fuel intensive energy backup options such as diesel generators with a battery backup can result in substantial environmental impact reductions. However, it is important to keep in mind that there are other factors such as economic considerations and overall system reliability that ultimately affect microgrid system choice in real world situations.

Scenario analysis of battery pack manufacturing revealed that the electricity grid mix used in battery cell production plays a significant role in system wide environmental impacts. Therefore, sourcing locations and their associated grid mix are important considerations for reducing life cycle impacts. Another key impact hotspot for the solar industry is the importance of establishing takeback and recycling programs. A scenario analysis comparing system wide end of life recycling versus a landfill process revealed a significant reduction in climate change, particulate matter, photochemical oxidants, and acidification impacts, especially in the case of PV-Battery systems. Further, recycling at end of life substantially reduces impacts in the freshwater eutrophication and human toxicity categories.

Without the existence of a takeback and recycling program, there is the potential for the PV-Battery system to have greater impacts compared to the other two systems within these categories. The substantial reduction in impacts due to recycling, therefore, helps reduce the potential for an environmental tradeoff for the PV-Battery system in these particular categories. Through specific scenario analyses this study identifies key impact hotspots, namely battery manufacturing and the establishment of takeback and recycling programs at end of life. Both of these considerations directly translate into opportunities for solar developers to consider environmental sustainability while developing PV microgrids.

Looking at the larger picture, solar developers are in the business of clean energy generation, making it crucial for them to understand how the overall process of creating, establishing and maintaining such energy generation systems affects the environment. By exploring impacts across a range of impact categories and performing scenario analyses, this project identifies specific components or processes that contribute to the overall environmental impact of the systems. In the case of microgrids, manufacturing of individual components occurs globally in multiple locations, making global impact categories such as climate change (kg CO₂e) significant indicators of the overall environmental performance of systems. That being said, specific impact categories such as particulate matter formation, photochemical oxidant formation, and terrestrial acidification explored in this study are also significant for solar developers in terms of regulation compliance in the local regions where manufacturing takes place. Furthermore, these impact categories are also important for developers because they are of great concern to the potential customers and users of these solar microgrids, namely the off-grid communities.

Off-grid communities

Off-grid communities in rural areas are another important group of stakeholders that can benefit from this study. Although these communities could potentially be connected to a central grid in the future, they are located in such remote areas that the wait time and capital

cost can be excessive. In such situations, the status quo is defined as having no electricity access. Communities depend on incumbent technologies such as diesel generators, kerosene lamps, or direct burning of biomass. These fossil fuel and biomass intensive energy options directly translate into negative environmental and health impacts for the communities. By comparing home diesel generator use and the extension of the marginal grid to entire PV-Battery microgrid systems, this analysis is able to compare the environmental impacts of potential energy access options, clearly highlighting the environmental advantage of PV-Battery microgrids.

Assessment of specific impact categories that quantify local environmental impacts are highly valuable to these off grid communities. The results clearly highlight significantly lower impacts in categories of local concern such as particulate matter, photochemical oxidant formation, and terrestrial acidification for PV-Battery systems microgrid systems compared to diesel generators and traditional electrification options.

Through the wide range of impact assessments, this study is also able to shed light on the existence of potential tradeoffs for the PV-Battery system, most notably in the freshwater eutrophication category. The end of life scenario analysis highlights that recycling of microgrids at the end of life can substantially reduce the potential for such tradeoffs. This is indicated by the 65% reduction in freshwater eutrophication impacts from the PV-Battery system upon substitution of landfilling with recycling at the end of life.

Additionally, electrification options such as PV microgrids are sometimes viewed as a stop-gap arrangement before central grid connections are provided to these communities. By designing microgrid systems to completely meet a community's demand, this project establishes the feasibility of setting up off-grid PV microgrid systems as an adaptable and potentially reliable long-term clean energy access solution.

In conclusion, by highlighting the environmental and health advantages of PV microgrid systems, especially those containing battery backup systems, in comparison to central grid expansion and incumbent electrification technologies, this analysis drives home the advantages of off-grid renewable energy solutions in rural communities and helps inform decision-making for energy access solutions.

Conclusion

Thirty-four million people in Kenya today live without access to electricity, which means only 19% of the total population has electricity. Off-grid communities are rapidly growing in number as countries in Sub-Saharan Africa face a growing gap between their energy supply and energy demand, fueled by population growth and an increase in energy demand associated with economic growth. Most of these off-grid communities are located in rural areas and the majority of them depend on kerosene and biomass for lighting and cooking, and small-scale diesel generators for electricity if they can be afforded. Rural Kenyans spend 26% of their income on lighting alone. Kerosene in these rural off-grid communities typically cost 46% more than at pump stations in urban areas (Lighting Global, 2014). More importantly, these incumbent energy sources are highly polluting and dangerous, and dependency on these sources locks people in a cycle of poverty where their income is drained and their health and environment is degraded (SunnyMoney, 2014). For instance, kerosene lamps have been documented to cause a wide range of negative impacts from accidental fires, to pneumonia caused by the release of concentrated particulate matter within small spaces (Mills & Jacobson, 2007) (Rao, 2012). Therefore, clean energy access is one of the prominent focus areas for effectively addressing economics, health and environmental concerns posing such rural off-grid communities.

This project's main significance lies in exploring PV microgrids as a potential clean energy access solution. By performing a system wide comparative assessment of three different PV microgrid designs, and evaluating them in comparison to small-scale diesel generators and the expansion of a traditional grid, this project is able to provide a comprehensive comparison of the environmental impacts across viable electrification options. The results clearly highlight the substantially lower environmental impacts of PV-Battery microgrid systems (PV microgrid system with a battery backup) as compared to other electrification options in Kenya. Analysis of a range of impact categories from climate change to human toxicity helped quantitatively assess the potential for each of these systems to cause a wide variety of health and ecological impacts over their life cycle. The climate change impact category provided insight on global impacts, while impact categories such as particulate matter and terrestrial acidification reflected more local environmental and health impacts. Based on this impact assessment, this analysis was able to highlight the clear health and environmental advantages of PV-Battery microgrid systems for off-grid communities in Kenya.

Developing renewable energy infrastructure forms a key part of sustainable development goals in nations such as Kenya. Although the contribution of renewable energy, primarily in the form of hydro, has been increased in the central electricity grid mix, the expansion of the central grid itself to remote and rural areas is a slow, expensive process. Off-grid renewable energy options like PV microgrids, which have a faster installation times, provide a two pronged advantage; immediate energy access resulting in subsequent improvement in economic opportunities, and a significant environmental and health advantage compared to other viable electrification

options. Thus, emphasizing that PV-Battery microgrids can contribute to a real improvement in quality of life for off-grid communities.

The key takeaway of this project for stakeholders is the provision of a tool for informed decision making in the area of off-grid energy access. National policies are an important determining factor that shapes the trajectory of renewable energy growth in any nation. By highlighting the potential for PV microgrids to be feasible, adaptable, long term energy access solutions, with health and environmental advantages over the expansion of central grids and existing incumbent energy options, this study highlights the need for national policies in developing nations like Kenya to provide suitable environments for the growth of PV microgrids, to work towards a clean energy future.

Appendix

Appendix 1: Component Benchmarking

Table 13: Benchmarking of Lifecycle GWP Impact for Major Microgrid Components

Component	Source	Impact indicator	GWP (kg CO2 eq.)/kg	GWP (kg CO2 eq.)/kwh	Notes
Li-ion Battery	Present Study	ReCiPe (h)	15	-	NCM li-ion battery
Li-ion Battery	Notter et al. (2011)	CML	6.0	-	-
Li-ion Battery	Ellingsen et al. (2013)	ReCiPe (h)	18.0	-	-
Li-ion Battery	Zackrisson et al. (2010)	unknown	15.9	-	This was for an LFP battery, which have lower impacts per kg
Li-ion Battery	Argonne (GREET) (2010)	unknown	12.5 [+6]	-	This was an average for all different cathode and anode pastes
Li-ion Battery	Rydh and Sanden (2005)	unknown	18.1	-	This number was taken from the Argonne paper above.
Li-ion Battery	Ishihara et al. 1999	unknown	18.2	-	This number was taken from the Argonne paper above.
Charge Controller	Present Study	ReCiPe (h)	8.1	-	Morningstar TS-MPPT-600v Charge controller
Charge Controller	Posorski et al. (2003)	unknown	6.0	-	
CdTe Modules	Present Study		-	0.011	

CdTe Modules	Kim et. al (2012) (NREL Harmonization)	unknown	-	.018-.052	Harmonization of 24 estimates. Older modules (lower efficiencies)
Mono-Si Modules	Present Study	ReCiPe (h)	-	0.029	
Mono-Si Modules	Hsu et. al (2012) (NREL Harmonization)	unknown	-	.019-.095	Harmonization of 41 estimates
Diesel Generator	Present Study	ReCiPe (h)	26.4		Calculated weighted efficiency based on varying operational load
Diesel Generator	C Smith, et al. (2015)	unknown	33		Assumed 100% operational load

Appendix 2: Life Cycle Inventories

Section A: PV Modules

Table A1: Life Cycle Inventory of Crystalline Silicon Production

Description	Amount	Unit
Output		
CZ single crystalline silicon photovoltaics*	1.00	kg
Inputs		
Water, cooling	5.09	m ³
Electricity, South Korea*	68.2	kWh
Natural Gas burned in low Nox furnace >100 kW	6.82E+01	MJ
Tap water	9.41E+01	kg
Water deionized	4.01	kg
Silicon, production mix	0.781	kg
Argon, liquid	1	kg
Hydrogen fluoride	0.01	kg
Nitric Acid, 50% in water	0.067	kg
Sodium Hydroxide, 50% in water	0.042	kg
Ceramic Tiles	0.167	kg
Lime, hydrated, packed	0.022	kg
transport, lorry >16ft.	0.912	tkm
transport, freight rail	1.41	tkm
Silicone plant	1E-11	unit
Disposal, waste, Si wafer production	0.167	kg

Emissions/Waste		
Waste Heat (to air)	2.46E+02	MJ
Hydroxide (to river)	0.367	kg
Biological Oxygen Demand (BOD5) (to river)	0.130	kg
Chemical Oxygen Demand (to river)	0.130	kg
Dissolved Organic Carbon (to river)	0.040	kg
Total Organic Carbon (to river)	0.040	kg
Nitrogen Oxides (to river)	0.034	kg
Nitrate (to river)	0.084	kg

*Indicates a process developed as part of this analysis as opposed to an existing Gabi/Ecoinvent process

Sources: 1) R. Frischknecht, R. Itten, P. Sinha, M. de Wild-Scholten, J. Zhang, V. Fthenakis, H. C. Kim, M. Raugei, M. Stucki, 2015, Life Cycle Inventories and Life Cycle Assessment of Photovoltaic Systems, IEA PVPS Task 12, Report T12-04:2015 (2015).

Table A2: Life Cycle Inventory of Mono Crystalline Silicon Wafer

Description	Amount	Unit
Output		
Mono-Si Wafer*	1.00	sqm
Inputs		
Electricity Medium Voltage (Malaysia)*	25.7	kwh
Natural gas burned low-Nox >100 kw	4	MJ
Tap water at user	6.00E-03	kg
Water deionised	1.80E+01	kg

CZ single crystalline silicon	1.58	kg
Silicon carbide	0.62048	kg
Silicon carbide, recycling	1.409435	kg
Flat glass, uncoated	0.009985	kg
Sodium hydroxide, 50% in H2O	0.014998	kg
Hydrochloric acid, 30% in H2O	0.0027	kg
Acetic acid, 98% in H2O	0.038996	kg
Triethylene glycol	0.217784	kg
Triethylene glycol, recycling	1.947732	kg
Dipropylene glycol monomethyl ether	0.299967	kg
Alkylbenzene sulfonate, linear, petrochemical	0.239974	kg
Acrylic binder, 34% in H2O	0.003854	kg
Brass	0.007438	kg
Steel, low-alloyed	0.797173	kg
Wire drawing, steel	0.80461	kg
Disposal, waste, silicon wafer production, 0% water, to underground deposit	0.170118	kg
Transport, lorry >16t, fleet average	9.29E-01	tkm
Transport, freight, rail	3.84E+00	tkm
Wafer factory	0.000004	unit
Emissions/Waste		
Heat, waste (to air)	92.45562	MJ

COD, Chemical Oxygen Demand (to river)	0.029545	kg
BOD5, Biological Oxygen Demand (to river)	0.029545	kg
DOC, Dissolved Organic Carbon (to river)	0.011095	kg
TOC, Total Organic Carbon (to river)	0.011095	kg

*Indicates a process developed as part of this analysis as opposed to an existing Gabi/Ecoinvent process

Sources: 1) R. Frischknecht, R. Itten, P. Sinha, M. de Wild-Scholten, J. Zhang, V. Fthenakis, H. C. Kim, M. Raugei, M. Stucki, 2015, Life Cycle Inventories and Life Cycle Assessment of Photovoltaic Systems, IEA PVPS Task 12, Report T12-04:2015 (2015).

Table A3: Life Cycle Inventory of Mono Crystalline Silicon Cell

Description	Amount	Unit
Output		
Mono-Si Cell*	1.00E+00	m ²
Inputs		
Tap water	1.71E+02	kg
Electricity Medium Voltage (Malaysia)*	1.44E+01	kWh
Natural Gas burned in low NOx furnace >100 kW	6.08E-02	MJ
Photovoltaic Cell Factory	4.00E-07	unit
Mono-Si Wafer	1.03E+00	m ²
Ammonia, liquid	2.19E-02	kg
Phosphoryl chloride	1.33E-02	kg
Isopropanol	1.77E-01	kg
Hydrochloric acid, 30% in H ₂ O	6.29E-04	kg
Hydrogen Fluoride	6.45E-04	kg

Copper Plating for Mono-Si cell*	5.85E-03	m ²
Sodium Hydroxide, 50% in H2O	6.04E-01	kg
Lime, hydrated, packed	1.51E-02	kg
Refrigerant R134a	3.12E-05	kg
Nitrogen, liquid	1.15E+00	kg
Silicon tetrahydride	2.91E-03	kg
Transport, lorry >16 ft.	2.74E-01	tkm
Transport, freight, rail	1.52E+00	tkm
Treatment, PV cell production effluent, to wastewater treatment, class 3	1.59E-01	m ³
Disposal, waste, Si wafer prod., inorg, 9.4% water, to residual material landfill	2.33E+00	kg
Disposal, solvents mixture, 16.5% water, to hazardous waste incineration	1.72E-01	kg
Transport, transoceanic freight ship	3.06E-02	tkm
Emissions/Waste		
Heat, waste (to air high population)	5.18E+01	MJ
Aluminum (to air high population)	7.73E-06	kg
Hydrogen fluoride (to air high population)	1.38E-04	kg
Lead (to air high population)	7.73E-06	kg
Silicon (to air high population)	3.17E-08	kg
Silver (to air high population)	7.73E-06	kg
Tin (to air high population)	7.73E-06	kg
Ammonia (to air high population)	3.73E-05	kg

Carbon dioxide, fossil (to air high population)	1.67E-01	kg
Chlorine (to air high population)	4.60E-05	kg
Hydrogen (to air high population)	1.10E-02	kg
2-Propanol (to air high population)	1.47E-02	kg
Acetaldehyde (to air high population)	6.33E-04	kg
Ethane, 1,1,1,2-tetrafluoro-, HFC-134a (to air high population)	3.12E-05	kg
Silicon (to air high population)	3.33E-04	kg
Silicon (to air high population)	2.63E-03	kg
NMVOC, non-methane volatile organic compounds, unspecified origin (to air high population)	1.26E-02	kg
Water (to air high population)	1.16E+01	kg

*Indicates a process developed as part of this analysis as opposed to an existing Gabi/Ecoinvent process

Sources: 1) R. Frischknecht, R. Itten, P. Sinha, M. de Wild-Scholten, J. Zhang, V. Fthenakis, H. C. Kim, M. Rauegi, M. Stucki, 2015, Life Cycle Inventories and Life Cycle Assessment of Photovoltaic Systems, IEA PVPS Task 12, Report T12-04:2015 (2015).

2) Sinha, Parikhit, and Mariska De Wild-Scholten. "LIFE CYCLE ASSESSMENT OF SILVER REPLACEMENT WITH COPPER BASED METALLIZATION IN TETRASUN PV MODULES." Proc. of 31st European Photovoltaic Solar Energy Conference and Exhibition, Germany, Hamburg. 2015. Print.

3) Tetra Sun Data Module Datasheet. Tempe, Arizona: First Solar, 2015. PDF.

Table A4: Life Cycle Inventory of Mono Crystalline Silicon Copper Plating

Description	Amount	Unit
Output		
Copper Plating for Mono-Si Cell*	1.00	m ²
Inputs		
Tin Plating	1	m ²
Tin	0.0001	kg
Selective Coating, aluminum sheet, nickel pigmented aluminum oxide	1	m ²
Nickel	0.0001	kg
Primary Copper	0.0001	kg

*Indicates a process developed as part of this analysis as opposed to an existing Gabi/Ecoinvent process

Sources: Atteq Ur Rehman, and Soo Hong Lee. "Review of the Potential of the Ni/Cu Plating Technique for Crystalline Silicon Solar Cells." Materials 7.2 (2014): 1318-341. Web.

Table A5: Life Cycle Inventory of Mono Crystalline Silicon Panel

Description	Amount	Unit
Output		
Mono-Si Panel*	1.00E+00	m ²
Inputs		
Electricity, medium voltage (Malaysia)*	3.73E+00	kWh
Diesel, burned in building machine	8.75E-03	MJ
Photovoltaic panel factory	4.00E-06	unit
Tap water	5.03E+00	kg
Tempering, flat glass	8.81E+00	kg

Copper wire drawing	1.03E-01	kg
Mono-Si Cell	9.35E-01	m ²
Aluminum alloy, AlMg3	2.13E+00	kg
Tin	1.29E-02	kg
Lead	7.25E-04	kg
Diode, unspecified	2.81E-03	kg
Polyethylene, HDPE, granulate	2.38E-02	kg
Solar glass, low-iron	8.81E+00	kg
Copper, primary	1.03E-01	kg
Glass fiber reinforced plastic, polyamide, injection molding	2.95E-01	kg
Ethylvinylacetate, foil	8.75E-01	kg
Polyethylene terephthalate, granulate, amorphous	4.58E-01	kg
Extrusion, plastic film	4.82E-01	kg
Silicone product	1.22E-01	kg
Corrugated board, mixed fiber, single wall	7.63E-01	kg
1-propanol	1.59E-02	kg
EUR-flat pallet	5.00E-02	unit
Hydrogen fluoride	6.24E-02	kg
Isopropanol	1.47E-04	kg
Potassium hydroxide	5.14E-02	kg
Soap	1.16E-02	kg
Transport, lorry >16t	5.85E+00	tkm
transport, freight, rail	7.55E+01	tkm

disposal, municipal solid waste, 22.9% water, to municipal incineration	3.00E-02	kg
disposal, polyvinylfluoride, 0.2% water, to municipal incineration	1.12E-01	kg
disposal, plastics, mixture, 15.3% water, to municipal incineration	1.64E+00	kg
disposal, used mineral oil, 10% water, to hazardous waste incineration	1.61E-03	kg
treatment, sewage, from residence, to wastewater treatment, class 2	5.03E-03	m3
Emissions/Waste		
Heat, waste (to air)	1.34E+01	MJ
NMVOC, non-methane volatile organic compounds, unspecified origin (to air)	8.06E-03	kg
Carbon dioxide, fossil (to air)	2.18E-02	kg

*Indicates a process developed as part of this analysis as opposed to an existing Gabi/Ecoinvent process

Sources: 1) R. Frischknecht, R. Itten, P. Sinha, M. de Wild-Scholten, J. Zhang, V. Fthenakis, H. C. Kim, M. Raugei, M. Stucki, 2015, Life Cycle Inventories and Life Cycle Assessment of Photovoltaic Systems, IEA PVPS Task 12, Report T12-04:2015 (2015).

2) Sinha, Parikhit, and Mariska De Wild-Scholten. "LIFE CYCLE ASSESSMENT OF SILVER REPLACEMENT WITH COPPER BASED METALLIZATION IN TETRASUN PV MODULES." Proc. of 31st European Photovoltaic Solar Energy Conference and Exhibition, Germany, Hamburg. 2015. Print.

3) Tetra Sun Data Module Datasheet. Tempe, Arizona: First Solar, 2015. PDF.

Table A6: Life Cycle Inventory of Module AC/DC Cabling

Description	Secondary Inputs	Amount	Unit
Output			
Module AC/DC Cabling*		1.00	m
Inputs			
Tube Insulation		0.48	kg
i) Nylon 6		0.24	kg
ii) Plastic Extrusion Profile		0.24	kg
	Thermal Energy from Natural Gas	0.103	MJ
	Compressed Air	0.00576	nm ³
	Polyvinyl Chloride Granulate	0.241	kg
	Lubricating Oil	3.39E-05	kg
	Electricity Grid Mix	0.662	MJ
Copper Wire		0.64	kg
	Electricity Grid Mix	3.3	MJ
	Copper Primary	0.64	kg
	Thermal Energy from Natural Gas	0.032	MJ
Processing			
	Copper Wire (6 mm)	0.64	kg

*Indicates a process developed as part of this analysis as opposed to an existing Gabi/Ecoinvent process

Sources: 1) Socolof et. al 2014; Design for the Environment (DfE) Wire and Cable Partnership. Rep. no. EPA 744R08001. United States Environmental Protection Agency

2) R. Frischknecht, R. Itten, P. Sinha, M. de Wild-Scholten, J. Zhang, V. Fthenakis, H. C. Kim, M. Rauegi, M. Stucki, 2015, Life Cycle Inventories and Life Cycle Assessment of Photovoltaic Systems, International Energy Agency (IEA) PVPS Task 12, Report T12-04:2015

3) 20150807_Series 4v2 Module Datasheet. Tempe, Arizona: First Solar, 07 Aug. 2015. PDF.

Table A7: Life Cycle Inventory of Solar Retaining Clip

Description	Secondary Inputs	Amount	Unit
Output			
Solar Retaining Clip*		1.00	Clip
Inputs			
Plastic Injection Molding Part		0.03	kg
	Tap Water, at user	0.0132	kg
	Polypropylene/Ethylene Propylene Diene Elastomer Granulate	0.0306	kg
	Electricity Grid Mix	0.199	MJ
Aluminum Die-Cast Part		0.25	kg
	Electricity Grid Mix	0.873	MJ
	Aluminum Ingot Mix	0.261	kg
	Thermal Energy from Natural Gas	0.475	MJ

*Indicates a process developed as part of this analysis as opposed to an existing Gabi/Ecoinvent process

Sources: 1) Product Catalogue Mounting System 34. Eberswalde, Germany: MP-Tec, 2013. PDF.

Section B: Module Balance of Systems (BOS)

Table B1: Life Cycle Inventory of Cadmium Telluride Module BOS

Description	Secondary Inputs	Amount	Unit
Output			
CdTe Ground BOS*		1.00E+00	m ²
Inputs			
Mounting			
BF Steel billet/ slab bloom PE		1.02E+01	kg
Section bar rolling, steel		1.02E+01	kg
Zinc coating, pieces		6.31E-01	m ²
Aluminum ingot mix IAI (2010) IAI		1.34E-01	kg
Section bar extrusion, aluminum		1.34E-01	kg
Vulcanization of synthetic rubber PE		6.20E-02	kg
	Synthetic rubber, at plant	6.20E-02	kg
	Electricity, medium voltage, production ES, at grid	2.87E-01	MJ
	Lubricating oil, at plant	8.77E-04	kg
	Water, ultrapure, at plant	3.26E-01	kg
Other Support Structures			
Concrete block, at plant/DE		3.74E+00	kg
Sawn timber, softwood, raw, air dried, 20%, at plant		1.00E-03	m ³

Polyvinylchloride, at regional storage		4.20E-02	kg
Construction			
Diesel, at regional storage		1.72E+00	kg
Electricity, medium voltage, at grid		1.30E-01	kWh
	Diesel, burned in building machine	7.71E+01	MJ
Transformer			
BF Steel billet/ slab bloom PE		7.52E-01	kg
Sheet rolling, steel		7.52E-01	kg
Copper, primary, at refinery		1.84E-01	kg
Wire drawing, copper		1.84E-01	kg
Plastic extrusion profile (unspecific) PE		3.30E-02	kg
	Polyethylene, HDPE, granulate, at plant	3.32E-02	kg
	Electricity, medium voltage, production ES, at grid	9.10E-02	MJ
	Thermal energy from natural gas PE	1.42E-02	MJ
	Lubricating oil, at plant	4.66E-06	kg
	Compressed air 7 bar (medium power consumption) PE	7.92E-04	Nm ³
	Electricity, medium voltage, production ES, at grid	3.42E-04	MJ
Transformer, high voltage use, at plant		3.30E-02	kg

Soybean oil, at oil mill		6.68E-01	kg
Inverter			
Inverter, 500kW, at plant		2.37E-04	p
Operation and Maintenance (O&M)			
Electricity, medium voltage, at grid		4.18E+00	MJ
Natural gas, at long-distance pipeline		1.60E-02	Nm ³
	Natural gas, burned in gas turbine	6.03E-01	MJ
Petrol, unleaded, at regional storage		5.40E-02	kg
	Operation, passenger car, petrol, fleet average	5.37E-01	vkm
Transport			
Transport, transoceanic freight ship/OCE U		2.74E+02	tkm
Transport, lorry >16t, fleet average/RER U		2.72E+00	tkm
Waste			
Treatment, sewage, unpolluted, to wastewater treatment, class 3		8.90E-02	m ³
Emissions/Waste			
Heat, waste		1.30E+02	MJ
Transformation, from permanent crops, non-irrigated		2.73E+00	m ²
Transformation, to industrial area, built up		1.15E+00	m ²

Transformation, to industrial area, vegetation		1.58E+00	m ²
Occupation, industrial area, built up		3.46E+01	m ² a
Occupation, industrial area, vegetation		7.74E+01	m ² a

*Indicates a process developed as part of this analysis as opposed to an existing Gabi/Ecoinvent process

Sources: 1) Sinha, Parikhit, and Mariska de Wild-Scholten. "Life Cycle Assessment of Utility-Scale CdTe PV Balance of Systems." 27th European Photovoltaic Solar Energy Conference, Frankfurt. 2012.

Table B2: Life Cycle Inventory of Mono Crystalline Silicon Module BOS

Description	Amount	Unit
Output		
Mono-Si Ground BOS*	1.00	m ²
Inputs		
Ground Mount for Mono-Si*	1	m ²
Inverter (BOS)*	0.000146	pcs.
O&M (BOS)*	0.617	pcs.
Transformer (BOS)*	1.03	kg
Module AC/DC Cabling	1.23	m

Table B3: Life Cycle Inventory of Mono Crystalline Silicon Module Mounting

Description	Amount	Unit
Output		
Ground Mount Mono-Si*	1.00	m²
Inputs		
Aluminum Production Mix, Wrought alloy	3.98	kg
Corrugated Board, Mixed Fiber	0.0864	kg
Polyethylene HDPE, granulate	0.000909	kg
Disposal building polystyrene isolation	0.00455	kg
Polystyrene high impact, HIPS	0.00455	kg
Chromium steel 18/8	0.247	kg
Reinforcing Steel	7.21	kg
Concrete, normal	0.000537	m ³
Aluminum section bar extrusion	3.98	kg
Steel Section Bar Rolling	6.15	kg
Wire Drawing, Steel	1.06	kg
Zinc Coating, pieces	0.156	m ²
Zinc Coating, coils	0.109	m ²
transport, lorry >16ft.	0.217	tkm
transport, freight rail	5.14	tkm
Transport van	1.14	tkm
Disposal packaging cardboard	0.0864	kg
Disposal building polyethylene/polypropylene	0.000909	kg

*Indicates a process developed as part of this analysis as opposed to an existing Gabi/Ecoinvent process

Sources: R. Frischknecht, R. Itten, P. Sinha, M. de Wild-Scholten, J. Zhang, V. Fthenakis, H. C. Kim, M. Raugei, M. Stucki, 2015, Life Cycle Inventories and Life Cycle Assessment of Photovoltaic Systems, IEA PVPS Task 12, Report T12-04:2015 (2015).

Section C: Life Cycle Inventory of Li-ion Battery pack and Charge Controller

Table C1: Life Cycle Inventory of a Lithium-ion Battery Pack.

Description	Secondary Inputs	Amount	Unit
Output			
Lithium-ion Battery Pack*		1.00	kg
Inputs			
Battery Cell		3.00E-01	kg
BMS		3.70E-01	kg
Battery Packaging		3.20E-01	kg
	Electricity Grid Mix	1.44E-03	MJ
	Transport, lorry >16ft fleet average	1.60E-01	tkm
	Transport, transoceanic freight ship	4.9	tkm

*Indicates a process developed as part of this analysis as opposed to an existing Gabi/Ecoinvent process

Sources: Ellingsen, Linda Ager-Wick, et al. "Life Cycle Assessment of a Lithium-Ion Battery Vehicle Pack." *Journal of Industrial Ecology* 18.1 (2014): 113-124

Table C2: Life Cycle Inventory of a Lithium-ion Battery Cell

Description	Secondary Inputs	Amount	Unit
Output			
Battery Cell*		1.00	kg
Inputs			
Lithium-ion battery Anode		3.90E-01	kg
Lithium-ion Battery Cathode		4.30E-01	kg
Electrolyte		1.60E-01	kg
Seperator		2.20E-02	kg
Cell Container		6.70E-03	kg
	Water, decarbonized, at plant	380	kg
	Electricity grid mix	1.01E+02	MJ
	Transport, lorry >32t, EURO3	1.00E-01	tkm
	Transport, freight, rail	2.60E-01	tkm
	facilities precious metal refinery	1.90E-08	piece

*Indicates a process developed as part of this analysis as opposed to an existing Gabi/Ecoinvent process

Sources: Ellingsen, Linda Ager-Wick, et al. "Life Cycle Assessment of a Lithium-Ion Battery Vehicle Pack." Journal of Industrial Ecology 18.1 (2014): 113-124

Table C3: Life Cycle Inventory of a Lithium-ion Battery Anode

Description	Secondary Inputs	Amount	Unit
Output			
Lithium-ion battery anode*		1.00E+00	kg
Inputs			
Negative Current Collector		5.70E-01	kg
	copper, primary, at refinery	5.70E-01	kg
	sheet rolling, copper	5.70E-01	kg
	metal working factory	2.62E-10	kg
	Transport, freight, rail	1.14E-01	tkm
	Transport, lorry >32t, EURO3	5.70E-02	tkm
Negative Electrode Paste		4.30E-01	kg

	Graphite, battery grade, at plant	4.13E-01	kg
	carboxymethyl cellulose, powder, at plant	8.60E-03	kg
	acrylic acid, at plant	8.60E-03	kg
	N-methyl-2-pyrrolidone, at plant	4.04E-01	kg
	chemical plant, organics	1.72E-10	piece
	Transport, freight, rail	5.16E-01	tkm
	Transport, lorry >32t, EURO3	8.17E-02	tkm
Transport, freight, rail		3.70E-01	tkm
Transport, lorry >32t, EURO3		1.00E-01	tkm

*Indicates a process developed as part of this analysis as opposed to an existing Gabi/Ecoinvent process

Sources: Ellingsen, Linda Ager-Wick, et al. "Life Cycle Assessment of a Lithium-Ion Battery Vehicle Pack." Journal of Industrial Ecology 18.1 (2014): 113-124

Table C4: Life Cycle Inventory of a Lithium-ion Battery Cathode

Description	Secondary Inputs	Amount	Unit
Output			
Lithium-ion battery cathode*		1.00E+00	kg
Inputs			
Positive Current Collector		1.10E-01	kg
	Aluminium ingot mix, IAI (2010)	5.70E-01	kg
	sheet rolling, aluminium	5.70E-01	kg
	aluminium casting plant	2.62E-10	kg
	Transport, freight, rail	1.14E-01	tkm
	Transport, lorry >32t, EURO3	5.70E-02	tkm
Positive Electrode Paste		8.90E-01	kg
	polyvinylfluoride, at plant	3.56E-02	kg
	Carbon black, at plant	1.78E-02	kg
	N-methyl-2-pyrrolidone, at plant	3.65E-01	kg
	NiCoMn(OH) ₂	8.37E-01	kg
	chemical plant, organics	3.56E-10	piece
	Transport, freight, rail	4.09E-01	tkm

	Transport, lorry >32t, EURO3	1.25E-01	tkm
Transport, freight, rail		5.50E-01	tkm
Transport, lorry >32t, EURO3		1.00E-01	tkm

*Indicates a process developed as part of this analysis as opposed to an existing Gabi/Ecoinvent process

Sources: Ellingsen, Linda Ager-Wick, et al. "Life Cycle Assessment of a Lithium-Ion Battery Vehicle Pack." Journal of Industrial Ecology 18.1 (2014): 113-124

Table C5: Life Cycle Inventory of Nickel Cobalt Manganese for Lithium-ion Battery Positive Electrode Paste.

Description	Secondary Inputs	Amount	Unit
Output			
NiCoMn(OH) ₂ *		1.00E+00	kg
Inputs			
Production of CoSO ₄		5.70E-01	kg
Production of NiSO ₄		5.70E-01	kg
Production of MnSO ₄		5.50E-01	kg
Soda, powder, at plant		8.80E-01	kg
	Transport, freight, rail	1.50E+00	tkm
	Transport, lorry >16t, fleet average	2.60E-01	tkm
	Chemical plant, organics	4.00E-10	piece

*Indicates a process developed as part of this analysis as opposed to an existing Gabi/Ecoinvent process

Sources: Ellingsen, Linda Ager-Wick, et al. "Life Cycle Assessment of a Lithium-Ion Battery Vehicle Pack." Journal of Industrial Ecology 18.1 (2014): 113-124

Table C6: Life Cycle Inventory of Cobalt Sulfate for NiCoMn(OH)₂* in a Lithium-ion Battery.

Description	Amount	Unit
Output		
CoSO₄, at plant*	1.00E+00	kg
Aluminium (+III) [Inorganic emissions to fresh water]	7.20E-06	kg
Arsenic (+V) [Heavy metals to fresh water]	2.50E-07	kg
Cadmium (+II) [Heavy metals to fresh water]	2.60E-08	kg
Calcium (+II) [Inorganic emissions to fresh water]	5.70E-02	kg
Carbon disulphide [Inorganic emissions to air]	4.20E-03	kg
Chemical oxygen demand (COD) [Analytical measures to fresh water]	8.70E-04	kg
Chromium (+VI) [Heavy metals to fresh water]	4.60E-08	kg
Cobalt [Heavy metals to fresh water]	6.80E-08	kg
Copper (+II) [Heavy metals to fresh water]	6.70E-07	kg
Cyanide [Inorganic emissions to fresh water]	1.60E-04	kg
Dust (> PM10) [Particles to air]	7.50E-04	kg
Dust (PM2,5 - PM10) [Particles to air]	7.70E-03	kg
Dust (PM2.5) [Particles to air]	6.70E-03	kg
Iron [Heavy metals to fresh water]	2.40E-05	kg
Lead (+II) [Heavy metals to fresh water]	2.30E-07	kg
Manganese (+II) [Heavy metals to fresh water]	2.10E-06	kg
Mercury (+II) [Heavy metals to fresh water]	3.50E-09	kg
Nickel (+II) [Heavy metals to fresh water]	1.60E-06	kg
Nitrogen [Inorganic emissions to fresh water]	1.90E-03	kg
Solids (dissolved) [Analytical measures to fresh water]	4.30E-04	kg
Sulphate [Inorganic emissions to fresh water]	2.00E-01	kg
Zinc (+II) [Heavy metals to fresh water]	6.40E-06	kg
Inputs		
Chemicals inorganic, at plant	3.20E-02	kg
Chemicals organic, at plant	1.00E-02	kg
hydrogen cyanide, at plant	1.50E-03	kg
limestone, milled, packed, at plant	1.90E-02	kg
Portland calcareous cement, at plant	1.40E+00	kg
sand, at mine	1.70E+01	kg
blasting	6.30E-02	kg
diesel, burned in building machine	4.60E+00	MJ
electricity, medium voltage, production UCTEat grid	6.40E+00	MJ
transport, lorry, >16t, fleet average	9.40E-01	tkm
aluminium hydroxide, plant	3.40E-10	piece
conveyor belt, at plant	1.60E-06	m
non-ferrous metal mine, underground	2.10E-09	piece

disposal, nickel smelter slag, 0% water, to residual material landfill	1.30E+01	kg
disposal, sulfidic tailings, off-site	25	kg

*Indicates a process developed as part of this analysis as opposed to an existing Gabi/Ecoinvent process

Sources: Majeau-Bettez, Guillaume, Troy R. Hawkins, and Anders Hammer Strømman. "Life cycle environmental assessment of lithium-ion and nickel metal hydride batteries for plug-in hybrid and battery electric vehicles." *Environmental science & technology* 45.10 (2011): 4548-4554

Table C7: Life Cycle Inventory of Nickel Sulfate for a Lithium-ion Battery Positive Electrode Paste

Description	Amount	Unit
Output		
NiSO₄, at plant*	1.00E+00	kg
Aluminium [Particles to air]	5.60E-04	kg
Aluminium (+III) [Inorganic emissions to fresh water]	5.20E-06	kg
Arsenic (+V) [Heavy metals to fresh water]	2.00E-06	kg
Arsenic (+V) [Heavy metals to air]	2.60E-07	kg
Biological oxygen demand (BOD) [Analytical measures to fresh water]	6.30E-04	kg
Cadmium (+II) [Heavy metals to fresh water]	3.10E-08	kg
Calcium (+II) [Inorganic emissions to fresh water]	4.20E-02	kg
Carbon dioxide [Inorganic emissions to air]	3.20E-01	kg
Carbon disulphide [Inorganic emissions to air]	3.00E-03	kg
Chemical oxygen demand (COD) [Analytical measures to fresh water]	6.30E-04	kg
Chromium (+VI) [Heavy metals to fresh water]	1.60E-07	kg
Cobalt [Heavy metals to fresh water]	4.70E-08	kg
Cobalt [Heavy metals to air]	4.20E-04	kg
Copper (+II) [Heavy metals to fresh water]	7.10E-07	kg
Copper (+II) [Heavy metals to air]	1.30E-04	kg
Cyanide [Inorganic emissions to fresh water]	1.10E-04	kg
Iron [Heavy metals to fresh water]	1.80E-05	kg
Lead (+II) [Heavy metals to fresh water]	2.40E-07	kg
Lead (+II) [Heavy metals to air]	1.20E-05	kg
Magnesium [Inorganic emissions to air]	3.30E-04	kg
Manganese (+II) [Heavy metals to fresh water]	1.50E-06	kg
Mercury (+II) [Heavy metals to fresh water]	3.50E-09	kg
Nickel (+II) [Heavy metals to fresh water]	1.60E-06	kg

Nickel (+II) [Heavy metals to air]	1.50E-04	kg
Nickel ore (1.2%) [Non renewable resources]	4.80E-01	kg
Nitrogen organic bounded [Inorganic emissions to fresh water]	1.40E-03	kg
NMVOC (unspecified) [Group NMVOC to air]	6.90E-05	kg
Particulates, < 2.5 um [ecoinvent long-term to air]	5.70E-03	kg
Particulates, > 10 um [ecoinvent long-term to air]	5.80E-04	kg
Particulates, > 2.5 um, and < 10um [ecoinvent long-term to air]	5.00E-03	kg
Silver [Heavy metals to air]	4.80E-08	kg
Solids (dissolved) [Analytical measures to fresh water]	3.10E-04	kg
Sulphate [Inorganic emissions to fresh water]	1.40E-01	kg
Sulphur dioxide [Inorganic emissions to air]	5.10E-01	kg
Tin (+IV) [Heavy metals to fresh water]	1.20E-07	kg
Tin (+IV) [Heavy metals to air]	2.30E-06	kg
Total dissolved organic bounded carbon [Analytical measures to fresh water]	1.25E-04	kg
Total organic bounded carbon [Analytical measures to fresh water]	1.25E-04	kg
Waste heat [Other emissions to air]	5.27E+01	MJ
Water, river [Water]	1.10E-02	m3
Water, well, in ground [Water]	6.10E-02	m3
Zinc (+II) [Heavy metals to fresh water]	2.50E-06	kg
Zinc (+II) [Heavy metals to air]	2.50E-06	kg
Inputs		
ammonia, liquid, at regional storehouse	3.20E-02	kg
chemicals, inorganic, at plant	2.30E-02	kg
chemicals, organic, at plant	6.80E-03	kg
hydrogen cyanide, at plant	1.10E-03	kg
hydrogen liquid, at plant	0.00E+00	kg
limestone, milled, packed, at plant	7.30E-01	kg
Portland calcareous cement, at plant	1.00E+00	kg
sand, at mine	1.30E+01	kg
silica sand, at plant	7.20E-01	kg
blasting	4.60E-02	kg
diesel, burned in building machine	3.10E+00	MJ
UCTE electricity, high voltage, production UCTE, at grid	4.10E+00	MJ
electricity, hydropower, at run-of-river, power plant	1.05E+01	MJ
electricity grid mix	1.70E+00	MJ
heat, at hard coal industrial furnace 1-10MW	7.10E-01	MJ
natural gas burned in industrial furnace >100kW	3.50E+00	MJ
heavy fuel oil, burned in industrial furnace >100kw	8.10E+00	MJ

transport, lorry >16t, fleet average	6.80E-01	tkm
non-ferrous metal mine, underground	1.50E-09	piece
non-ferrous metal smelter	1.30E-11	piece
aluminium hydroxide, plant	2.50E-10	piece
conveyor belt, at plant	1.20E-06	m
disposal, nickel smelter slag, 0% water, to residual material landfill	3.60E+00	kg
disposal, sulfidic tailings, off-site	2.70E+01	kg

*Indicates a process developed as part of this analysis as opposed to an existing Gabi/Ecoinvent process

Sources: Majeau-Bettez, Guillaume, Troy R. Hawkins, and Anders Hammer Strømman. "Life cycle environmental assessment of lithium-ion and nickel metal hydride batteries for plug-in hybrid and battery electric vehicles." *Environmental science & technology* 45.10 (2011): 4548-4554

Table C8: Life Cycle Inventory of MnSO₄ for Lithium-ion Battery Positive Electrode Paste

Description	Amount	Unit
Output		
MnSO₄, at plant*	1.00E+00	kg
GLO: disposal, non-sulfidic tailings, off-site [residual material landfill facility]	0.71	kg
Waste heat [ecoinvent long-term to air]	1.5	MJ
Inputs		
GLO: hard coal coke, at plant [fuels]	1.43E+00	MJ
GLO: manganese concentrate, at beneficiation [Beneficiation]	1.10E+00	kg
GLO: non-ferrous metal mine, underground [Beneficiation]	1.60E-14	piece
RER: aluminium hydroxide, plant [Beneficiation]	2.40E-10	piece
RER: natural gas, high pressure, at consumer [fuels]	3.60E-02	MJ
RER: sulphuric acid, liquid, at plant [inorganics]	6.50E-01	kg
RER: transport, freight, rail [Railway]	3.90E-01	tkm
RER: transport, lorry >16t, fleet average [Street]	6.00E-02	tkm
Electricity grid mix	7.70E-02	MJ

*Indicates a process developed as part of this analysis as opposed to an existing Gabi/Ecoinvent process

Sources: Majeau-Bettez, Guillaume, Troy R. Hawkins, and Anders Hammer Strømman. "Life cycle environmental assessment of lithium-ion and nickel metal hydride batteries for plug-in hybrid and battery electric vehicles." *Environmental science & technology* 45.10 (2011): 4548-4554

Table C9: Life Cycle Inventory of Electrolyte for a Lithium-ion Battery.

Description	Amount	Unit
Output		
Electrolyte*	1.00E+00	kg
Inputs		
CN: ethylene carbonate, at plant [organics]	8.80E-01	kg
CN: lithium hexafluorophosphate, at plant [inorganics]	1.20E-01	kg
RER: chemical plant, organics [organics]	4.00E-10	pcs.
RER: transport, freight, rail [Railway]	6.00E-01	tkm
RER: transport, lorry >32t, EURO3 [Street]	1.00E-01	tkm

*Indicates a process developed as part of this analysis as opposed to an existing Gabi/Ecoinvent process

Sources: Ellingsen, Linda Ager-Wick, et al. "Life Cycle Assessment of a Lithium-Ion Battery Vehicle Pack." Journal of Industrial Ecology 18.1 (2014): 113-124

Table C10: Life Cycle Inventory of a Separator in a Lithium-ion Battery

Description	Amount	Unit
Output		
Separator*	1.00E+00	kg
Inputs		
RER: injection molding [processing]	1.00E+00	kg
RER: plastics processing factory [production of components]	7.40E-10	pcs.
RER: polypropylene, granulate, at plant [polymers]	1.00E+00	kg
RER: transport, freight, rail [Railway]	2.00E-01	tkm
RER: transport, lorry >32t, EURO3 [Street]	1.00E-01	tkm

*Indicates a process developed as part of this analysis as opposed to an existing Gabi/Ecoinvent process

Sources: Ellingsen, Linda Ager-Wick, et al. "Life Cycle Assessment of a Lithium-Ion Battery Vehicle Pack." Journal of Industrial Ecology 18.1 (2014): 113-124

Table C11: Life Cycle Inventory of a Cell Container in a Lithium-ion Battery.

Description	Secondary Inputs	Amount	Unit
Output			
Cell Container*		1.00E+00	kg
Inputs			
Aluminium tab		2.20E-01	kg
	RER: aluminium casting, plant [Benefication]	3.30E-11	pcs.
	RER: aluminium, production mix, at plant [Benefication]	2.20E-01	kg
	RER: sheet rolling, aluminium [processing]	2.20E-01	kg
	RER: transport, freight, rail [Railway]	4.40E-02	tkm
	RER: transport, lorry >32t, EURO3 [Street]	2.20E-02	tkm
Copper Tab		3.80E-01	kg
	GLO: copper, primary, at refinery [Benefication]	3.80E-01	kg
	RER: metal working factory [General manufacturing]	1.75E-20	pcs.
	RER: sheet rolling, copper [processing]	3.80E-01	kg
	RER: transport, freight, rail [Railway]	7.60E-02	tkm
	RER: transport, lorry >32t, EURO3 [Street]	3.80E-02	tkm
Multilayer Pouch		4.00E-01	kg
	RER: aluminium casting, plant [Benefication]	3.08E-11	pcs.
	RER: aluminium, production mix, at plant [Benefication]	2.00E-01	kg
	RER: injection moulding [processing]	1.88E-01	kg
	RER: nylon 6, at plant [polymers]	3.20E-02	kg
	RER: packaging film, LDPE, at plant [processing]	1.00E-02	kg
	RER: plastics processing factory [production of components]	1.40E-10	pcs.

	RER: polyethylene terephthalate, granulate, amorphous, at plant [polymers]	3.12E-02	kg
	RER: polypropylene, granulate, at plant [polymers]	1.28E-01	kg
	RER: sheet rolling, aluminium [processing]	2.00E-01	kg
RER: transport, lorry >32t, EURO3 [Street]		1.00E-01	tkm
RER: transport, freight, rail [Railway]		2.00E-01	tkm

*Indicates a process developed as part of this analysis as opposed to an existing Gabi/Ecoinvent process

Sources: Ellingsen, Linda Ager-Wick, et al. "Life Cycle Assessment of a Lithium-Ion Battery Vehicle Pack." Journal of Industrial Ecology 18.1 (2014): 113-124

Table C12: Life Cycle Inventory of a Battery Management System (BMS) of a Lithium-ion Battery

Description	Amount	Unit
Output		
BMS*	1.00E+00	kg
Inputs		
GLO: printed wiring board, through-hole mounted, unspec., Pb free, at plant [Module]	8.90E-02	kg
High Voltage System [Valuable substances]	3.00E-01	kg
IBIS [Valuable substances]	4.80E-01	kg
IBIS Fastener [Valuable substances]	3.00E-03	kg
Low voltage system [Valuable substances]	1.30E-01	kg
RER: transport, freight, rail [Railway]	2.00E-01	tkm
RER: transport, lorry >32t, EURO3 [Street]	1.00E-01	tkm

*Indicates a process developed as part of this analysis as opposed to an existing Gabi/Ecoinvent process

Sources: Ellingsen, Linda Ager-Wick, et al. "Life Cycle Assessment of a Lithium-Ion Battery Vehicle Pack." Journal of Industrial Ecology 18.1 (2014): 113-124

Table C13: Life Cycle Inventory of an IBIS for a Lithium-ion Battery.

Description	Amount	Unit
Output		
IBIS*	1.00E+00	kg
Inputs		
CH: brass, at plant [Benefication]	5.70E-03	kg
CH: casting, brass [processing]	5.70E-03	kg
GLO: connector, clamp connection, at plant [Parts]	2.10E-02	kg
GLO: electronic component production plant [Parts]	2.00E-08	pcs.
GLO: integrated circuit, IC, logic type, at plant [Parts]	1.70E-05	kg
GLO: printed wiring board, through-hole mounted, unspec., Pb free, at plant [Module]	1.10E-01	kg
RER: acrylonitrile-butadiene-styrene copolymer, ABS, at plant [polymers]	2.00E-04	kg
RER: injection moulding [processing]	0.0088	kg
RER: nylon 6, at plant [polymers]	0.0019	kg
RER: polyethylene terephthalate, granulate, amorphous, at plant [polymers]	0.0068	kg
RER: steel product manufacturing, average metal working [General manufacturing]	0.85	kg
RER: steel, low-alloyed, at plant [Benefication]	0.85	kg
RER: transport, freight, rail [Railway]	0.17	tkm
RER: transport, lorry >32t, EURO3 [Street]	0.087	tkm

*Indicates a process developed as part of this analysis as opposed to an existing Gabi/Ecoinvent process

Sources: Ellingsen, Linda Ager-Wick, et al. "Life Cycle Assessment of a Lithium-Ion Battery Vehicle Pack." Journal of Industrial Ecology 18.1 (2014): 113-124

Table C14: Life Cycle Inventory of an IBIS Fastener for a Lithium-ion Battery.

Description	Amount	Unit
Output		
IBIS fastener*	1.00E+00	kg
Inputs		
RER: metal working factory [General manufacturing]	4.60E-10	pcs.
RER: steel product manufacturing, average metal working [General manufacturing]	1.00E+00	kg
RER: steel, low-alloyed, at plant [Benefication]	1.00E+00	kg
RER: transport, freight, rail [Railway]	2.00E-01	tkm
RER: transport, lorry >32t, EURO3 [Street]	1.00E-01	tkm

*Indicates a process developed as part of this analysis as opposed to an existing Gabi/Ecoinvent process

Sources: Ellingsen, Linda Ager-Wick, et al. "Life Cycle Assessment of a Lithium-Ion Battery Vehicle Pack." Journal of Industrial Ecology 18.1 (2014): 113-124

Table C15: Life Cycle Inventory of a BMS High Voltage System within a Lithium-ion Battery.

Description	Amount	Unit
Output		
BMS High Voltage System*	1.00E+00	kg
Inputs		
GLO: cable, ribbon cable, 20-pin, with plugs, at plant [Parts]	4.50E-01	kg
GLO: copper, primary, at refinery [Benefication]	2.71E-01	kg
GLO: electronic component production plant [Parts]	2.00E-08	pcs.
GLO: polyphenylene sulfide, at plant [polymers]	3.20E-02	kg
RER: aluminium product manufacturing, average metal working [General manufacturing]	1.20E-01	kg
RER: aluminium, production mix, at plant [Benefication]	0.12	kg
RER: copper product manufacturing, average metal working [General manufacturing]	0.27	kg
RER: injection moulding [processing]	0.14	kg
RER: metal product manufacturing, average metal working [General manufacturing]	0.016	kg
RER: nylon 66, at plant [polymers]	0.044	kg

RER: polyethylene terephthalate, granulate, amorphous, at plant [polymers]	0.057	kg
RER: steel product manufacturing, average metal working [General manufacturing]	0.0014	kg
RER: steel, low-alloyed, at plant [Benefication]	0.0014	kg
RER: synthetic rubber, at plant [polymers]	0.0036	kg
RER: tin, at regional storage [Benefication]	0.016	kg
RER: transport, freight, rail [Railway]	0.11	tkm
RER: transport, lorry >32t, EURO3 [Street]	0.055	tkm

*Indicates a process developed as part of this analysis as opposed to an existing Gabi/Ecoinvent process

Sources: Ellingsen, Linda Ager-Wick, et al. "Life Cycle Assessment of a Lithium-Ion Battery Vehicle Pack." Journal of Industrial Ecology 18.1 (2014): 113-124

Table C16: Life Cycle Inventory of a BMS Low Voltage System within a Lithium-ion Battery

Description	Amount	Unit
Output		
BMS Low Voltage System*	1.00E+00	kg
Inputs		
GLO: electronic component production plant [Parts]	2.00E-08	pcs.
GLO: electronic component, passive, unspecified, at plant [Parts]	9.70E-01	kg
RER: injection moulding [processing]	2.90E-02	kg
RER: nylon 66, at plant [polymers]	2.90E-02	kg
RER: transport, freight, rail [Railway]	2.00E-01	tkm
RER: transport, lorry >32t, EURO3 [Street]	1.00E-01	tkm

*Indicates a process developed as part of this analysis as opposed to an existing Gabi/Ecoinvent process

Sources: Ellingsen, Linda Ager-Wick, et al. "Life Cycle Assessment of a Lithium-Ion Battery Vehicle Pack." Journal of Industrial Ecology 18.1 (2014): 113-124

Table C17: Life Cycle Inventory of Battery Packaging in a Lithium-ion Battery

Description	Amount	Unit
Output		
Battery Packaging*	1.00E+00	kg
Inputs		
Battery Retention [Valuable substances]	1.10E-01	kg
Battery Tray [Valuable substances]	3.00E-01	kg
Module Packaging [Valuable substances]	5.90E-01	kg
OCE: transport, transoceanic freight ship [Water]	4.80E+00	tkm
RER: transport, lorry >16t, fleet average [Street]	1.50E-01	tkm

*Indicates a process developed as part of this analysis as opposed to an existing Gabi/Ecoinvent process

Sources: Ellingsen, Linda Ager-Wick, et al. "Life Cycle Assessment of a Lithium-Ion Battery Vehicle Pack." Journal of Industrial Ecology 18.1 (2014): 113-124

Table C18: Life Cycle Inventory of a Battery Retention System within a Lithium-ion Battery

Description	Amount	Unit
Output		
Battery Retention*	1.00E+00	kg
Inputs		
Heat Transfer Plate [Valuable substances]	4.90E-01	kg
Lower Retention [Valuable substances]	3.80E-01	kg
RER: synthetic rubber, at plant [polymers]	1.30E-01	kg
RER: transport, freight, rail [Railway]	2.00E-01	tkm
RER: transport, lorry >32t, EURO3 [Street]	1.00E-01	tkm

*Indicates a process developed as part of this analysis as opposed to an existing Gabi/Ecoinvent process

Sources: Ellingsen, Linda Ager-Wick, et al. "Life Cycle Assessment of a Lithium-Ion Battery Vehicle Pack." Journal of Industrial Ecology 18.1 (2014): 113-124

Table C19: Life Cycle Inventory of a Lower Retention System within a Lithium-ion Battery

Description	Amount	Unit
Output		
Lower Retention*	1.00E+00	kg
Inputs		
RER: metal working factory [General manufacturing]	4.60E-10	pcs.
RER: steel product manufacturing, average metal working [General manufacturing]	1.00E+00	kg
RER: steel, low-alloyed, at plant [Benefication]	1.00E+00	kg
RER: transport, freight, rail [Railway]	2.00E-01	tkm
RER: transport, lorry >32t, EURO3 [Street]	1.00E-01	tkm

*Indicates a process developed as part of this analysis as opposed to an existing Gabi/Ecoinvent process

Sources: Ellingsen, Linda Ager-Wick, et al. "Life Cycle Assessment of a Lithium-Ion Battery Vehicle Pack." Journal of Industrial Ecology 18.1 (2014): 113-124

Table C20: Life Cycle Inventory of a Heat Transfer Plate for a Lithium-ion Battery

Description	Amount	Unit
Output		
Heat Transfer Plate*	1.00E+00	kg
Inputs		
RER: metal working factory [General manufacturing]	4.60E-10	pcs.
RER: steel product manufacturing, average metal working [General manufacturing]	1.00E+00	kg
RER: steel, low-alloyed, at plant [Benefication]	1.00E+00	kg
RER: transport, freight, rail [Railway]	2.00E-01	tkm
RER: transport, lorry >32t, EURO3 [Street]	1.00E-01	tkm

*Indicates a process developed as part of this analysis as opposed to an existing Gabi/Ecoinvent process

Sources: Ellingsen, Linda Ager-Wick, et al. "Life Cycle Assessment of a Lithium-Ion Battery Vehicle Pack." Journal of Industrial Ecology 18.1 (2014): 113-124

Table C21: Life Cycle Inventory of Battery Pack Module Packaging

Description	Amount	Unit
Output		
Module Packaging*	1.00E+00	kg
Inputs		
Inner frame [Valuable substances]	4.60E-01	kg
Outer Frame [Valuable substances]	5.40E-01	kg
RER: transport, freight, rail [Railway]	2.00E-01	tkm
RER: transport, lorry >32t, EURO3 [Street]	1.00E-01	tkm
SE: facilities precious metal refinery [Benefication]	1.90E-08	pcs.

*Indicates a process developed as part of this analysis as opposed to an existing Gabi/Ecoinvent process

Sources: Ellingsen, Linda Ager-Wick, et al. "Life Cycle Assessment of a Lithium-Ion Battery Vehicle Pack." *Journal of Industrial Ecology* 18.1 (2014): 113-124

Table C21: Life Cycle Inventory of Battery Pack Outer Frame

Description	Amount	Unit
Output		
Outer Frame*	1.00E+00	kg
Inputs		
RER: aluminum casting, plant [Benefication]	1.10E-10	pcs.
RER: aluminum, production mix, at plant [Benefication]	7.00E-01	kg
RER: anodising, aluminum sheet [processing]	3.00E-02	m ²
RER: injection molding [processing]	3.00E-01	kg
RER: nylon 66, glass-filled, at plant [polymers]	3.00E-01	kg
RER: plastics processing factory [production of components]	2.20E-10	pcs.
RER: sheet rolling, aluminum [processing]	0.7	kg
RER: transport, freight, rail [Railway]	0.2	tkm
RER: transport, lorry >32t, EURO3 [Street]	0.1	tkm

*Indicates a process developed as part of this analysis as opposed to an existing Gabi/Ecoinvent process

Sources: Ellingsen, Linda Ager-Wick, et al. "Life Cycle Assessment of a Lithium-Ion Battery Vehicle Pack." Journal of Industrial Ecology 18.1 (2014): 113-124

Table C23: Life Cycle Inventory of Battery Pack Inner Frame

Description	Amount	Unit
Output		
Inner Frame*	1.00E+00	kg
Inputs		
RER: aluminum casting, plant [Benefication]	1.00E-10	pcs.
RER: aluminum, production mix, at plant [Benefication]	6.50E-01	kg

RER: anodising, aluminum sheet [processing]	3.00E-02	sqm
RER: injection molding [processing]	3.50E-01	kg
RER: nylon 66, glass-filled, at plant [polymers]	3.50E-01	kg
RER: plastics processing factory [production of components]	2.60E-10	pcs.
RER: sheet rolling, aluminum [processing]	6.50E-01	kg
RER: transport, freight, rail [Railway]	2.00E-01	tkm
RER: transport, lorry >32t, EURO3 [Street]	1.00E-01	tkm

*Indicates a process developed as part of this analysis as opposed to an existing Gabi/Ecoinvent process

Sources: Ellingsen, Linda Ager-Wick, et al. "Life Cycle Assessment of a Lithium-Ion Battery Vehicle Pack." Journal of Industrial Ecology 18.1 (2014): 113-124

Table C24: Life Cycle Inventory of Battery Tray

Description	Amount	Unit
Output		
Battery Tray*	1.00E+00	kg
Inputs		
RER: transport, freight, rail [Railway]	1.00E-01	tkm
RER: transport, lorry >32t, EURO3 [Street]	2.00E-01	tkm
Tray lid [Valuable substances]	2.10E-01	kg
Tray with fasteners [Valuable substances]	7.90E-01	kg

*Indicates a process developed as part of this analysis as opposed to an existing Gabi/Ecoinvent process

Sources: Ellingsen, Linda Ager-Wick, et al. "Life Cycle Assessment of a Lithium-Ion Battery Vehicle Pack." Journal of Industrial Ecology 18.1 (2014): 113-124

Table C25: Life Cycle Inventory of Battery Tray Lid

Description	Amount	Unit
Output		
Tray Lid*	1.00E+00	kg
Inputs		
RER: injection molding [processing]	1.00E+00	kg
RER: plastics processing factory [production of components]	7.40E-10	pcs.
RER: polypropylene, granulate, at plant [polymers]	1.00E+00	kg
RER: transport, freight, rail [Railway]	2.00E-01	tkm
RER: transport, lorry >32t, EURO3 [Street]	0.1	tkm

*Indicates a process developed as part of this analysis as opposed to an existing Gabi/Ecoinvent process

Sources: Ellingsen, Linda Ager-Wick, et al. "Life Cycle Assessment of a Lithium-Ion Battery Vehicle Pack." Journal of Industrial Ecology 18.1 (2014): 113-124

Table C26: Life Cycle Inventory of Battery Tray with Fasteners

Description	Amount	Unit
Output		
Tray Lid with Fasteners*	1.00E+00	kg
Inputs		
RER: metal working factory [General manufacturing]	4.60E-10	pcs.
RER: steel product manufacturing, average metal working [General manufacturing]	1.00E+00	kg
RER: steel, low-alloyed, at plant [Benefication]	1.00E+00	kg
RER: transport, freight, rail [Railway]	2.00E-01	tkm
RER: transport, lorry >32t, EURO3 [Street]	0.1	tkm

*Indicates a process developed as part of this analysis as opposed to an existing Gabi/Ecoinvent process

Sources: Ellingsen, Linda Ager-Wick, et al. "Life Cycle Assessment of a Lithium-Ion Battery Vehicle Pack." *Journal of Industrial Ecology* 18.1 (2014): 113-124

Table C27: Life Cycle Inventory of Charge Controller Manufacturing

Description	Secondary Inputs	Amount	Unit
Output			
Charge Controller*		1.00E+00	pc.
Inputs			
Heat Sink*		1.00E+00	pc.
i) Aluminum Part		2.83E+00	kg
	Aluminum Ingot	2.96E+00	kg
	Electricity	9.88E+00	MJ
	Thermal Energy from Heavy Fuel Oil	5.38E+00	MJ
Printed Wiring Board*		1.00E+00	pc.
i) printed wiring board, mixed mounted, solder mix		1.50E-02	m ²
ii) Copper		2.55E-03	kg
Enclosure Box*		1.00E+00	pc.
i) Steel part		1.36E+00	kg
	Steel electro-galvanised coil	1.43E+00	kg
	lubricating oil, at plant [organics]	1.81E-04	kg
	Compressed air 7 bar	1.03E-01	Nm ³
	Electricity grid mix	2.82E-01	MJ

*Indicates a process developed as part of this analysis as opposed to an existing Gabi/Ecoinvent process

Sources: 1) Marcellino, Joe (Morningstar Corp. technical support), email to author, 24 Nov. 2015 2) Dutta, Debashish (Electrical Engineer, <http://www.opengreenenergy.in>), personal communication, 3 Dec. 2015. 3) Morningstar TS-MPPT-600V operation manual

Section D: Life Cycle Inventory of Diesel Generator

Table D1: Life Cycle Inventory of Diesel Generator Production

Description	Secondary Inputs	Amount	Unit
Output			
Diesel Generator		1.00	kg
Inputs			
Aluminum die cast part		0.35	kg
i) Primary Aluminum Ingot (cast part)		0.37	kg
	Thermal Energy from Natural Gas	0.67	MJ
	Electricity, Medium Voltage	1.23	MJ
Steel cast part		0.30	kg
	Thermal Energy from Natural Gas	1.03	MJ
	Electricity, Medium Voltage	1.48	MJ
Steel		0.30	kg
Copper (wire)		0.03	kg
Plastic (Polypropylene part)		0.02	kg

Source: Smith, Cameron, John Burrows, Eric Scheier, Amberli Young, Jessica Smith, Tiffany Young, and Shabbir H. Gheewala. "Comparative Life Cycle Assessment of a Thai Island's Diesel/PV/wind Hybrid Microgrid." *Renewable Energy* 80 (2015): 85-100. Web.

Table D2: Life Cycle Inventory of Diesel Generator Use Phase

Description	Amount	Unit
Output		
Electricity	1.00E+00	MJ
Inputs		
Diesel burned in generator	1.00E+00	MJ
i) Diesel	2.34E-02	kg
ii) Lubricating oil	6.69E-05	kg
iii) Mineral oil	6.69E-05	kg

Source: Smith, Cameron, John Burrows, Eric Scheier, Amberli Young, Jessica Smith, Tiffany Young, and Shabbir H. Gheewala. "Comparative Life Cycle Assessment of a Thai Island's Diesel/PV/wind Hybrid Microgrid." *Renewable Energy* 80 (2015): 85-100. Web.

Section E: Life Cycle Inventory of Microgrid Distribution and Security Systems

Table E1: Life Cycle Inventory of Residential Electricity Meters

Description	Secondary Inputs	Amount	Unit
Output			
Residential Electricity Meter*		1.00E+00	m
Inputs			
Plastic Injection Molding Part		4.00E+00	kg
	Tap Water, at user	1.76E+00	kg
	Polycarbonate Granulate	4.08E+00	kg
	Electricity Grid Mix	2.66E+01	MJ
Aluminum Die-Cast Part		4.00E-01	kg
	Electricity Grid Mix	1.40E+00	MJ
	Aluminum Ingot Mix	4.18E-01	kg
	Thermal Energy from Natural Gas	7.60E-01	MJ
LCD glass		1.00E+00	kg
Electronics for Control Units		2.00E-01	kg
Backlight LCD screen		2.00E-01	

*Indicates a process developed as part of this analysis as opposed to an existing Gabi/Ecoinvent process

Sources: 1) CENTRON II C1219. Liberty Lake, Washington: Itron, 2014. PDF.

2) Marshall, Vin. "The Dissection: A Home Electric Meter." Popular Science. N.p., 14 Oct. 2009. Web.

Table E2: Life Cycle Inventory of Copper Electricity Wiring

Description	Secondary Inputs	Amount	Unit
Output			
Copper Electricity Wiring*		1.00E+00	m
Inputs			
Tube Insulation		2.00E-02	kg
i) Nylon 6		1.00E-02	kg
ii) Tube Elastomere*		1.00E-02	kg
	Thermal Energy from Natural Gas	4.29E-02	MJ
	Compressed Air	2.40E-03	nm ³
	Polyvinyl Chloride Granulate	1.00E-02	kg
	Lubricating Oil	1.41E-06	kg
	Electricity Grid Mix	2.76E-02	MJ
	Processing		
	Plastic Extrusion Profile	1.00E-02	kg
Copper Wire		1.85E-02	kg
	Electricity Grid Mix	9.54E-02	MJ
	Copper Mix	1.85E-02	kg
	Thermal Energy from Natural Gas	9.25E-04	MJ
	Processing		
	Copper Wire (6 mm)	1.85E-02	kg

*Indicates a process developed as part of this analysis as opposed to an existing Gabi/Ecoinvent process

Sources: 1) Socolof et. al 2014; Design for the Environment (DfE) Wire and Cable Partnership. Rep. no. EPA 744R08001. United States Environmental Protection Agency

Table E3: Life Cycle Inventory of Security Fencing

Description	Secondary Inputs	Amount	Unit
Output			
Chain Link Fence*		1.00E+00	m
Inputs			
Steel Wire Rod		2.35E+01	kg
	BF Steel Billet	2.48E+01	kg
Steel Fence Post*		3.33E-01	Posts
	Steel Welded Pipe	5.52E+00	kg

*Indicates a process developed as part of this analysis as opposed to an existing Gabi/Ecoinvent process

Sources: 1) Chain-link-fabric-weights. Sharon, Pennsylvania: Wheatland Tube, 2014. PDF.

2) Chain Link Fence Manufacturers Institute Product Manual. Columbia, Maryland: Chain Link Fence Manufacturers Institute, 2011. PDF.

Section F: Life Cycle Inventory of Microgrid End of Life

Table F1: Life Cycle Inventory of PV-Hybrid Microgrid Landfilling

Description	Amount	Unit
Output		
Microgrid Landfilling*	1.00	Pieces
Inputs		
aluminum waste [Valuable substances]	700	kg
Ferro-metals waste [Valuable substances]	280	kg
glass waste [Resources]	280	kg
plastic waste [Valuable substances]	140	kg
steel waste [Valuable substances]	1400	kg

*Indicates a process developed as part of this analysis as opposed to an existing Gabi/Ecoinvent process

Table F2: Life Cycle Inventory of Cadmium Telluride Module Takeback and Recycling

Description	Amount	Unit
Output		
Recycling, CdTe Module*	1.00E+00	sqm
Inputs		
Transport, lorry >16t, fleet average	1.12E+01	tkm
Electricity, medium voltage, at grid	4.38E+00	kWh
Sulphuric acid, liquid, at plant	8.33E-02	kg

Water, deionised, at plant/CH U	5.42E+00	kg
Hydrogen peroxide, 50% in H ₂ O, at plant	5.71E-01	kg
Sodium hydroxide, 50% in H ₂ O, production mix, at plant	1.04E-01	kg
Treatment, PV cell production effluent, to wastewater treatment, class 3	4.79E-03	m ³
Disposal, plastics, mixture, 15.3% water, to municipal incineration	6.16E-01	kg
Disposal, inert waste, 5% water, to inert material landfill	1.28E-01	kg
Avoided Burden		
Cadmium sludge, from zinc electrolysis, at plant	2.84E-02	kg
Copper telluride cement, from copper production	3.22E-02	kg
Silica sand, at plant	8.27E+00	kg
Soda, powder, at plant	3.28E+00	kg
Limestone, milled, packed, at plant	5.72E+00	kg
Natural gas, high pressure, at consumer	1.96E+01	MJ
Heavy fuel oil, at regional storage	3.17E-01	kg
Copper, primary, at refinery	7.89E-02	kg
Emissions/Waste		
Cadmium, ion	8.92E-08	kg
Cadmium	5.89E-09	kg

*Indicates a process developed as part of this analysis as opposed to an existing Gabi/Ecoinvent process

Sources: 1) Bergesen, Joseph D., et al. "Thin-film photovoltaic power generation offers decreasing greenhouse gas emissions and increasing environmental co-benefits in the long term." *Environmental science & technology* 48.16 (2014): 9834-9843.

Table F3: Life Cycle Inventory of BOS Recycling

Description	Amount	Unit
Output		
Recycling, CdTe Ground BOS*	1.00E+00	m ²
Inputs		
Transport, lorry >16t, fleet average	1.08E+00	tkm
Aluminum, secondary, from old scrap, at plant/RER U	1.35E-01	kg
Steel, electric, un- and low-alloyed, at plant/RER U	9.86E+00	kg
Copper, secondary, at refinery/RER U	8.09E-01	kg
Avoided Burden		
Aluminum ingot mix IAI (2010) IAI	1.35E-01	kg
BF Steel billet/ slab/ bloom PE	9.86E+00	kg
Copper, primary, at refinery	8.09E-01	kg

*Indicates a process developed as part of this analysis as opposed to an existing Gabi/Ecoinvent process

Sources: 1) Bergesen, Joseph D., et al. "Thin-film photovoltaic power generation offers decreasing greenhouse gas emissions and increasing environmental co-benefits in the long term." *Environmental science & technology* 48.16 (2014): 9834-9843.

Table F4: Life Cycle Inventory of Pyrometallurgical Recycling of Battery Pack

Description	Secondary processes	Amount	Unit
Output			
Aluminum scrap [Waste for recovery]		1.81E-01	kg
	RER: Aluminum, secondary, from old scrap, at plant	-1.71E-01	kg
Copper scrap [Waste for recovery]		1.33E-01	kg
	RER: Copper, secondary, at refinery	-1.26E-01	
GLO: cobalt, at plant [Beneficiation]		-4.32E-02	kg
GLO: manganese concentrate, at beneficiation [Beneficiation]		-4.10E-02	kg
Steel scrap [Waste for recovery]		1.24E-01	kg
	DE: EAF Steel billet / Slab / Bloom PE	-1.17E-01	kg
CH: disposal, plastics, mixture, 15.3% water, to municipal incineration [municipal incineration]		2.00E-01	kg
CH: treatment, sewage, to wastewater treatment, class 3 [wastewater treatment]		1.00E-03	m ³
Chlorine [ecoinvent long-term to fresh water]		4.00E-02	kg
Dust (PM10) [Particles to air]		2.08E-04	kg
GLO: Co powder, pyrometallurgical processing Li-ion batteries, at plant [Recycling]		7.49E-02	kg

GLO: MnO ₂ powder, pyrometallurgical processing Li-ion batteries, at plant [Recycling]		1.00E-02	kg
secondary mixed polymer [Valuable substances]		8.00E-02	kg
Sulphur dioxide [Inorganic emissions to fresh water]		4.00E-02	kg
Sulphur dioxide [ecoinvent long-term to air]		4.80E-05	kg
Inputs			
CH: electricity, medium voltage, at grid [supply mix]		2.88E+00	MJ
RER: sodium hydroxide, 50% in H ₂ O, production mix, at plant [inorganics]		2.10E-01	kg
RER: tap water, at user [Appropriation]		1.00E+00	kg
spent battery pack, pyro [Valuable substances]		1.00E+00	kg

Sources: Fisher, Karen, et al. "Battery waste management life cycle assessment." Final report for publication. Environmental Resources Management (2006).

Table F5: Life Cycle Inventory of Hydrometallurgical Recycling of Battery Pack

Description	Secondary processes	Amount	Unit
Output			
Copper scrap [Waste for recovery]		1.33E-01	kg
	RER: Copper, secondary, at refinery	-1.26E-01	kg
GLO: cobalt, at plant [Benefication]		-4.28E-02	kg

GLO: lithium carbonate, at plant [inorganics]		-4.94E-04	kg
RER: aluminum scrap, old, at plant [Benefication]		1.81E-01	kg
	RER: Aluminum, secondary, from old scrap, at plant	-1.71E-01	kg
Steel scrap (St) [Waste for recovery]		1.24E-01	kg
	DE: EAF Steel billet / Slab / BloomPE	-1.17E-01	kg
CH: treatment, sewage, to wastewater treatment, class 3 [wastewater treatment]		3.37E-01	m3
Cobalt [ecoinvent long-term to fresh water]		1.67E-08	kg
COD, Chemical Oxygen Demand [ecoinvent long-term to fresh water]		3.00E-07	kg
Copper [Heavy metals to fresh water]		1.67E-08	kg
Fluoride [ecoinvent long-term to fresh water]		3.00E-08	kg
Gypsum [Waste for recovery]		3.39E-01	kg
Hydrocarbons (unspecified) [Hydrocarbons to fresh water]		1.00E-08	kg
Nickel, ion [ecoinvent long-term to fresh water]		1.67E-08	kg
NMVOC, non-methane volatile organic compounds, unspecified origin [ecoinvent long-term to air]		2.50E-07	kg

Paper (unspecified) [Consumer waste]		6.50E-02	kg
Plastic (without metal; unspecified) [Waste for recovery]		6.50E-02	kg
Sulphur dioxide [Inorganic emissions to air]		4.50E-07	kg
Suspended solids, unspecified [Particles to fresh water]		1.20E-07	kg
Waste in landfill (inert material, sanitary and residual material landfill) [Consumer waste]		2.02E-01	kg
Inputs			
CH: lime, hydrated, packed, at plant [Binder]		1.16E-01	kg
FR: electricity, medium voltage, production FR, at grid [production mix]		5.04E-01	MJ
GLO: chemicals inorganic, at plant [inorganics]		2.50E-02	kg
RER: sulphuric acid, liquid, at plant [inorganics]		2.31E-01	kg
RER: tap water, at user [Appropriation]		7.20E-01	kg
Spent Battery Pack, Hydro [Valuable substances]		1.00E+00	kg

Sources: Fisher, Karen, et al. "Battery waste management life cycle assessment." Final report for publication. Environmental Resources Management (2006).

Table F6: Life Cycle Inventory of Diesel Generator Recycling

Description	Secondary Inputs	Amount	Unit
Output			
Diesel Generator – Recycled*		1.00E+00	kg
Inputs			
Primary Aluminum Ingot		-9.62E-01	kg
Steel		-9.52E-01	kg
Processing			
	Aluminum Recycling	1.00E+00	kg
	EAF Steel Billet	1.00E+00	kg
	Copper Recycling Potential	1.00E+00	kg

*Indicates a process developed as part of this analysis as opposed to an existing Gabi/Ecoinvent process

Source: Smith, Cameron, John Burrows, Eric Scheier, Amberli Young, Jessica Smith, Tiffany Young, and Shabbir H. Gheewala. "Comparative Life Cycle Assessment of a Thai Island's Diesel/PV/wind Hybrid Microgrid." *Renewable Energy* 80 (2015): 85-100. Web.

Section G: Life Cycle Inventory of Electricity Grid Mixes

Table G1: Life Cycle Inventory of Average Kenya Electricity Grid Mix

Description	Amount	Unit
Output		
Kenya Electricity Mix*	3.60E+00	MJ
Inputs		
Electricity from Heavy Fuel Oil	1.11E+00	MJ
Electricity from Hydro	1.60E+00	MJ
Electricity from Photovoltaic	4.07E-04	MJ
Electricity from Biomass	7.26E-02	MJ
Electricity from Wind	7.30E-03	MJ
Electricity from Geothermal	8.14E-01	MJ

*Indicates a process developed as part of this analysis as opposed to an existing Gabi/Ecoinvent process

Sources: 1) IEA (2010) Energy Statistics for different countries. Electricity/Heat Data. Retrieved June 2011

Table G2: Life Cycle Inventory of the Marginal Kenya Electricity Grid Mix

Description	Amount	Unit
Output		
Kenya Electricity Mix*	3.60	MJ
Inputs		
Electricity from Heavy Fuel Oil	0.1	MJ
Electricity from Hydro	0.23	MJ
Electricity from Coal	1.1	MJ
Electricity from Natural Gas	0.61	MJ
Electricity from Wind	0.36	MJ
Electricity from Geothermal	1.2	MJ

*Indicates a process developed as part of this analysis as opposed to an existing Gabi/Ecoinvent process

Sources: 1) 10 YEAR POWER SECTOR EXPANSION PLAN 2014-2024. N.p.: Republic of Kenya, June 2014. PDF.

Table G3: Life Cycle Inventory of Malaysia Electricity Grid Mix

Description	Amount	Unit
Output		
Malaysia Electricity Mix*	3.60E+00	MJ
Inputs		
Electricity from Natural Gas	2.29E+00	MJ
Electricity from Hard Coal	9.68E-01	MJ
Electricity from Heavy Fuel Oil	6.80E-02	MJ
Electricity from Hydro	2.78E-01	MJ

*Indicates a process developed as part of this analysis as opposed to an existing Gabi/Ecoinvent process

Sources: 1) IEA (2010) Energy Statistics for different countries. Electricity/Heat Data. Retrieved June 2011

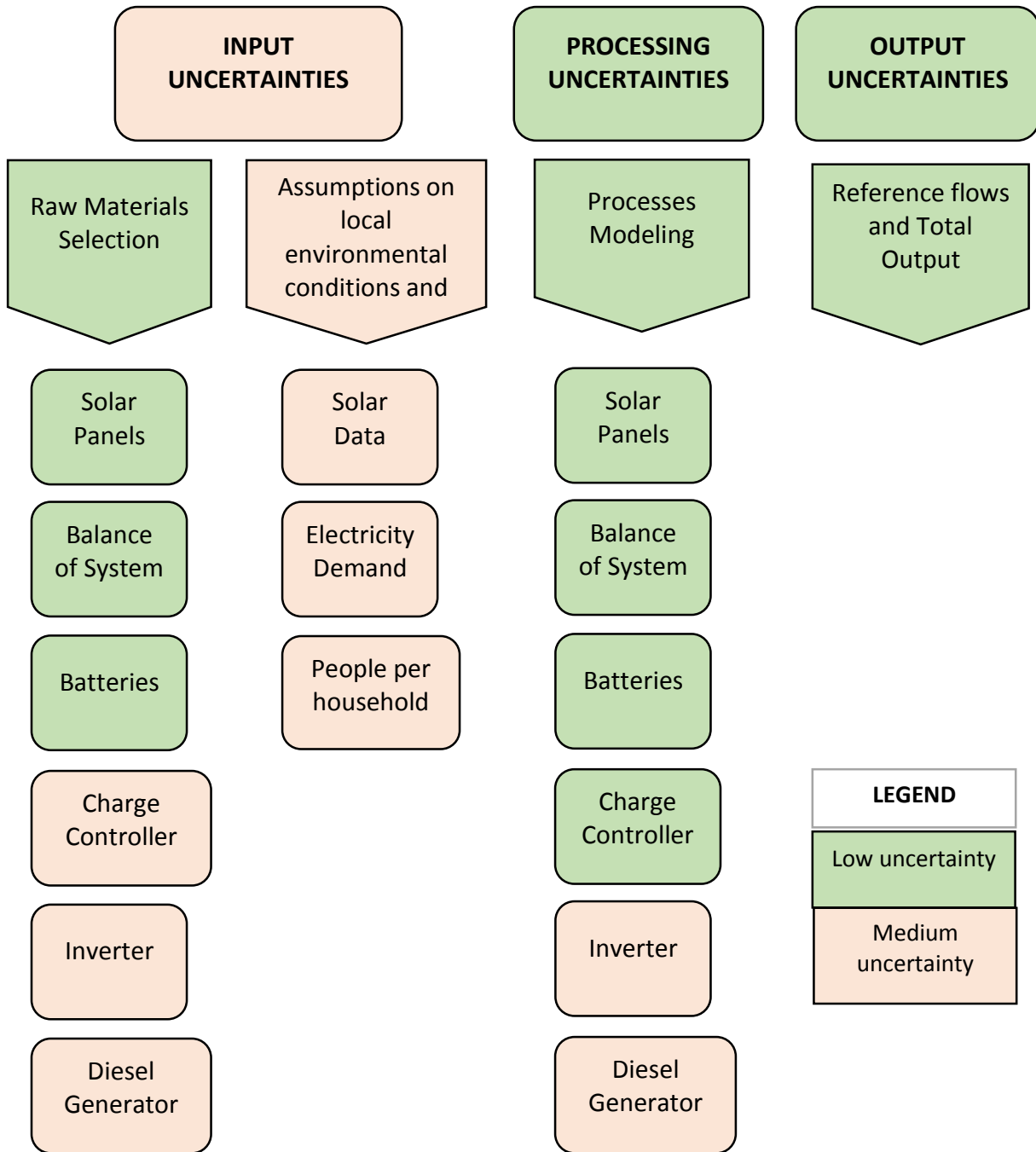
Table G4: Life Cycle Inventory of South Korean Electricity Grid Mix

Description	Amount	Unit
Output		
South Korea Electricity Mix*	3.60E+00	MJ
Inputs		
Electricity from Heavy Fuel Oil	1.24E-01	MJ
Electricity from Photovoltaic	2.16E-03	MJ
Electricity from Biomass	3.60E-04	MJ
Electricity from Wind	3.60E-03	MJ
Electricity from Geothermal	8.14E-01	MJ
Electricity from Nuclear	1.21E+00	MJ
Electricity from Waste	5.04E-03	MJ
Electricity from Hard Coal	1.43E+00	MJ
Electricity from Natural Gas	7.82E-01	MJ

*Indicates a process developed as part of this analysis as opposed to an existing Gabi/Ecoinvent process

Sources: 1) IEA (2010) Energy Statistics for different countries. Electricity/Heat Data. Retrieved June 2011

Appendix 3: Breakdown of Uncertainties



Appendix 4: PV-Hybrid and PV-Diesel Contribution Analysis

For the climate change, particulate matter, photochemical oxidant, and acidification categories, the majority of the PV-Hybrid impacts came from the generator use and the battery. In total, 11-36% of the hybrid impacts came from the lithium-ion battery. The substantial drop in battery contribution from the PV-Battery model is due in large part to the use of the diesel generator which ended up contributing over 55-83% of the total impacts (**Figure 21**).

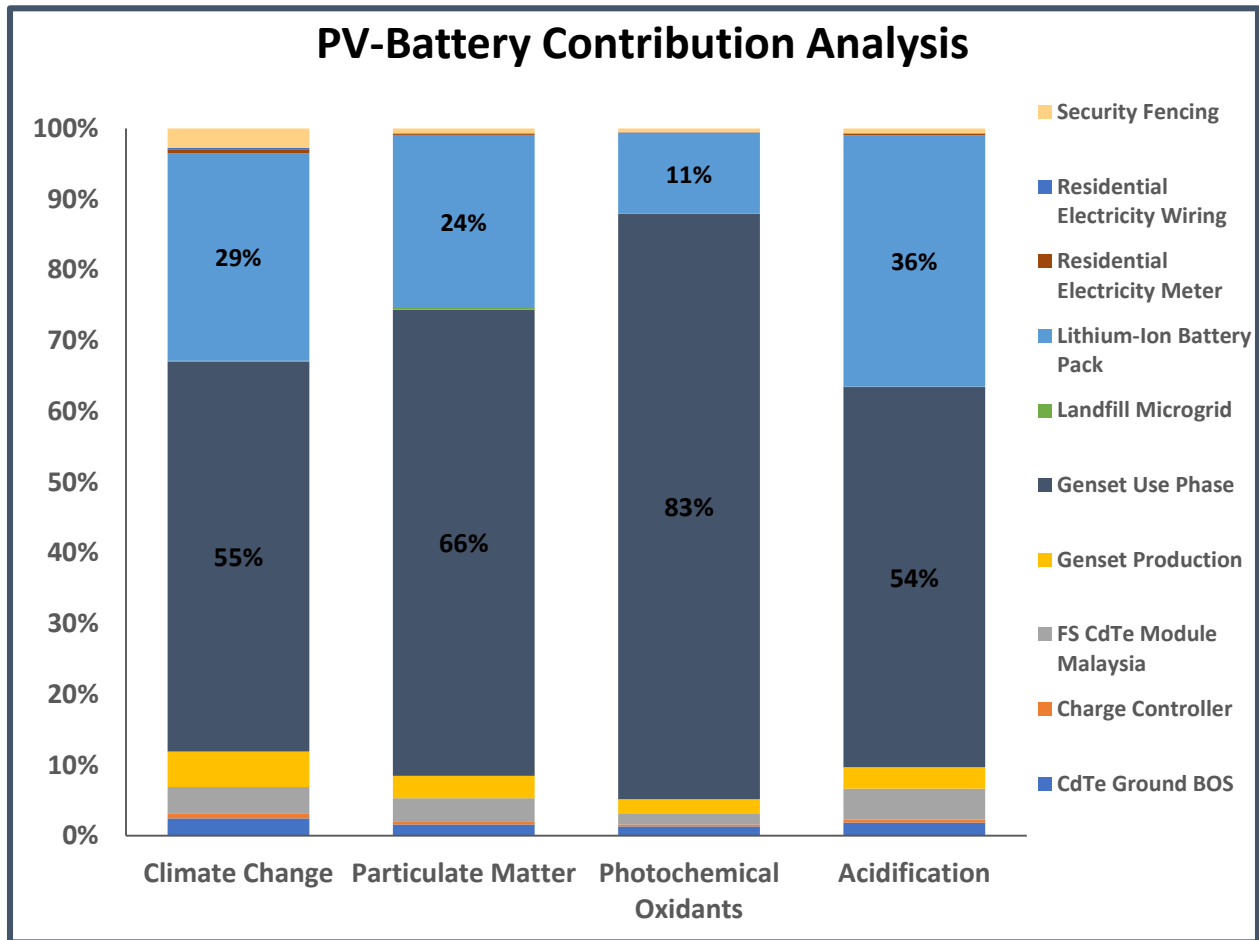


Figure 21: Contribution of PV-Hybrid Components. Contribution of individual PV-Hybrid microgrid components to overall microgrid climate change (kg CO₂e), PM (kg PM₁₀ eq.), photochemical oxidant formation (kg NMVOC), and terrestrial acidification (kg SO₂ eq.) impact.

As was seen in the PV-Battery system, the battery cell production also dominates the total battery impact for all four categories for the PV-Hybrid system contributing 73-86% of the total battery impacts (**Figure 22**).

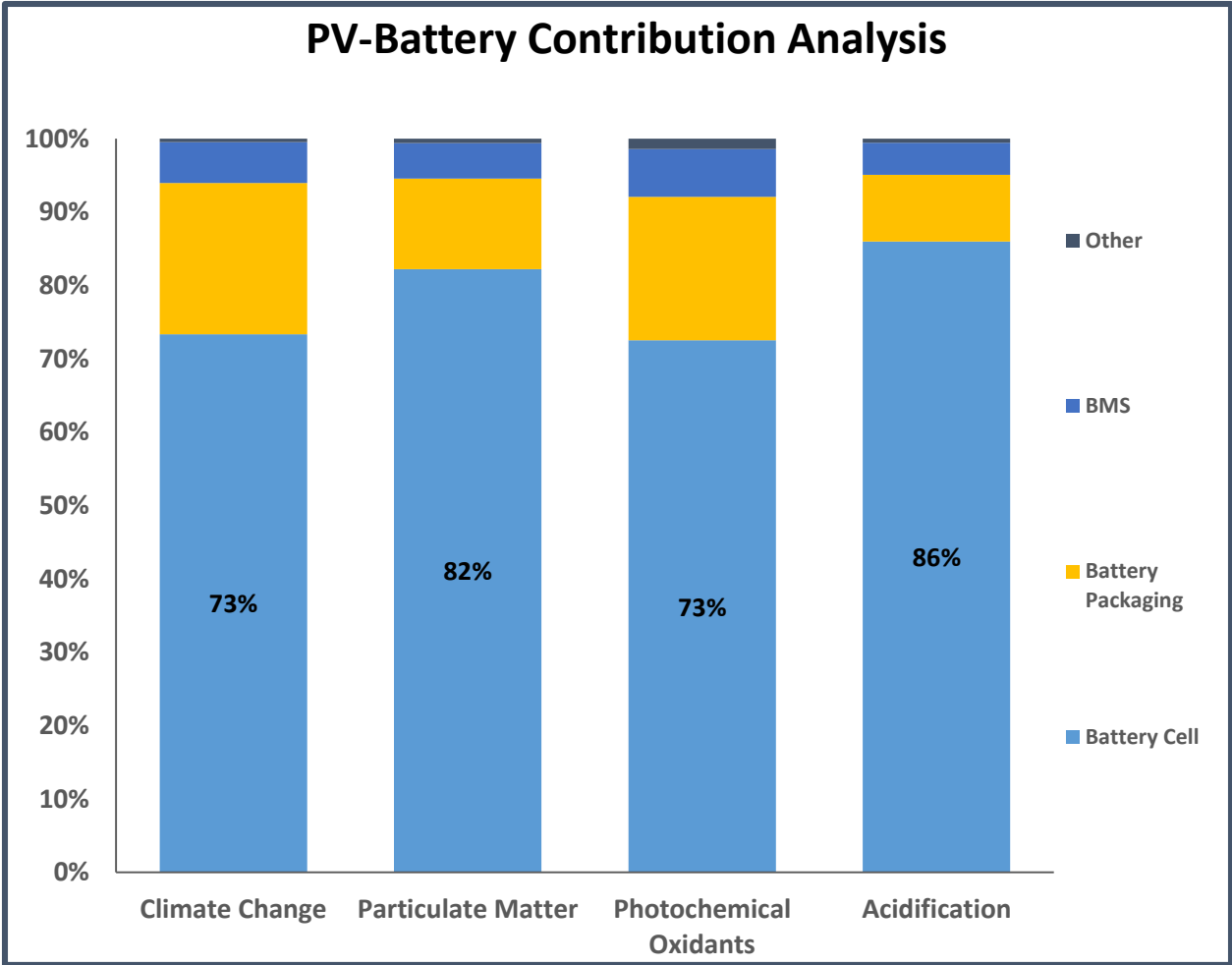


Figure 22: Contribution Analysis of Lithium-ion Battery Components. Contribution of individual lithium-ion battery components to overall Li-ion battery climate change (kg CO₂e), PM (kg PM₁₀ eq.), photochemical oxidant formation (kg NMVOC), and terrestrial acidification (kg SO₂ eq.) impact in the PV-Hybrid system.

Within the battery cell process, the majority of the climate change impacts (69%) came from the electricity used in production, whereas, again, the other three categories are more evenly split between the cathode and anode processes (**Figure 23**).

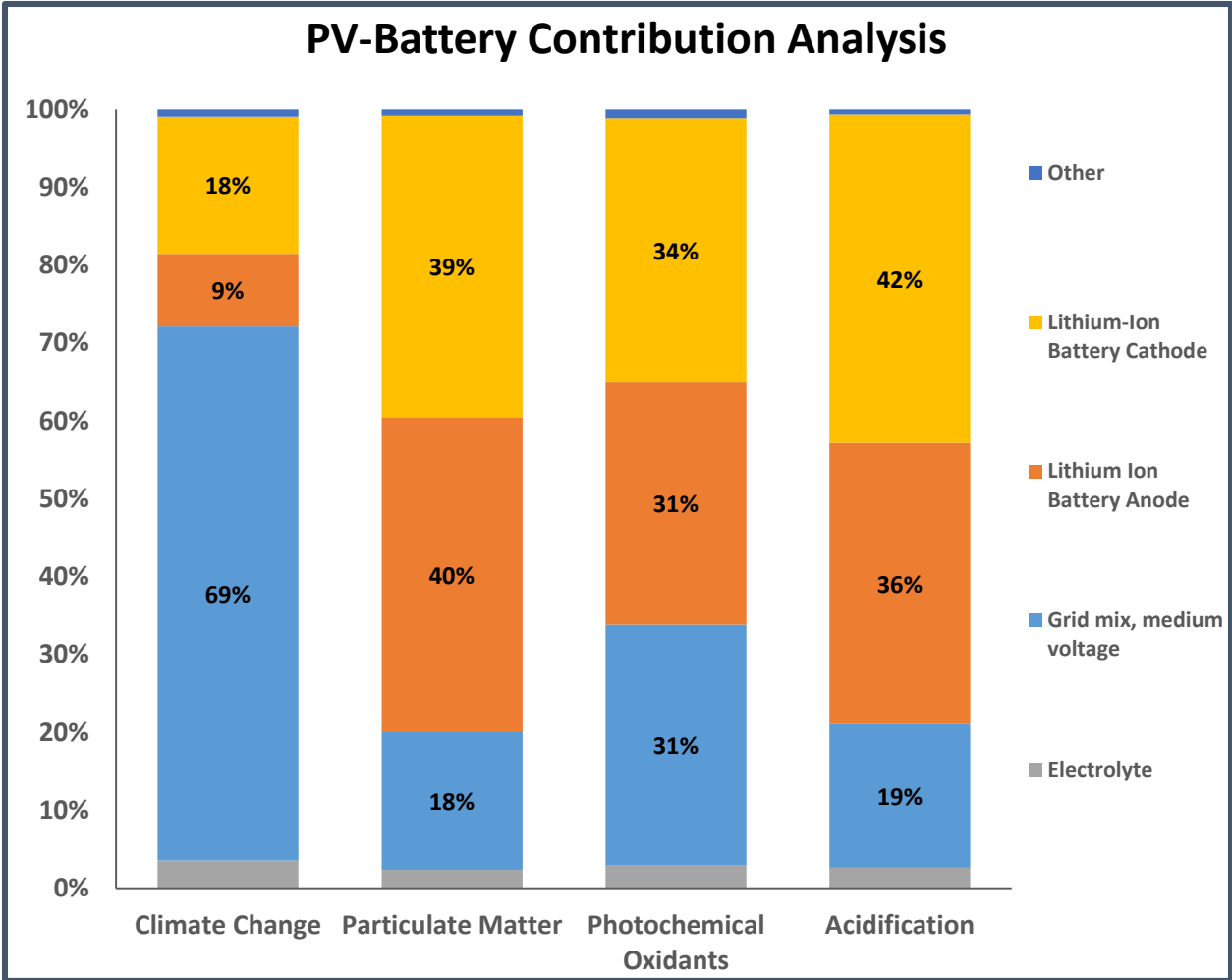


Figure 23: Contribution Analysis of Battery Cell Components. Contribution of individual battery cell components to overall Li-ion battery climate change (kg CO₂e), PM (kg PM₁₀ eq.), photochemical oxidant formation (kg NMVOC), and terrestrial acidification (kg SO₂ eq.) impact in the PV-Hybrid system.

In both indicator categories, the PV-Diesel system had much higher impacts than the two battery microgrids because of the large amounts of diesel burned. In fact over 98% of the climate change impacts and 99% of the PM impacts for the PV-Diesel system came from the burning of diesel in the generator.

Works Cited

- Aranda, E. D., Galan, J. G., de Cardona, M. S., & Marquez, J. A. (2009). Measuring The I-V Curve Of PV Generators. *IEEE Industrial Electronics Magazine*, 3(3).
- Arsenio, J. (2015, November 25). Personal Communication.
- Arsenio, J., Afonso, D., Dourado, S., Maia Alves, J., & Centeno Brito, M. (2014). 312 KW Solar PV-Diesel Minigrid in Bambadinca, Guinea-Bissau. *1st Africa Photovoltaic Solar Energy Conference and Exhibition Proceedings* (pp. 66-73). Durban, South Africa: 1st Africa Photovoltaic Solar Energy Conference.
- Attigah, B., & Mayer-Tasch, L. (2013). *The Impact of Electricity Access on Economic Development: A Literature Review*. Productive Use of Energy (PRODUSE).
- Aurora. (n.d.). *Aurora 4kW Diesel Generator – Technical specifications sheet*. Retrieved from Aurora Generators: <http://www.auroragenerators.com/downloads/AGi4P-SpecSheet.pdf>
- Bakhiyi, B., Labreche, F., & Zayed, J. (2014). The photovoltaic industry on the path to a sustainable future — Environmental and occupational health issues. *Environment International*, 73, 224-234.
- Barnes, D. F., & Floor, W. M. (1996). Rural energy in developing countries: A challenge for economic development. *Annual Review of Energy and the Environment*, 21(1), 497-530.
- Bergesen, J., Heath, G., Gibon, T., & Suh, S. (2014). Thin-film photovoltaic power generation offers decreasing greenhouse gas emissions and increasing environmental co-benefits in the long term. *Environmental Science and Technology*, 48(16).
- Chain Link Manufacturers Institute. (2011). *Chain Link Fence Manufacturers Institute Product Manual*. Retrieved from Contractors- Masterhalco: <http://contractors.masterhalco.com/Contract.nsf/CLFMIProdMan.pdf>
- Chen, W., Shen, H., Shu, B., Qin, H., & Deng, T. (2007). Evaluation Of Performance Of MPPT Devices In PV Systems With Storage Batteries. *Renewable Energy*, 32(9), 1611-1622.
- Cummins Onan. (2007, 03). *Cummins Diesel Generator – Technical specifications sheet*. Retrieved from Colorado Standby: https://coloradostandby.com/media/custom/upload/document_technical_a-1483.pdf
- de Koning, H. W., Smith, K. R., & Last, J. M. (1985). Biomass fuel combustion and health. *Bulletin of the World Health Organization*, 63(1), 11.
- Deichmann, U., Meisner, C., Siobhan, M., & Wheeler, D. (2011). The economics of renewable energy expansion in rural Sub-Saharan Africa. *Energy Policy*, 39(1), 215-227.

- Di, X., Nie, Z., Yuan, B., & Zuo, T. (2007). Life cycle inventory for electricity generation in China. *The International Journal of Life Cycle Assessment*, 12(4), 217-224.
- Dunlop, J., & Farhi, B. (2001). *Recommendations for maximizing battery life in photovoltaic systems: a review of lessons learned*. Cocoa, FL: Florida Solar Energy Center.
- Dunn, B., Kamath, H., & Tarascon, J. M. (2011). Electrical energy storage for the grid: a battery of choices. *Science*, 928-935.
- Dutta, D. (2015, 12 3). Personal Communication.
- Ellingsen, L.-w., Majeau-bettez, G., Singh, B., Srivastava, A., Valoen, L., & Stromman, A. (2014). Life cycle assessment of a lithium-ion battery vehicle pack. *Journal of Industrial Ecology*, 18(1), 113-124.
- Ezzati, M., & Kammen, D. M. (2001). Indoor air pollution from biomass combustion and acute respiratory infections in Kenya: an exposure-response study. *The Lancet*, 358(9282), 619-624.
- FG Wilson. (n.d.). *FG Wilson 6.8 kW Diesel Generator – Technical specifications sheet*. Retrieved from FG Wilson: <http://s7d2.scene7.com/is/content/Caterpillar/C10545256>
- First Solar. (2014). First Solar Analyst Day Presentation.
- First Solar. (2015). *20150807_Series 4v2 Module Datasheet*. Tempe, Arizona: First Solar.
- First Solar. (2015). *Approved Retaining Clips for FS Modules*. Tempe, Arizona: First Solar.
- First Solar. (2015). *Tetra Sun Module Datasheet*. Tempe, Arizona: First Solar.
- Fisher, K., Wallen, E., Laenen, P., & Collins, M. (2006). *Battery waste management life cycle assessment*. Environmental Resources Management.
- Frischknecht, R., Itten, P., Sinha, P., de Wild-Scholten, M., Zhang, J., Fthenakis, V., . . . Stucki, M. (2015). *Life Cycle Inventories and Life Cycle Assessment of Photovoltaic Systems*. IEA PVPS Task 12.
- Fthenakis, V., Kim, H., Frischknecht, R., Raugei, M., Sinha, P., & Stucki, M. (2011). *Life Cycle Inventories and Life Cycle Assessment of Photovoltaic Systems*. International Energy Agency.
- Goedkoop, M., Heijungs, R., Huijbregts, M., de Schryver, A., & van Zelm, R. (2009). *ReCiPe 2008: A Life Cycle Impact Assessment Method Which Comprises Harmonised Category Indicators at the Midpoint and the Endpoint Level*.
- Grimm, M., Sparrow, R., & Tasciotti, L. (2015). Does electrification spur the fertility transition? Evidence from Indonesia. *Demography*, 52(5), 1773-1796.

- Grzesiak, W. (2006). MPPT Solar Charge Controller For High Voltage Thin Film PV Modules. *Proceedings of IEEE 4th World Conference on Photovoltaic Energy Conference*. IEEE 4th World Conference on Photovoltaic Energy Conference.
- Hsu, D. D., O'donoghue, P., Fthenakis, V., Heath, G. A., Kim, H., Sawyer, P., . . . Turney, D. E. (2012). Life Cycle Greenhouse Gas Emissions of Crystalline Silicon Photovoltaic Electricity Generation. *Journal of Industrial Ecology*, 16, S122-S135.
- International Atomic Energy Agency. (2014). *Nuclear Share of Electricity Generation in 2014*. Retrieved from Power Reactor Information System: <https://www.iaea.org/PRIS/WorldStatistics/NuclearShareofElectricityGeneration.aspx>.
- International Energy Agency. (2010). *Energy Statistics for different countries*. Retrieved from International Energy Agency: <http://www.iea.org/stats/prodresult.asp?PRODUCT=Electricity/Heat>.
- International Energy Agency. (2011). *OECD- Electricity and heat generation*. Retrieved from Electricity Information Statistics Database: <http://www.oecd-ilibrary.org/energy/>
- International Energy Agency. (2015). *Energy Access Database*. Retrieved from World Energy Outlook: <http://www.worldenergyoutlook.org/resources/energydevelopment/energyaccessdatabase/>
- International Organization for Standardization. (2010). *ISO 14040:2006 Environmental Management-Life Cycle Assessment-Principles and framework*. Geneva: International Organization for Standardization.
- Itron. (2014). *CENTRON II C1219*. Retrieved from Itron: <https://www.itron.com/PublishedContent/CENTRON%20II%20C1219.pdf>
- Itten, R., Frischknecht, R., & Stucki, M. (2014). *Life Cycle Inventories of Electricity Mixes and Grid*. Uster: treeze Ltd.
- Jacobson, A. (2007). Connective Power: Solar electrification and Social Change in Kenya. *World Development*, 35(1), 144-162.
- Jolliet, O., Saade-Sbeih, M., Shaked, S., Jolliet, A., & Crettaz, P. (2015). Chapter 6: Interpretation. In O. Jolliet, M. Saade-Sbeih, S. Shaked, A. Jolliet, & P. Crettaz, *Environmental Life Cycle Assessment* (pp. 149-197). CRC Press.
- Jordan, D. C., & Kurtz, S. R. (2013). Photovoltaic Degradation Rates—an Analytical Review. *Progress in Photovoltaics: Research and Application*, 21(1), 12-29.
- Jorge, R., Hawkins, T., & Hertwich, E. (2012). Life cycle assessment of electricity transmission and distribution—part 2: transformers and substation equipment. *The International Journal of Life Cycle Assessment*, 17(2), 184-191.

- Joulie, M., Laucournet, R., & Billy, E. (2014). Hydrometallurgical recovery of value metals from spent lithium ion batteries. *Journal of Power Sources*, 551-555.
- Kalhammer, F. R., Kopf, B. M., Swan, D. H., Roan, V. P., & Walsh, M. P. (2007). *Status and prospects for zero emissions vehicle technology*. Sacramento, California: California Air Resources Board.
- Kanagawa, M., & Nakata, T. (2008). Assessment of Access to Electricity and the Socio-economic Impacts in Rural Areas of Developing Countries. *Energy Policy*, 36(6), 2016.
- Kang, D., Chen, M., & Ogunseitan, O. A. (2013). Potential Environmental And Human Health Impacts Of Rechargeable Lithium Batteries In Electronic Waste. *Environmental Science & Technology*, 47(10), 5495-5503.
- Kim, H., Cha, K., Fthenakis, V., Sinha, P., & Hur, T. (2014). Life Cycle Assessment of Cadmium Telluride Photovoltaic (CdTe PV) Systems. *Solar Energy*, 103, 78-88.
- Kim, H., Fthenakis, V., Choi, J.-k., & Turney, D. E. (2012). Life Cycle Greenhouse Gas Emissions of Thin-film Photovoltaic Electricity Generation. *Journal of Industrial Ecology*, 16, S110-S121.
- Kirubi, C., Kammen, D. M., Jacobson, A., & Mills, A. (2009). Community-Based Electric Micro-Grids Can Contribute to Rural Development: Evidence from Kenya. *World Development*, 37(7), 1208-1221.
- Kohler. (n.d.). *Kohler 5.5 kW Diesel Generator – Technical specifications sheet*. Retrieved from Kohler Power: <http://www.kohlerpower.com.sg/onlinecatalog/pdf/KM6M.pdf>
- Lee, K.-M., Lee, S.-Y., & Hur, T. (2004). Life cycle inventory analysis for electricity in Korea. *Energy*, 29(1), 87-101.
- Lighting Africa. (2011). *The off-grid lighting market in Sub-Saharan Africa: market research synthesis report*. Washington DC: The World Bank Group.
- Lighting Global. (2014, August). Energy and Carbon Benefits of Pico-powered Lighting. *Eco Design Notes*(4).
- Lukuyu, J., & Cardell, J. (2014). Hybrid Power System Options for Off-Grid Rural Electrification in Northern Kenya. *Smart Grid and Renewable Energy*, 5(5), 89-106.
- Majeau-Bettez, G., Hawkins, T. R., & Stromman, A. (2011). Life cycle environmental assessment of lithium-ion and nickel metal hydride batteries for plug-in hybrid and battery electric vehicles. *Environmental Science & Technology*, 45(10), 4548-4554.
- Malhotra, A., Battke, B., Beuse, M., Stephan, A., & Schmidt, T. (2016). Use cases for stationary battery technologies: A review of the literature and existing projects. *Renewable and Sustainable Energy Reviews*, 705-721.

- Marcellino, J. (2015, 11 24). Email with Morningstar technical support.
- Marshall, V. (2009, October 14). *The Dissection: A Home Electric Meter*. Retrieved from Popular Science: <http://www.popsci.com/diy/article/2009-10/electric-meter-dissection?image=5>
- Mills, E. (2012). Health impacts of fuel-based lighting. *3rd International Off-Grid Lighting Conference*. Dakar, Senegal.
- Mills, E. (2014). *Lifting the Darkness on the Price of Light: Assessing the Effect of Fuel Subsidies in the Off-Grid Lighting Market*. Geneva, Switzerland: UNEP.
- Mills, E. (2016). Identifying and reducing the health and safety impacts of fuel-based lighting. *Energy for Sustainable Development*, 39-50.
- Mills, E., & Jacobson, A. (2007). *The Lumina Project Vol. 1 Research Memo*.
- Miret, S. (2015, February 03). *Energy Access Across the World*. Retrieved from Berkeley Energy Resources Collaborative: <http://berc.berkeley.edu/energy-access-across-world/>
- Morningstar Corporation. (2013). *TriStar MPPT 600V Installation and Operation Manual*. Retrieved from Morningstar Corp: <http://www.morningstarcorp.com/wp-content/uploads/2014/02/600V-TS-MPPT-Operators-Manual.pdf>
- Morningstar Corporation. (2015). *Morningstar TS-MPPT-600v specification sheet*. Retrieved from Morningstar Corp: <http://www.morningstarcorp.com/wp-content/uploads/2014/02/MSC-Data-Sheet-TS-MPPT-600V-150526-04-MG.pdf>
- MP-Tec. (2013). *Product Catalogue Mounting System 34*. Eberswalde, Germany: MP-Tec.
- Mwangangi, S., Njeru, R., Koech, W., Ngari, P., Akinala, J., Omwega, T., . . . Shalleh, A. (2010, June). *Environmental and Social Impact Assessment Project Report For Proposed Two 250 kW Wind Turbines at Marsabit*. Kenya Power and Lighting Company. Retrieved from Kenya Power and Lighting Company: http://www.kplc.co.ke/fileadmin/user_upload/Documents/ESIA/ESIA%20of%20Two%20250%20KW%20Wind%20Turbines%20at%20Marsabit%20District.pdf
- NASA. (2016). Nasa Surface Meteorology and Solar Energy. Retrieved from <https://eosweb.larc.nasa.gov/sse>
- National Renewable Energy Laboratory. (2016). *Life Cycle Assessment Harmonization*. Retrieved from National Renewable Energy Laboratory: http://www.nrel.gov/analysis/sustain_lcah.html
- Navigant Consulting. (2013). *Microgrid Deployment Tracker 2Q13: Commercial/Industrial, Community/Utility, Institutional/Campus, Military, and Remote Microgrids: Operating, Planned, and Proposed Projects*. Boulder, CO: Navigant Consulting.

- Nordic Green. (2010). *Miljøbil Grenland AS*. Retrieved from Nordic Green: <http://www.nordicgreen.net/startups/energy-storage/milj-bil-grenland>
- Notter, D. A., Gauch, M., Widmer, R., Wager, P., Stamp, A., Zah, R., & Althaus, H.-J. (2010). Contribution of Li-ion batteries to the environmental impact of electric vehicles. *Environmental Science & Technology*, 44(17), 6550-6556.
- Palanisamy, K., & Fathima, A. H. (2015). Optimization in microgrids with hybrid energy systems—A review. *Renewable and Sustainable Energy Reviews*, 45, 431-446.
- Poullikkas, A. (2013). A comparative overview of large-scale battery systems for electricity storage. *Renewable and Sustainable Energy Reviews*, 27, 778.
- Rao, N. D. (2012). Kerosene subsidies in India: When energy policy fails as a social policy. *Energy for Sustainable Development* 16.1, 35-43.
- Rebitzer, G., Ekvall, T., Frischknecht, R., Hunkeler, D., Norris, G., Rydberg, T., . . . Pennington, D. W. (2004). Life cycle assessment: Part 1: Framework, goal and scope definition, inventory analysis, and applications. *Environment International*, 701-720.
- Republic of Kenya. (2014). *10 Year Power Sector Expansion Plan 2014-2024*.
- RV Solar Connection. (2008). *Morningstar Solar Charge Controllers*. Retrieved from RV Solar Connection: <http://www.rvsolarconnection.com/solar-controllers/morningstar-solar-controllers.htm>
- Rydh, C., & Sanden, B. A. (2005). Energy analysis of batteries in photovoltaic systems. Part I: Performance and energy requirements. *Energy Conversion and Management*, 46(11), 1957-1979.
- Schnitzer, D., Lounsbury, D., Carvallo, J., Deshmukh, R., Apt, J., & Kammen, D. M. (2014). *Microgrids for rural electrification: A critical review of best practices based on seven case studies*. The United Nations Foundation.
- Shuva, M., & Kurny, A. (2013). Hydrometallurgical Recovery of Value Metals from Spent Lithium Ion Batteries. *American Journal of Materials Engineering and Technology*, 1(1), 8-12.
- Simon, B., & Weil, M. (2013). Analysis of materials and energy flows of different lithium ion traction batteries. *Revue de Métallurgie*, 110(1), 65-76.
- Sinha, P. (2013). Life Cycle Materials and Water Management for CdTe Photovoltaics. *Solar Energy Materials and Solar Cells*, 119, 271.
- Sinha, P., & de Wild-Scholten, M. (2012). Life Cycle Assessment of Utility-Scale CdTe PV Balance of Systems. *Proceedings of 27th European Photovoltaic Solar Energy Conference and Exhibition* (pp. 4657-4660). 27th European Photovoltaic Solar Energy Conference and Exhibition.

- Sinha, P., & de Wild-Scholten, M. (2015). Life Cycle Assessment of Silver Replacement With Copper Based Metallization in Tetrasun PV Modules. *Proceedings of 31st European Photovoltaic Solar Energy Conference and Exhibition* (pp. 2424-2429). 31st European Photovoltaic Solar Energy Conference and Exhibition.
- Sinha, P., Cossette, M., & Menard, J. F. (2012). End-of-Life CdTe PV Recycling with Semiconductor Refining. *Proceedings of 27th European Photovoltaic Solar Energy Conference and Exhibition* (pp. 4653-4656). 27th European Photovoltaic Solar Energy Conference and Exhibition.
- Smith, C., Burrows, J., Scheier, E., Young, A., Smith, J., Young, T., & Gheewala, S. H. (2015). Comparative Life Cycle Assessment of a Thai Island's Diesel/PV/wind Hybrid Microgrid. *Renewable Energy*, 80, 85-100.
- Socolof, M. L., Smith, J., Cooper, D., & Amarakoon, S. (2014). *Design for the Environment: Wire and Cable Partnership*. Washington DC: Environmental Protection Agency.
- Strevel, N., Trippel, L., Kotarba, C., & Khan, I. (2013). Improvements in CdTe module reliability and long-term degradation through advances in construction and device innovation. *Photovoltaics International*, 22.
- Sullivan, J. L., & Gaines, L. (2012). Status of life cycle inventories for batteries. *Energy Conversion and Management*, 58, 134-148.
- Sullivan, J., & Gaines, L. (2010). *A review of battery life-cycle analysis: state of knowledge and critical needs*. Argonne, Illinois: Argonne National Laboratory.
- Sunny Money. (2014). *SolarAid Impact Report 2014*. Sunny Money.
- Swiss Federal Office of Energy. (2015, March 06). *Hydropower*. Retrieved from Swiss Federal Office of Energy SFOE:
<http://www.bfe.admin.ch/themen/00490/00491/index.html?lang=en>
- Turconi, R., Simonsen, C., Byriel, I., & Astrup, T. (2014). Life cycle assessment of the Danish electricity distribution network. *The International Journal of Life Cycle Assessment*, 19(1), 100-108.
- United Nations Development Programme. (2011). *Poverty Reduction: Scaling Up Local Innovations For Transformational Change*. New York: United Nations.
- United Nations Development Programme. (2015). *Sustainable Development Goals Booklet*. United Nations Development Programme.
- Ur Rehman, A., & Hong Lee, S. (2014). Review of the Potential of the Ni/Cu Plating Technique for Crystalline Silicon Solar Cells. *Materials*, 7(2), 1318-1341.
- Van Gerven, M. (2015, December 17). *Enel, Powerhive Partner on Landmark Rural Electrification Project*. Retrieved from The Current: First Solar's Blog:

<http://www.firstsolar.com/en/About-Us/Press-Center/Blog/2015/November/Powerhive.aspx>

- Wang, H., Vest, M., & Friedrich, B. (2011). Hydrometallurgical processing of Li-Ion battery scrap from electric vehicles. *EMC 2011*. Aachen.
- Wang, X., Palazoglu, A., & El-Farra, N. H. (2015). Operational optimization and demand response of hybrid renewable energy systems. *Applied Energy*, 143, 324-335.
- Warner, J. (2015). *Handbook of Lithium-Ion Battery Pack Design – Chemistry, components, Types and Terminology – Introduction*. Elsevier.
- Weber, C. L., Jaramillo, P., Marriott, J., & Samaras, C. (2010). Life cycle assessment and grid electricity: what do we know and what can we know? *Environmental Science & Technology*, 44(6), 1895-1901.
- Wheatland Tube. (2014). *Chain Link Fabric Average Weights*. Retrieved from Wheatland: <http://www.wheatland.com/images/specs/Chain-link-fabric-weights.pdf>
- Widiyanto, Maruyama, Kato, Nishimura, & Sampattagul. (2003). Environmental impacts evaluation of electricity grid mix systems in four selected countries using a life cycle assessment point of view. *EcoDesign 3rd International Symposium on Environmentally Conscious Design and Inverse Manufacturing 2003*, (pp. 26-33).
- Williams, N. J., Jaramillo, P., Taneja, J., & Ustun, T. (2015). Enabling private sector investment in microgrid-based rural electrification in developing countries: A review. *Renewable and Sustainable Energy Reviews*, 52, 1268.
- World Bank (ESMAP). (2003). *Rural electrification and development in the Philippines: Measuring the social and economic benefits*. Washington DC.
- World Bank (IEG). (2004). *Books, buildings, and learning outcomes: An impact evaluation of World Bank support to basic education in Ghana*. Washington DC: World Bank.
- World Bank. (2008). *The Welfare Impact of Rural Electrification: A Reassessment of the Costs and Benefits*. The World Bank.
- World Bank. (2010). *Sustainable Energy For All*. Retrieved from World Bank Data: <http://data.worldbank.org/data-catalog/sustainable-energy-for-all>
- Zackrisson, M., Avellan, L., & Orlenius, J. (2010). Life cycle assessment of lithium-ion batteries for plug-in hybrid electric vehicles—Critical issues. *Journal of Cleaner Production*, 18(15), 1519-1529.
- Zeyringer, M., Pachauri, S., Schmid, E., Schmidt, J., Worrell, E., & Morawetz, U. (2015). Analyzing grid extension and stand-alone photovoltaic systems for the cost effective electrification of Kenya. *Energy for Sustainable Development*, 25, 75-86.

Zhu, S.-g., He, W.-z., Li, G.-m., Zhou, X., Zhang, X.-j., & Huang, J.-w. (2012). Recovery of Co and Li from spent lithium-ion batteries by combination method of acid leaching and chemical precipitation. *Transactions of Nonferrous Metals Society of China*, 22(9), 2274-2281.